An Investigation of Control-Related Issues In Transcritical R744 and Subcritical R134a Mobile Air Conditioning Systems

R. P. McEnaney, J. M. Yin, C. W. Bullard, and P. S. Hrnjak

ACRC CR-19 July 1999

For additional information:

Air Conditioning and Refrigeration Center
University of Illinois
Mechanical & Industrial Engineering Dept.
1206 West Green Street
Urbana, IL 61801

(217) 333-3115

The Air Conditioning and Refrigeration Center was founded in 1988 with a grant from the estate of Richard W. Kritzer, the founder of Peerless of America Inc. A State of Illinois Technology Challenge Grant helped build the laboratory facilities. The ACRC receives continuing support from the Richard W. Kritzer Endowment and the National Science Foundation. The following organizations have also become sponsors of the Center.

Amana Refrigeration, Inc.
Brazeway, Inc.
Carrier Corporation
Caterpillar, Inc.
Chrysler Corporation
Copeland Corporation
Delphi Harrison Thermal Systems
Frigidaire Company
General Electric Company
Hill PHOENIX
Honeywell, Inc.
Hussmann Corporation
Hydro Aluminum Adrian, Inc.
Indiana Tube Corporation
Lennox International, Inc.
Modine Manufacturing Co.
Peerless of America, Inc.
The Trane Company
Thermo King Corporation
Visteon Automotive Systems
Whirlpool Corporation
York International, Inc.

For additional information:

Air Conditioning & Refrigeration Center
Mechanical & Industrial Engineering Dept.
University of Illinois
1206 West Green Street
Urbana IL 61801

217 333 3115

Table of Contents

List of Tables

List of Figures

Figure Page

Nomenclature

A/C—air conditioning

Condensate—evaporator condensate removal rate

COP—coefficient of performance

c_p—specific heat at constant pressure

cycle time—time to complete one full on/off cycle, cycling period

cycling limits—same as temperature limits

(dot operator)—partial derivative with respect to time

DPca—pressure change across gas cooler, airside

DPcr—pressure change across gas cooler, refrigerant side

DPea—pressure change across evaporator, airside

Dper—pressure change across evaporator, refrigerant side

e—error between temperature setpoint and cabin temperature

H—enthalpy

IHX—internal heat exchanger, same as SLHX

m—mass

mr—mass flow rate of refrigerant

m_ca—mass flow rate, gas cooler air

m_ea—mass flow rate, evaporator air

m_dot—mass flow rate

on time—portion of on/off cycle with compressor clutch engaged

P—pressure

power—compressor power

P_{cri}—pressure, gas cooler refrigerant inlet

P_{cro}—pressure, gas cooler refrigerant outlet

P_{eri}—pressure, evaporator refrigerant inlet

P_{ero}—pressure, evaporator refrigerant outlet

P_{ratio}—ratio of compressor discharge pressure to compressor suction pressure

P_{rcpi}—pressure, compressor refrigerant inlet

P_{rcpo}—pressure, compressor refrigerant outlet

Q—cooling capacity

QC—gas cooler heat transfer rate

QE—evaporator heat transfer rate

Q_lat—evaporator latent heat transfer rate

Q_sens—evaporator sensible heat transfer rate

Region 1)—operating regime where capacity is greater than load

Region 2)—operating regime where capacity and load are approximately equal

Region 3)—operating regime where load is greater than capacity

RH—relative humidity

SLHX—suction line heat exchanger, same as IHX

Tdp_cabin—cabin dew point temperature

temperature limits—evaporator air outlet temperature limits used in cycling

T_{cabin}, T_cabin—cabin temperature

T_{cai}—temperature, gas cooler air inlet

T_{cao}—temperature, gas cooler air outlet

T_{cri}—temperature, gas cooler refrigerant inlet

T_{cro}—temperature, gas cooler refrigerant outlet

T_{eai}—temperature, evaporator air inlet

T_{eao}—temperature, evaporator air outlet

T_{eri}—temperature, evaporator refrigerant inlet

T_{ero}—temperature, evaporator refrigerant outlet

T_{evap}—temperature, refrigerant evaporation

T_{ori}—temperature, expansion device refrigerant inlet

T_{rcpi}—temperature, compressor refrigerant inlet

T_{rcpo}—temperature, compressor refrigerant outlet

T_{set}—setpoint temperature

T_{shi}—temperature, suction line heat exchanger low side inlet

T_{sho}—temperature, suction line heat exchanger low side outlet

TXV—thermostatic expansion valve

UA—overall heat transfer coefficient

Vc—compressor speed

VOV—variable orifice valve

W_{comp}—compressor power

ΔQ—change in amount of air conditioning capacity

ΔT—change in temperature across component

η_i—compressor isentropic efficiency

η_v—compressor volumetric efficiency

1 Automotive A/C Systems in This Study

This section will provide some brief background on the types of systems that were the focus of this study, their components, and their operation. There were two major types of systems tested, a conventional subcritical vapor compression system using R134a as the refrigerant, and a transcritical vapor compression system using R744 (CO_2) as the refrigerant. Under each of these headings, several component choices were possible, but the systems that were tested are shown in Table 1.1.

Table 1.1. Different Automotive Air Conditioning Systems Tested

Working Fluid	Compressor	Expansion Device
R744	Fixed Reciprocating, Clutched	Backpressure Regulator Valve
		Needle Valve
R134a	Fixed Reciprocating, Clutched	Orifice Tube

1.1 System Configurations and Components

Even though the subcritical and transcritical cycles behave very differently, the basic layout of the system is nearly identical. Each system has a compressor, a heat exchanger designed to reject heat from the refrigerant to the environment (condenser or gas cooler), an expansion device, and an evaporator. Also, each system used some type of reservoir to store extra charge, in both cases, a suction accumulator. Special to the CO_2 system was an internal heat exchanger (IHX) that exchanged heat from the refrigerant exiting the gas cooler to the refrigerant entering the compressor. The purpose of this component is to create a lower refrigerant quality at the evaporator inlet, which increases both capacity and COP, as shown in Boewe (1). All of these components are shown in the schematic, Figure 1.2. The solid lines represent circuiting for the R134a system, and the dashed lines show the addition of the IHX for the R744 system. The systems investigated here are the size of those that would be used in a typical compact car.

1.2 Operation with Steady Inputs and Steady Refrigerant Flow

The parameter space for any given automotive A/C system consists of many variables relating to vehicle operation. The parameters which determine the operating condition for a

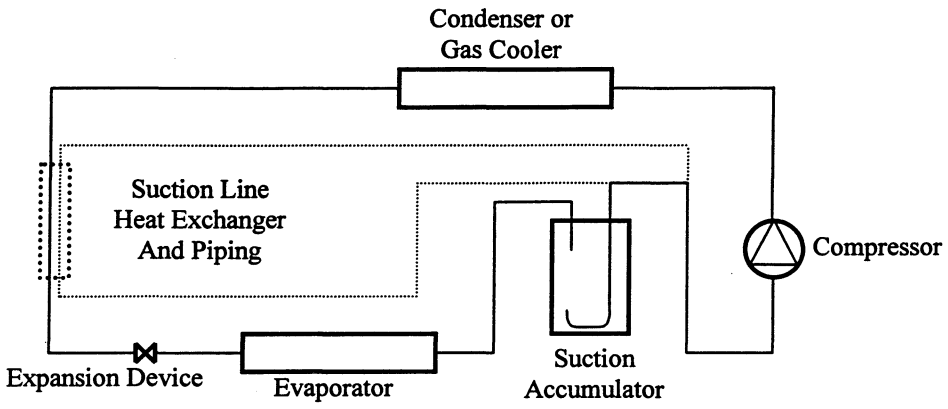

Figure 1.2. Schematic of Automotive A/C Systems in This Study

given system can be divided into three major areas: evaporator conditions, condenser or gas cooler conditions, and vehicle conditions. The parameters concerning the evaporator are the evaporator air flow rate (selected by the passenger) and the evaporator air inlet temperature and humidity (mainly a function of cabin conditions, but also vehicle air handling design). Likewise, the important variables for the condenser are the air flow rate (function of vehicle speed) and condenser air inlet temperature (function of ambient conditions and under-hood recirculation). The final important parameter is the engine speed. This is important because the compressor uses the main automobile engine as its power source.

The operation principles of these systems in this mode of operation can be explained conventionally by looking at some ideal cycles on a p-h diagram. Figure 1.3 shows the p-h diagram for the transcritical R744 vapor compression cycle with internal heat exchange on the left and the corresponding cycle for the R134a system on the right. Of course, the major difference is that the heat rejection (process 2→3) is above the critical point in the R744 system. Also, it is evident that the IHX (process 3→4 and 6→1 on the CO_2 diagram) can reduce the refrigerant inlet quality to the evaporator significantly for the R744 system. Finally, the operating pressures for R744 are much higher.

1.3 Realistic Operation

An automotive A/C system almost never operates with steady inputs and steady refrigerant flow. In almost all situations, the automotive A/C system operates in a transient fashion, whether that be due to changing inputs or varying refrigerant flow (compressor speed).

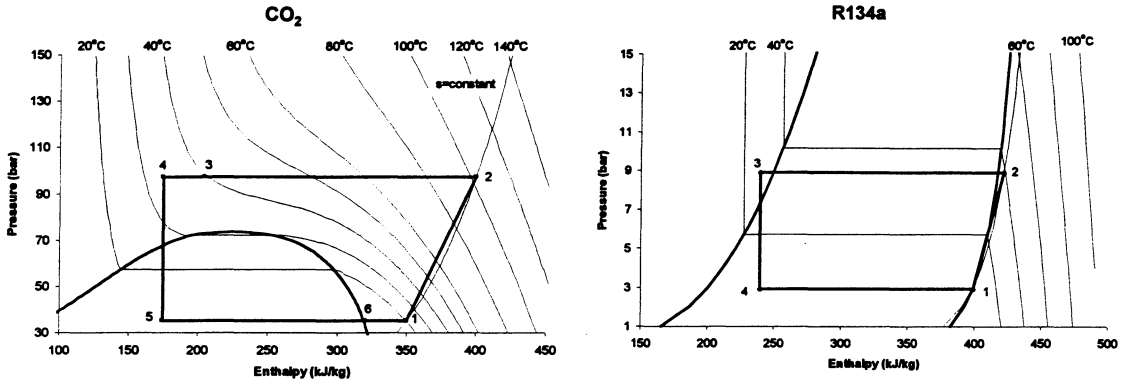

Figure 1.3. Vapor Compression Cycles on p-h Coordinates

First, the compressor is usually run directly from the vehicle's main engine. Since the engine speed changes often, unless the vehicle is being operated on an open, flat road, the compressor speed changes often. Second, when the vehicle speed changes, the air flow rate over the condenser (or gas cooler) also changes. Finally, until the cabin temperature and humidity reach an equilibrium, they are also varying parameters.

Unfortunately, testing the true operation of an automotive A/C system would require an actual vehicle doing simulated driving in a wind tunnel large enough to fit the entire car, with simulated solar load as well. The way in which the system behaves during transients is a strong function of several variables of the actual vehicle design. Our program was focused on breadboard systems that had the evaporator and condenser (gas cooler) placed in separate wind tunnels. This step in the program was focused on steady state operation, whether that be continuous steady refrigerant flow, or steady state cycling. That is, cycling that behaves in a repeating, or steady, pattern. By testing a wide variety of steady state conditions, one can get a good idea of how the system would behave under real operating conditions.

2 Role of Control Systems in Automotive A/C

There may be several reasons to have a control system on an automotive A/C system. However, the main role of a control system is to regulate cooling capacity. Although in reality the operating regime for an automotive A/C system is continuous, it is helpful to imagine three main regimes of A/C system operation: 1) when system capacity is greater than the load on the system, 2) when system capacity and load are about equal and 3) when system capacity is not enough to meet the load demand. These regimes are shown in Figure 2.1. Each of these regimes requires its own control strategy for optimum performance across a wide range of operating conditions. The focus here will be on control strategies to exploit properties of the transcritical R744 mobile A/C system, however some of the methodologies can be extended to the R134a system which uses a normal subcritical vapor compression cycle.

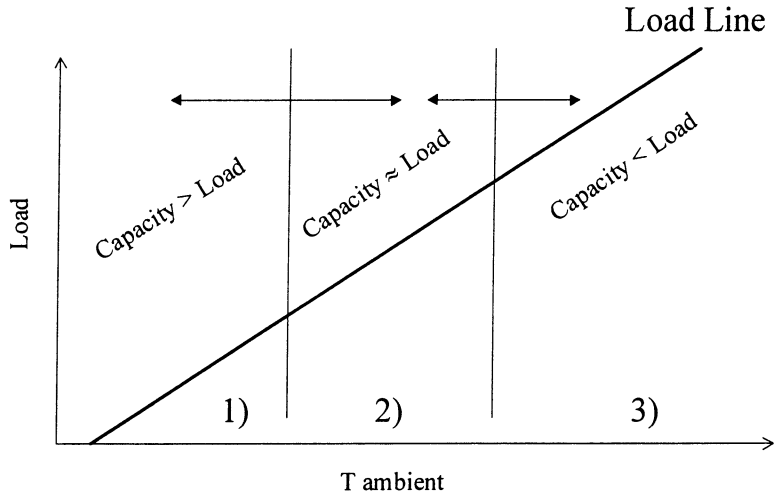

Figure 2.1. Division of Operating Regimes for Mobile A/C Systems

In addition to the main goal, there are some secondary goals that could be achieved through the use of variable components (control systems). Typical secondary goals include efficient operation, as well as safe operation. In more specific terms, these goals may include controlling the amount of superheat at the evaporator exit, or preventing system pressures from going too high or too low.

The major difference between the transcritical cycle and the subcritical cycle is high-pressure side operation. In the transcritical cycle, the traditional condensing process is replaced by a single phase supercritical heat rejection. That is, the working fluid is not saturated, so the

temperature and pressure are not linked. Also, it has been found that there is a high side pressure that will yield a maximum COP for each set of operating conditions. This pressure at which maximum COP occurs is not constant, but is a function of operating conditions and, according to Pettersen (2), was observed as early as the end of the 19th century, when CO_2 systems were used in marine applications. Therefore, some type of device to control the high side pressure is necessary if one wants to operate the transcritical cycle at close to maximum COP across a wide range of operating conditions.

It is also known that in the transcritical R744 cycle, the high side pressure which maximizes COP is usually not the same high side pressure which yields the highest cooling capacity, as shown in Figure 2.2, and in Boewe (1). Therefore, in regions 2) and 3) described above, it might be possible to 'trade' COP for Q and vice-versa depending on the operating needs (Figure 2.3).

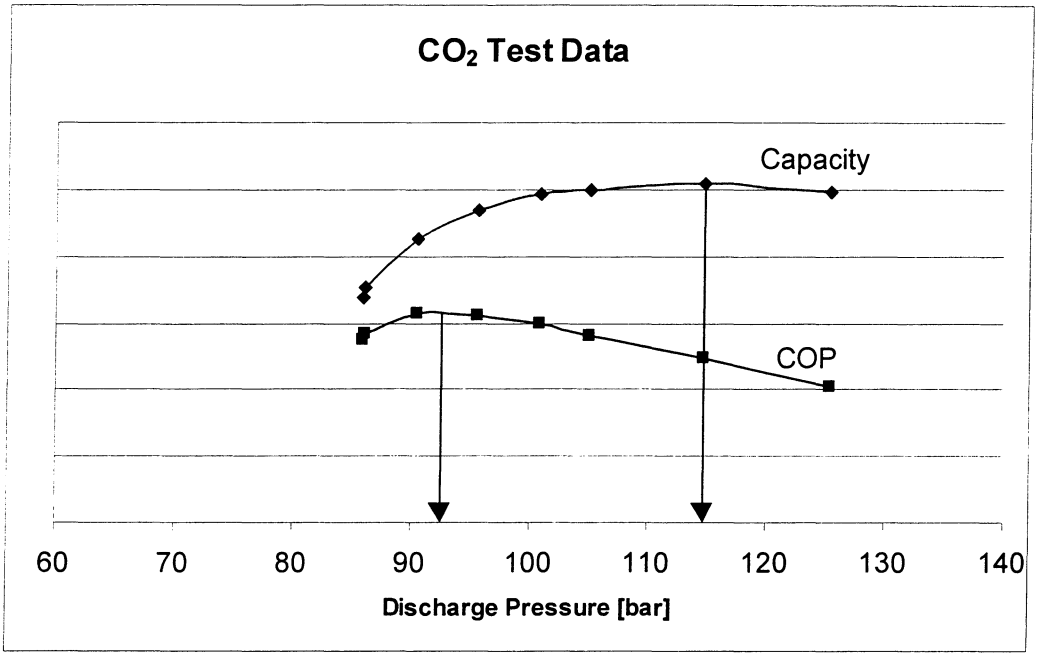

Figure 2.2. Maximum COP and Maximum Capacity are at Different Pressures

In region 1), the strategy is altogether different. In that region where cooling capacity is greater than needed, some type of capacity regulation is needed. Of course, in the R744 case, this could be done by controlling the high side pressure, however, this strategy reduces COP. There are many better ways to regulate capacity in this operating regime. The strategies

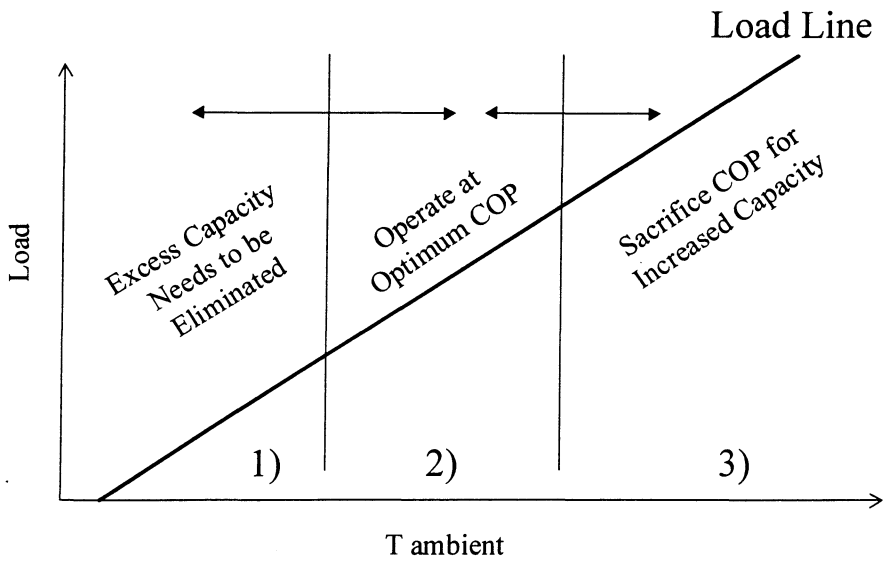

Figure 2.3. Possible Strategies for R744 in Operating Regimes

investigated here are concerned with different types of compressors. That is, the compressor is somehow able to reduce the mass flow of refrigerant to a more reasonable level for the operating conditions. These types of compressors can be used in both transcritical and subcritical vapor compression cycles. Types of compressor modulation include clutch-cycling, variable speed compressors, both internally and externally controlled variable displacement compressors, and variable capacity scroll compressors.

When variable compressors are put into the system, the three separate regions of load / capacity begin to dissolve into one another. This is because the compressor will adjust its displacement to more closely match the delivered capacity to the required capacity across a wide range of operating conditions. However, it is still helpful to think of the regions as existing, to have some idea of how the displacement needs to be adjusted.

The conditions being investigated in region 1) are those for which the A/C system capacity is not its maximum. Or, another way to think about it is that the compressor is not working 100%. The reason for this mode of operation usually is to prevent frosting of the evaporator coil. If the evaporator coil were to begin freezing, this would restrict airflow and bring the refrigerant temperature down further, thus causing more and more ice buildup. Therefore, some method is needed to prevent this event from occurring.

Another reason for running the A/C system at less than maximum capacity would be to try to match the system capacity to the load that is coming in. This scenario could occur when the conditions in the cabin are quite comfortable, but there is a small load coming in which the A/C system needs to remove. In present systems, there are two ways to accomplish this task. First, the A/C system would remove much more energy than necessary, then use waste heat from the engine to reheat the cooled air to the desired temperature. Another way to do this to avoid cooling the air too much is to raise the average evaporating temperature by clutch cycling. The second method is more efficient because it uses less compressor power to generate less cooling power.

Even though these conditions do exist, one might think they are very special conditions which do not occur often in the ordinary operation of a mobile A/C system. However, studies of driving patterns, weather data, and system test data show that these modes of operation make up a very significant portion of the total compressor operating hours.(3) Therefore, an understanding of what is occurring and what can be done to improve the efficiency in these operating regimes could contribute a great deal to the overall energy efficiency of these systems.

3 Variable Components

3.1 Valve Types

There are several types of variable expansion devices that are in use in modern systems. Although the construction and operation of the devices is quite varied, the idea for all of them is the same. Their job is to react to operating conditions to allow the system to operate better than using just a fixed area expansion device. A thermostatic expansion valve (TXV) uses the temperature at the evaporator exit as a signal to open and close the valve, Figure 3.1. The changing exit temperature changes the pressure in the bulb line. The evaporating temperature determines the pressure inside the valve. The valve is then moved until the spring force and two pressure forces are balanced, corresponding to a designated superheat. The picture shows both a remote bulb setup to measure the temperature, as well as a block type TXV, popular in automotive applications.

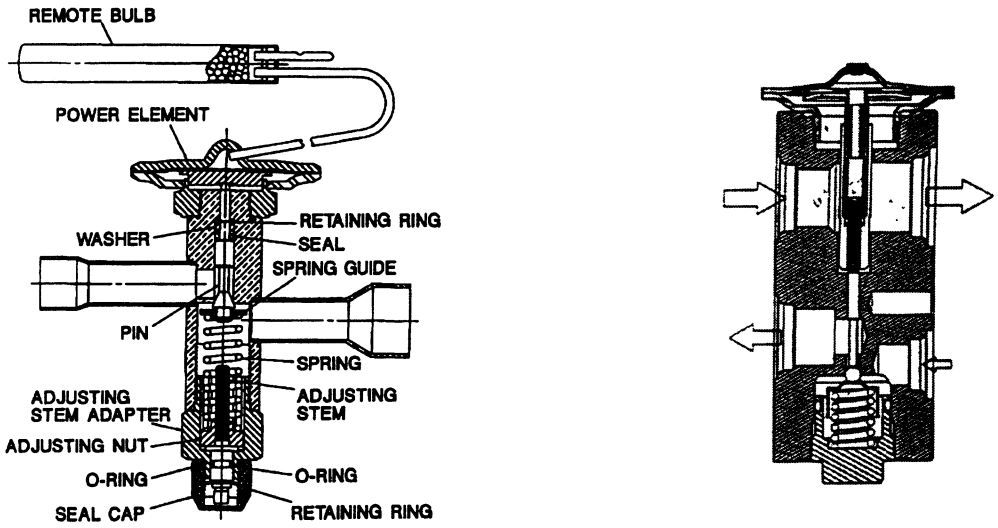

Figure 3.1. Schematic of Bulb and Block Type Thermostatic Expansion Valves (4) (5)

A variable orifice valve (VOV) uses the temperature of the refrigerant entering the orifice to adjust the orifice size, Figure 3.2. A bimetal coil responds to the temperature and is used to actuate the valve. This type of valve was planned to go into selected '99 model Chrysler automobiles. (6) (7)

An electronic expansion device uses a microprocessor, possibly linked to several parameters in the system to decide how much the valve should be open. The valve could either be driven by a stepper motor or pulse-width modulation and is the most versatile.

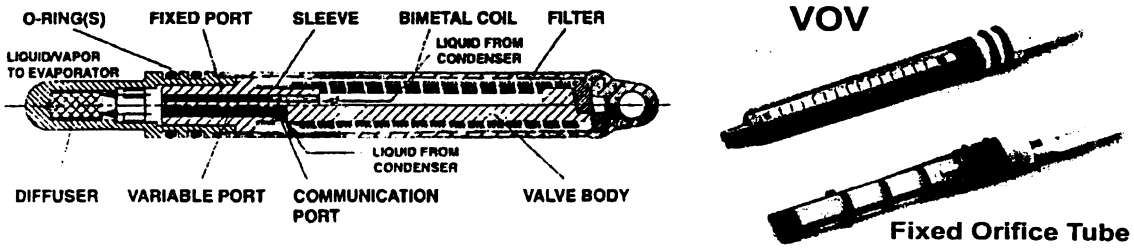

Figure 3.2. Variable Orifice Valve (7)

3.2 Compressor Types

3.2.1 Fixed Displacement, Cycling

Cycling is perhaps the simplest and least expensive way to achieve the effects of a variable compressor. This method allows a fixed displacement compressor to provide less than maximum cooling capacity by modulating the compressor on and off to get an average cooling capacity that more closely matches what is required. In a setup that uses cycling, there is a magnetic clutch placed between the input pulley on the compressor and the compressor shaft. The magnetic clutch is actuated by an electrical signal that corresponds to some type of system sensor, such as a pressure switch located on the suction accumulator. When the accumulator pressure drops below a certain value (corresponding to the evaporating temperature dropping below a certain value), the clutch will disengage. Then, when the accumulator pressure comes back up to a specified level, the clutch engages, and the cycle repeats.

3.2.2 Improved Cycling

Although typically the clutch is controlled by a pressure switch on the accumulator, there might be better inputs with which to control the clutch. One method that has been investigated is using the air temperature after the evaporator as a control variable. By varying the temperature limits, as in Figure 3.3, a system can achieve a better match of capacity and can operate at a higher COP.

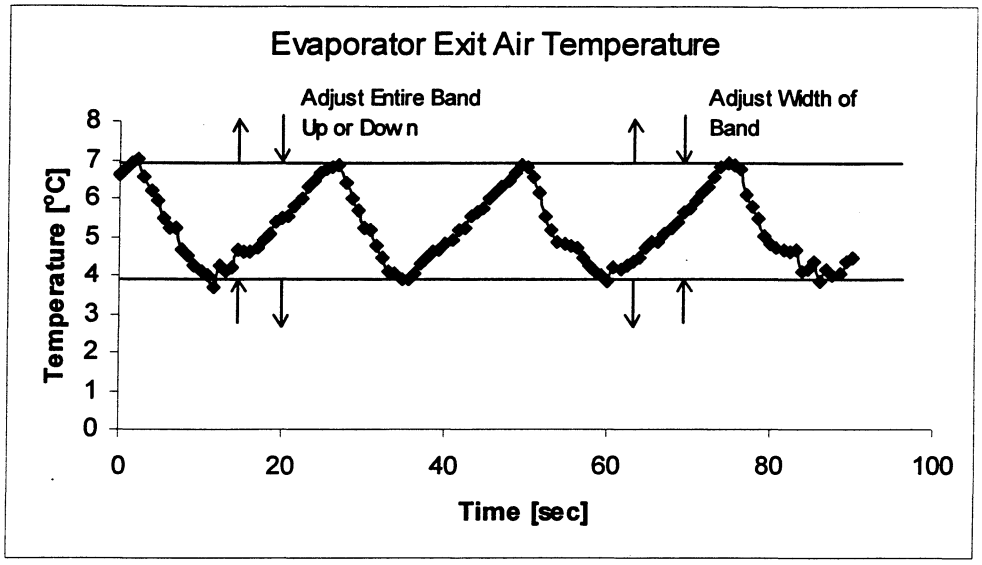

Figure 3.3. Adjustable Exit Air Temperature Limits in Cycling

3.2.3 Variable Speed

In a typical mobile A/C system, the compressor input pulley is belt driven from the engine. Therefore, the compressor speed is proportional to engine speed. However, as technology progresses, a compressor which is electrically driven may be an excellent alternative. In the future, more and more vehicles will most likely switch from using the internal combustion engine to some type of electrically driven drivetrain. Also, if one could use an electrically driven compressor, the compressor design could change from open to hermetic (thus eliminating a significant source of refrigerant emissions).

3.2.4 Variable Displacement

There are two main types of variable displacement compressors, internally and externally controlled. The internally controlled model uses the low side system pressure to vary the displacement of the compressor. As the suction pressure falls, the displacement of the compressor is reduced, thus reducing the cooling capacity. The externally controlled model uses some type of electronic or mechanical controller to perhaps blend several system parameters as inputs to calculate what the displacement of the compressor should be. In either case, the displacement is altered by adjusting the piston stroke via a variable angle wobble plate or swash

plate design, as illustrated in Figure 3.4. The variable displacement concept was introduced in the late 1950s and patented by Heidorn. (8)

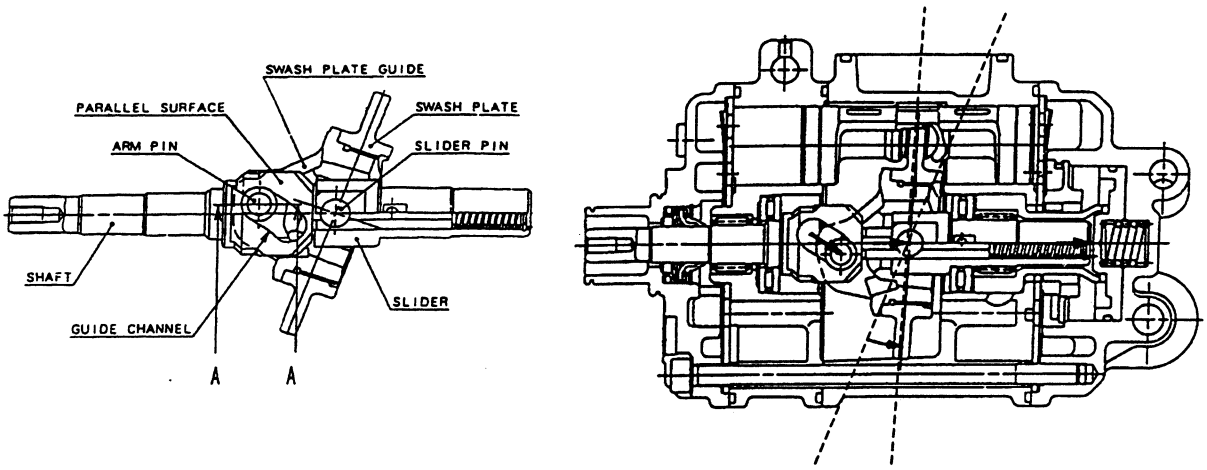

Figure 3.4. Variable Displacement Compressor Using Variable Swash Plate Angle (9)

3.2.5 Variable Capacity Scroll

This is the analog to the variable displacement reciprocating compressor. The variable capacity scroll compressor basically has an adjustable inlet/outlet volume ratio. The machine accomplishes this task by 'moving' the suction port along the spiral path used to compress the refrigerant, as shown in Figure 3.5. Since the trapping of the gas will happen later in the process, the volume ratio of beginning to end will change.

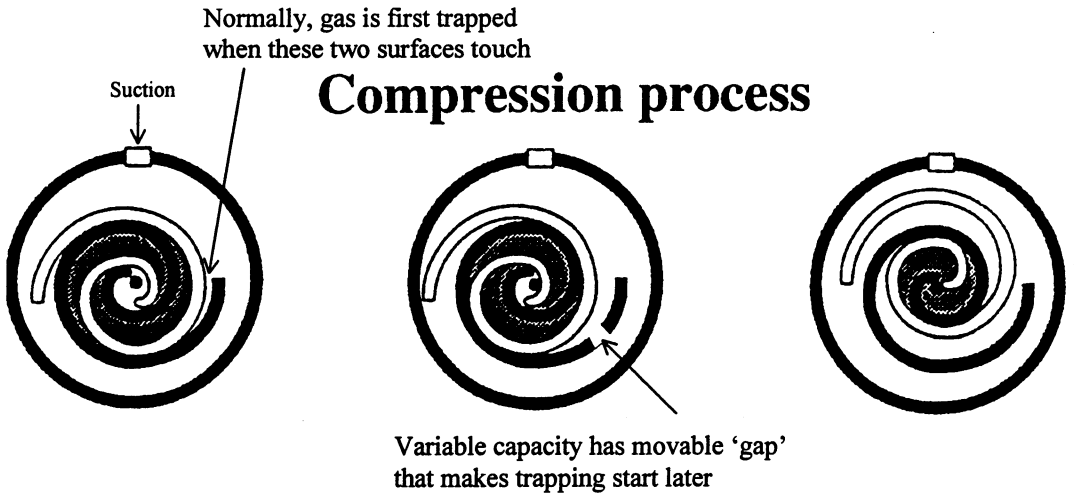

Figure 3.5. Schematic of Variable Capacity Scroll

4 Test Facility and Procedure

For a detailed explanation of the experimental apparatus and procedures, see (10), (11), (12). In addition to the test procedures described there, special considerations were necessary to operate the system in cycling mode. The fundamental difficulty is that during cycling, system parameters are changing much more rapidly than the sampling rate of the data acquisition system could capture. Therefore, it was necessary to speed up the data acquisition system to capture the dynamics of the A/C system. The main purpose of the increased sampling rate was to be able to calculate compressor power more accurately. Initially, this was done by reducing the number of data channels from 80 to 6. These six channels were only the most important parameters such as time, compressor torque, compressor speed, refrigerant mass flow rate, and inlet and exit air temperatures across the evaporator. This reduced the sampling time from 6 sec. per sample to approximately 0.3 sec. per sample. This speed was deemed reasonable to capture the dynamics of the A/C system, see Figure 4.1. A 10 minute data set sampled at 0.3 sec per sample was used to calculate compressor power. Typical cycle times for the mobile system ranged from 10 sec to 60 sec, thus anywhere from 10 to 60 cycles were captured this way. The system capacities were still calculated using the 6 second sampling rate over a 10 minute total period. This was possible because the energy balance methods used to find the system capacity, as described in (10), had very slow dynamics, especially in the case of the chamber energy balance.

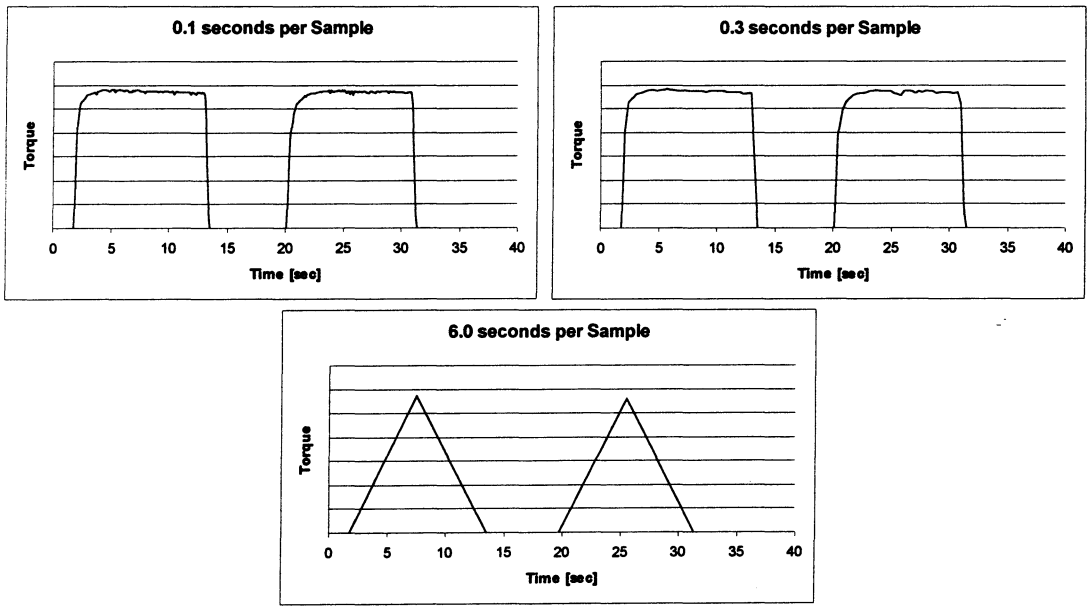

Figure 4.1. Torque Signal Sampled at Various Sampling Rates

Although this method was sufficient for calculating system parameters, it did not give a very good insight into what was happening elsewhere in the system. After further investigation, it was discovered that the equipment was actually capable of sampling much faster, if the technique was modified. The modified technique consisted of storing all of the raw voltage data in the onboard memory in the data acquisition system, then downloading all of the numbers in memory to a Microsoft Excel sheet and post-processing all of the voltages to get readings of pressures, temperatures, flow rates, etc. Drawbacks to using this technique are that each data set consumes a large amount of resources and the operator does not get real-time feedback about what is going on in the system. Therefore, usually only 1 or 2 complete cycles were captured in order to keep the data sets to a reasonable size. Again, these very fast sampled data sets were used only for visualization of what was happening in the system. Therefore, it was not really necessary to capture 10 minutes worth of data, as in the data sets used to calculate system capacities and compressor power.

Two different controllers were used to cause the system to cycle. In the case of the R134a system, the factory-installed switch on the suction accumulator served as the controller. The switch was of mechanical type and caused the circuit to open (disengage the clutch) when pressure dropped below 2.52-2.59 bar and caused the circuit to close above a pressure of 3.69-4.17 bar (absolute). These pressure ranges correspond to saturation temperatures of –3.7°C and 9°C.

For cycling the R744 system, a prototype controller was constructed to mimic the design of the pressure switch on the suction accumulator used in the R134a system. This controller used the signal from an electronic pressure transducer as the control variable. The upper and lower limits of the controller were set to match the saturation pressures of R744 at the same saturation temperatures as used in the R134a system. This corresponded to 31.5 bar as the lower limit and 43.9 bar as the upper limit. When this controller was installed in the system, it was found that this control strategy did not work. The pressure in the low side of the system did not rise rapidly enough and the clutch did not engage within a reasonable amount of time. Another control strategy was needed.

The next attempt was to use the temperature of the air exiting the evaporator as the control variable. The exit thermocouple was attached to a Red Lion model TCU10000 Temperature Control Unit. This unit was fully digital and the user could adjust the upper and

lower limits with a resolution of 0.1°C. It was found that this controller allowed the R744 system to mimic the behavior of the R134a system, important during preliminary R744 testing. This was the controller used to cycle the R744 system in all of the test data presented here.

After the data was collected, it was processed using software written in-house. The data sets used to calculate these parameters were approximately 10 minutes long, which yielded anywhere from 10 to 60 cycles to analyze. This software would analyze the data and output, among other items, an average compressor power. The software was also able to keep track of total time the compressor was engaged or disengaged, thus giving compressor on-time percentages. The software was written so as to discard any partial cycles that were at the beginning or the end of the data set. See Figure 4.2 for a graphical representation of the analysis technique.

The most important parameter, average compressor power was calculated by multiplying the instantaneous torque measurement by the instantaneous speed measurement, giving instantaneous power. Then, this power number was integrated with respect to time using the trapezoidal method. This generated a total energy usage for the compressor. When this total energy was divided by the total time over the analysis period, this yielded average compressor power. The shaded region represents the portion of the data set that was integrated using the trapezoidal method. The ends of the data set shown would be discarded because they are not complete cycles.

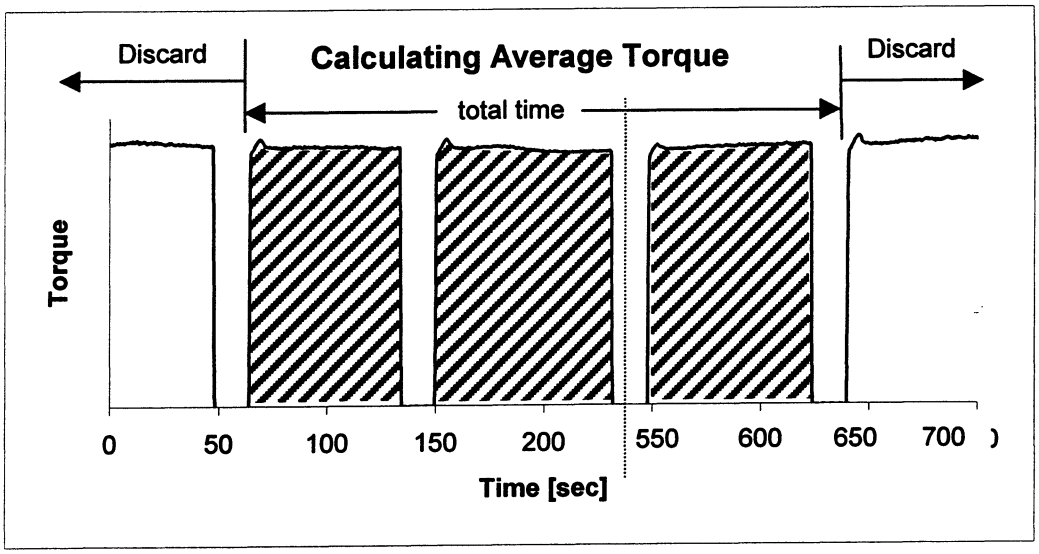

Figure 4.2. Computation of Average Compressor Torque

5 Modeling of Transcritical R744 System

5.1 Cycle Description

The behavior of the transcritical refrigeration cycle is quite different than the conventional, subcritical cycle. The major difference between the transcritical and subcritical cycles is high-pressure side operation. In the transcritical cycle, the traditional condensing process is replaced by a single phase supercritical heat rejection. That is, the working fluid is not saturated, so the temperature and pressure are not linked. Also contrary to operation in subcritical mode, as the high side pressure is raised, the coefficient of performance (COP) of the transcritical system may increase or decrease. It has been found that there is a high side pressure that will yield a maximum, or peak, COP for each set of operating conditions. This pressure at which maximum COP occurs is not constant, but is a function of operating conditions, and was observed as early as the end of the 19th century, when CO_2 systems were used in marine applications. (2) Thus, knowledge of how the system behaves with varying high side pressure is necessary if one wants to operate the transcritical cycle at close to maximum COP across a wide range of operating conditions.

In Inokuty (13), the basic thermodynamic relation describing the pressure corresponding to the maximum COP is shown to be: $-\partial H/\partial P$ along isotherm at gas cooler exit = COP * $\partial H/\partial P$ along the compression isentrope. This relationship is defined for the ideal cycle with no internal heat exchanger. If we reshape that relation somewhat to include an internal heat exchanger, we find that the maximum COP occurs when (ΔQ / Q = ΔW / W), or when the percentage increase in capacity is equal to the percentage increase in work. See Figure 5.1.

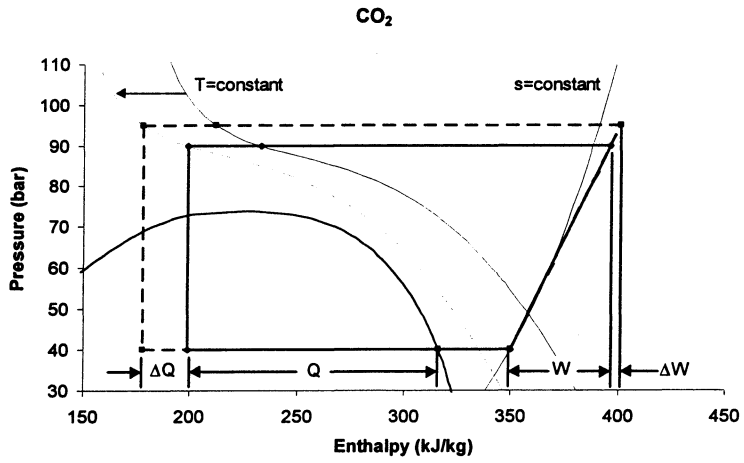

Figure 5.1. P-H Diagram With Incremental Increases in Work and Capacity

5.2 Sensitivity Model Construction

A model of this system was created using EES software linked to REFPROP 5, which provided the CO_2 properties. The model was constructed semi-empirically, that is, some observations about the way the prototype system behaved, as well as some of the numbers describing the prototype system were input into the model. The purpose of constructing this model was to provide insights on how sensitive certain types of system behavior are to various changes, which is especially useful in constructing control strategies. The most important output from the model was COP. However, it was not necessarily the magnitude that was of interest, but how COP varied as compressor discharge pressure was varied. The inputs to the model were evaporating temperature, high side pressure, overall heat transfer coefficient for the suction line heat exchanger, and gas cooler refrigerant exit temperature. The intermediate parameters consisted of refrigerant state points around the loop, as well as refrigerant mass flow. The output parameters were Q and COP. The information flow is represented graphically in Figure 5.2.

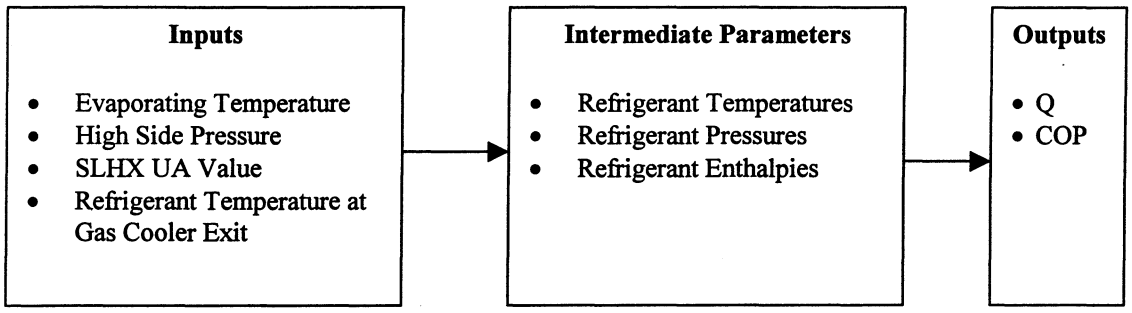

Figure 5.2. Information Flow in Maximum COP Model

The compressor is one component whose values are determined empirically from the data gathered from the prototype system, as described in (11). The two parameters that are input into the model are isentropic efficiency (η_i) and volumetric efficiency (η_v). These two parameters are treated as a function of pressure ratio, the ratio of compressor discharge pressure to compressor suction pressure.

The gas cooler did not need to be modeled in this simulation. The condition at the inlet of the gas cooler was assumed to be the same as the exit of the compressor. The condition at the outlet of the gas cooler was fixed by inputs into the model. That is, the compressor discharge pressure was assumed to be the pressure for the entire high side of the system, and the refrigerant

temperature out of the gas cooler, T_{cro}, was an input into the model. This could be done because the goal of the model was to develop a relationship between the refrigerant temperature exiting the gas cooler and the high side pressure at maximum COP.

The internal, or suction line heat exchanger (SLHX) was modeled as a cocurrent flow heat exchanger. This was because most of the data collected for the system was taken using this flow orientation through the SLHX. An overall heat transfer coefficient was assumed for the SLHX, and it was divided into 5 parts. In each part of the heat exchanger, the arithmetic mean temperature between the inlet and outlet for each side was used to calculate the refrigerant properties. Also, the arithmetic mean temperature difference between the low side and high side of the heat exchanger was used as the driving potential for the heat transfer. A schematic is shown in Figure 5.3. These assumptions could be made because it was also assumed that there was never any two phase refrigerant in either side of the heat exchanger. This is based on observation of the real system which showed that the high side refrigerant was always single phase (supercritical), and the low side refrigerant generally entered with a quality of 0.98 to 1.00. Finally, the overall heat transfer coefficient for the SLHX was an input parameter, and was varied. For a more detailed description of the heat exchanger used in the prototype R744 system, see (11), (14).

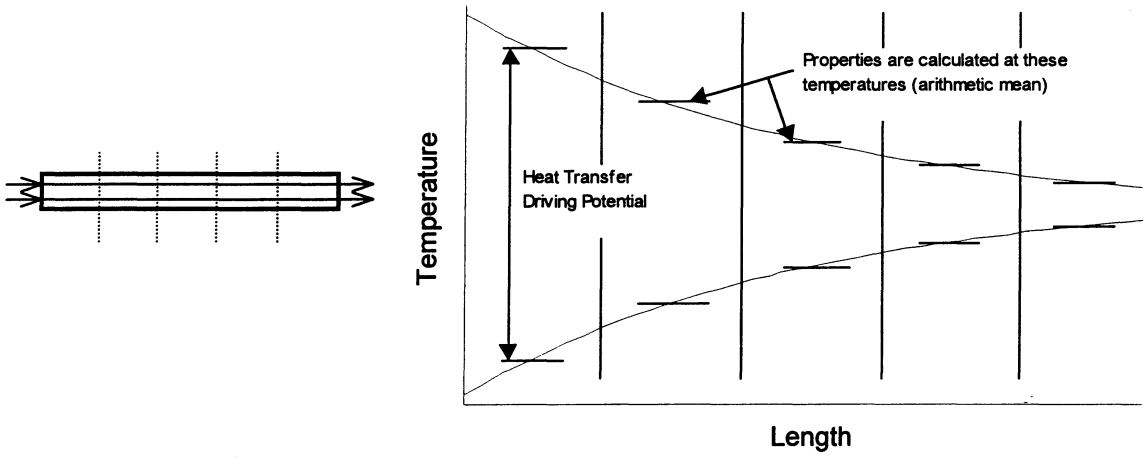

Figure 5.3. SLHX Schematic used in Maximum COP Model

The evaporator also did not need to be modeled in this simulation. The entrance condition for the evaporator was determined by an isenthalpic process from the high side exit of the SLHX, down to the pressure corresponding to the evaporation temperature (an input to the

model). The refrigerant exiting the evaporator was assumed to be of quality 1.0 for all conditions, based on the observation in the real system that the exit quality was generally between 0.95 and 0.98. The reason this occurs is that the only location that liquid is stored in this system is in the suction accumulator, unlike a conventional R134a system. In a subcritical system, the condensing pressure is a function of the condenser drainage. Liquid accumulated in the condenser reduces condensing area and thus increases the pressure. In contrast, the R744 system has only supercritical vapor in the high side. So, if the evaporator was unable to evaporate all of the refrigerant, the remaining liquid would go to the suction accumulator and would be trapped there. It is possible that the 2 to 5% difference between the exit condition and saturated vapor is due to the liquid that is put back into the suction line from the suction accumulator. Finally, no pressure drop was assumed through the evaporator, or through any other components in the model, except the expansion device.

6 Influence of Selected Parameters on System Performance

Before investigating the influences of operating conditions and components on the system behavior, it is first necessary to have a good understanding of the importance of the high side pressure, as introduced earlier in this text. In Figure 6.1, test data is presented for a single operating condition for a range of high side pressures. This figure shows data that are representative of most operating conditions. That is, one can observe that as the discharge pressure is increased, the cooling capacity begins to increase, then saturates. The COP begins to increase, reaches a peak, then decreases. Finally, it is seen that the compressor power increases linearly as discharge pressure is increased. These behaviors are also seen in Figure 6.2, which plots the cycles for the points labeled 'a', 'b', and 'c' in Figure 6.1. These cycles show the same behaviors as explained in the text in chapter 5.

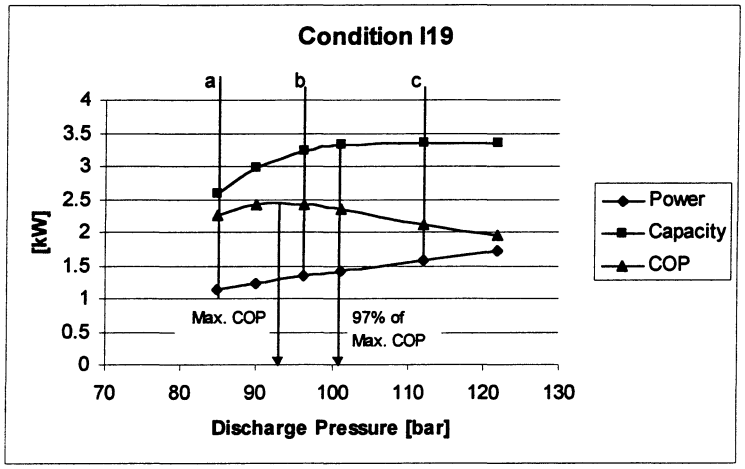

Figure 6.1. System Behavior as High Side Pressure is Varied

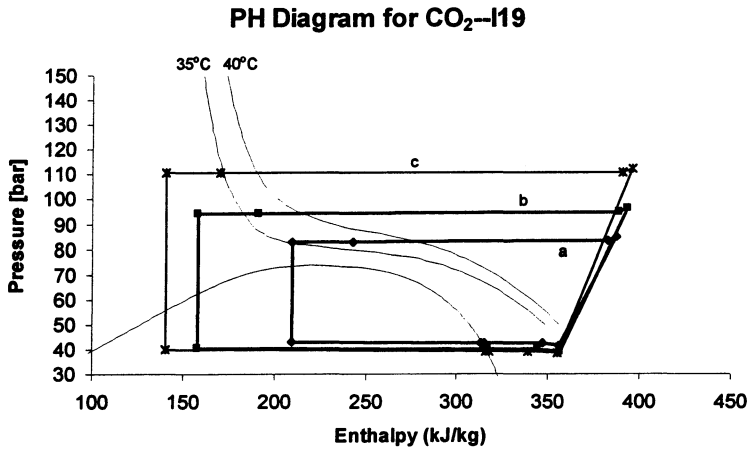

Figure 6.2. Cycles for Selected Operating Conditions

In Park (15), data is presented that shows the influence of external operating conditions such as air inlet temperatures and flow rates over both heat exchangers on system COP and capacity. Rather than do the same type of analysis, this study is more focused on system behavior as determined by refrigerant side conditions. For example, increasing either the airflow rate over the evaporator or the air inlet temperature to the evaporator would be an example of changing an external operating condition. The effect of either of these would be to increase the evaporating temperature. Thus, this study would consider the effects of system behavior due to a change in evaporating temperature as compared to separate studies of changing evaporator airflow rates and inlet temperatures. This also has the advantage of removing most of the details of the heat exchanger designs since those designs have a great impact on what happens to the refrigerant as it passes through.

6.1 Gas Cooler Refrigerant Exit Temperature

Perhaps the most influential parameter on the COP maximizing high side pressure is the refrigerant temperature exiting the gas cooler, T_{cro}. In relating to operating parameters, this single temperature would at least capture the effects of the air temperature and flow rate entering the gas cooler, and the gas cooler design. This point deserves some discussion, especially as to why this parameter, and not the condition at the exit of the high side of the suction line heat exchanger, is the most indicative.

In (15), the effects of many of the operating parameters were shown on the value of COP maximizing high side pressure. If one were to look at the cycle (Figure 6.3), it is seen that it is the condition at the exit of the high side of the SLHX (labeled 4) that determines the quality at the inlet of the evaporator. Therefore, at first it seems that maybe this could be the most important parameter, not T_{cro}. However, upon further investigation, it is seen that the temperature at the exit of the SLHX is a function not only of the heat exchanger design, heat transfer coefficient, and inlet temperature, but it is also a function of the evaporating temperature. Since in this study it will be shown that the evaporating temperature does not play a large part in changing the COP maximizing high side pressure, using the exit temperature may introduce effects that should not be included. This is apparent when considering the scenarios shown in Table 6.4. First, the model was run with a gas cooler exit temperature of 37°C and an evaporating temperature of 3°C. The model showed that the pressure for maximum COP was

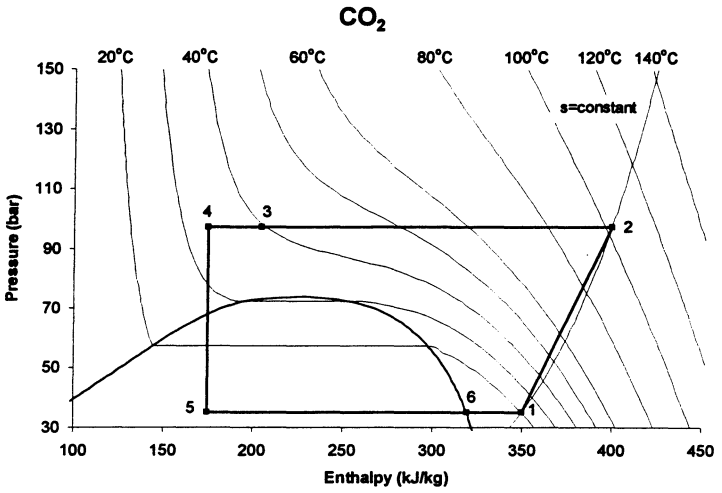

Figure 6.3. Transcritical R744 Vapor Compression Cycle on P-H Coordinates

around 90.5 bar and the SLHX exit temperature is 32.9°C. Next, a scenario with a gas cooler exit temperature of 35°C was run with an evaporating temperature of 9°C. The maximum COP high side pressure was 85.5 bar, but the SLHX exit temperature for this case was also 32.9°C. Therefore, if one were developing a relationship for a controller to locate the COP maximizing high side pressure, this parameter is not a wise choice because of non-uniqueness.

Table 6.4. Model Results Showing Non-Uniqueness of SLHX Exit Temperatures

T_{cro} [°C]	Evaporating Temperature [°C]	Pressure @ max COP [bar]	SLHX Exit Temperature [°C]
37.0	3.0	90.5	32.9
35.0	9.0	85.5	32.9

The effects of changing T_{cro} are shown in Figure 6.5. The two figures shown represent model predictions and actual test data for a range of T_{cro}. There are two items of importance shown in each of these two figures. First, as T_{cro} is increased, the corresponding COP maximizing high side pressure also increases. Second, as T_{cro} is increased, the COP curves tend to flatten out and the maxima become less well-defined.

6.2 Effect of SLHX

This effect would capture changing either the SLHX size (as was done in the experimental work presented here), or design, or both. The model was run for several gas cooler

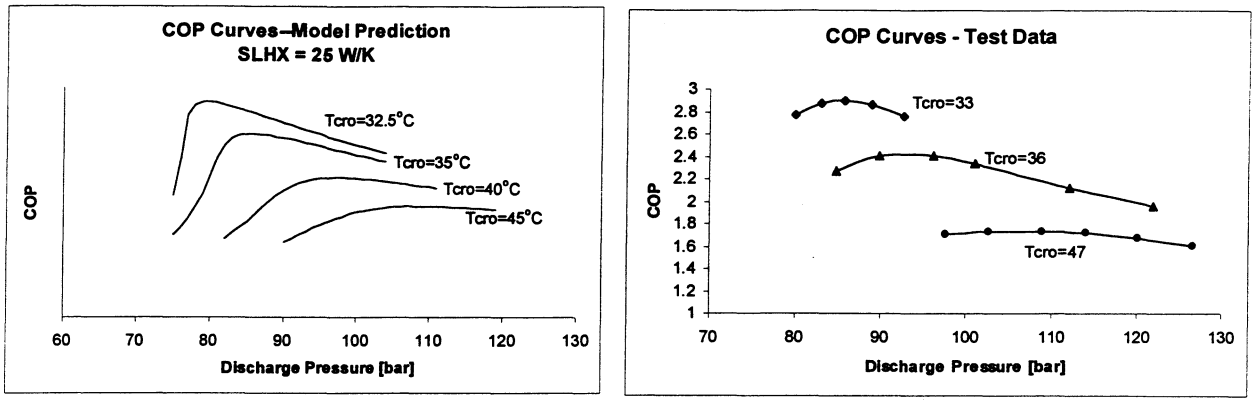

Figure 6.5. Effect of Changing Gas Cooler Exit Temperature on COP Curves

refrigerant exit temperatures with an evaporating temperature of 5°C. A range of SLHX overall heat transfer coefficients (UA value) from 0 (no SLHX) to 25 W/K was used. This upper value is in the range of 15-36 W/K that was observed in the test data. Table 6.6 shows the COP maximizing high side pressure as a function of SLHX UA value for these model runs. It is seen that there is a larger difference between the values of the COP maximizing pressure for the 0 and 5 W/K values than there is for the range from 5 to 25 W/K. This seems to suggest that the change in the value of COP maximizing high side pressure occurs even when a very small SLHX is added, but the effect begins to decrease from there. The model predictions are verified by looking at the test data presented in Figure 6.7. It is seen that there are two groups of locations for the COP maximizing high side pressure. One group contains the data taken with the various length SLHXs installed, and the second 'group' is the single curve that shows no SLHX. The numbers on the figure represent the approximate range of UA values for each actual SLHX.

Table 6.6 Model Predicted COP Maximizing High Side Pressure for Different SLHXs

SLHX UA Tcro [oC]	0 (no SLHX)	5 W/K	25 W/K
32.5	81 [bar]	80	80
35	87	86	86
40	101	99	97
45	116	110	107
50	132	123	119

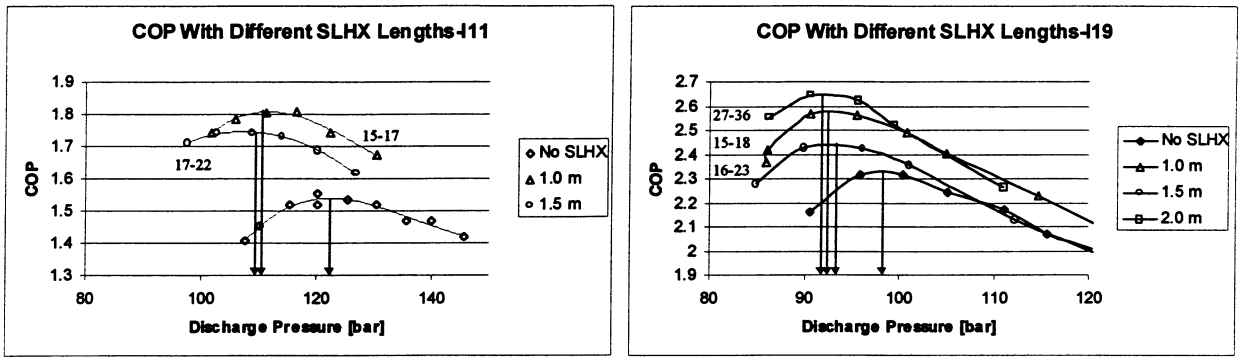

*numbers denote UA value range in W/K

Figure 6.7. Real Effect of Changing SLHX Heat Transfer Coefficient

What was observed is that this large range of values for the SLHX heat transfer did not have a great impact on the system behavior, at least in the behaviors that were the study of this work. This fact was also verified with actual test data, Figure 6.7. The explanation for this phenomenon is the following: since the evaporation temperature was assumed to be constant as the pressure was varied, and T_{cro} was held constant while the pressure was varied, the specific enthalpy change over the SLHX does not vary much. On the PH diagram (Figure 6.3), this means that the length of line 3-4 does not change with a variation in high side pressure. Therefore, since the length of the line is fixed, and we follow the isotherm with point 3, it is really the slope of that isotherm that determines the behavior at the exit of the SLHX. Since the evaporator in the real system always evaporated to a quality of around 0.98, the specific capacity only depends on the enthalpy at the evaporator entrance, which is the enthalpy at the SLHX outlet, which is a constant offset from the gas cooler outlet condition. Looking at the compression process shown in the p-h diagram, the effect of the amount of heat transfer in the SLHX is to determine the compressor inlet condition. Looking at the two sensitivity curves shown in Figure 6.8, we see that the (ΔW / W) curve is the same for both cases while the (ΔQ / Q) curve shifts left with an increase in SLHX heat transfer. This causes the intersection to be at a lower pressure.

There are two ways to get an increase in the (ΔQ / Q) term. Either the ΔQ term can be increased, or the Q term can be decreased. Note that by going to lower pressures, both occur at the same time. Looking at the slopes of the isotherms (Figure 6.3), we see that at lower values of T_{cro}, the change in slope is quite pronounced and the slope itself is such that the ΔQ term is quite

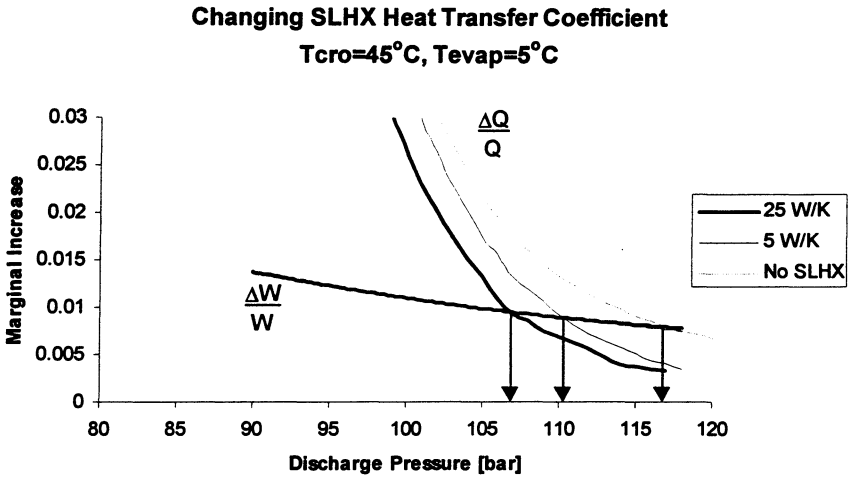

Figure 6.8. Sensitivity Curves for a Change in SLHX Heat Transfer

sensitive to pressure change around the pressures that correspond to the maximum COPs. That is why the pressure corresponding to maximum COP does not change much at lower values of T_{cro}.

However, when looking at the isotherms of higher values of T_{cro}, it is seen that they are becoming more linear and vertical around the pressures corresponding to maximum COPs. Therefore, a greater change in pressure is necessary at these higher temperatures, as compared to the lower values of T_{cro}, to get the same value for (ΔQ / Q). In this case, the reduction of Q plays a more important role in the increase of the overall term.

6.3 Effect of Evaporation Temperature

In order to capture the effects of changing conditions such as different airflow rates, temperatures, humidities, and designs, the evaporation temperature was changed over a wide range from 5°C to 20°C. This is a very extreme range for an automotive A/C application. The effects seen are shown in Figure 6.9, along with the results from the SLHX variation. The lines for the locations of the maximum COP are quite close. The change is almost insignificant when it is realized that the shaded region represents a region in which the system operates at greater than 97% of its maximum COP (for the baseline configuration). If we attempt the same analysis as described in the previous section, shown in Figure 6.10, we see that the actual values for the (ΔQ / Q) and (ΔW / W) terms change, but the high side pressure for maximum COP, (the intersection of the curves) does not move much.

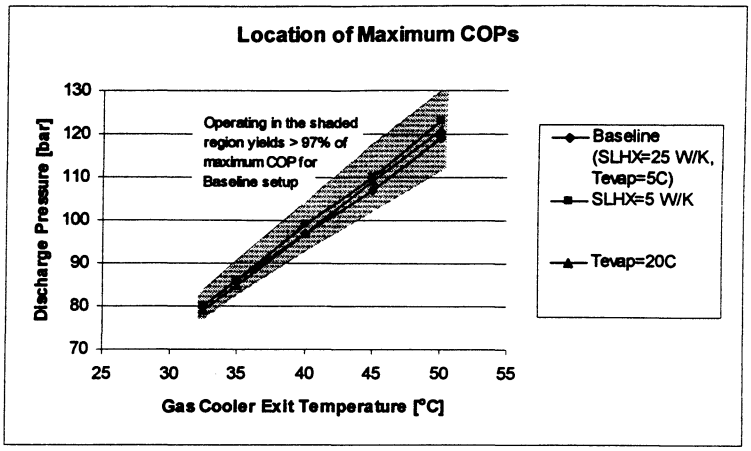

Figure 6.9. Discharge Pressure for Maximum COP for Varying Assumptions

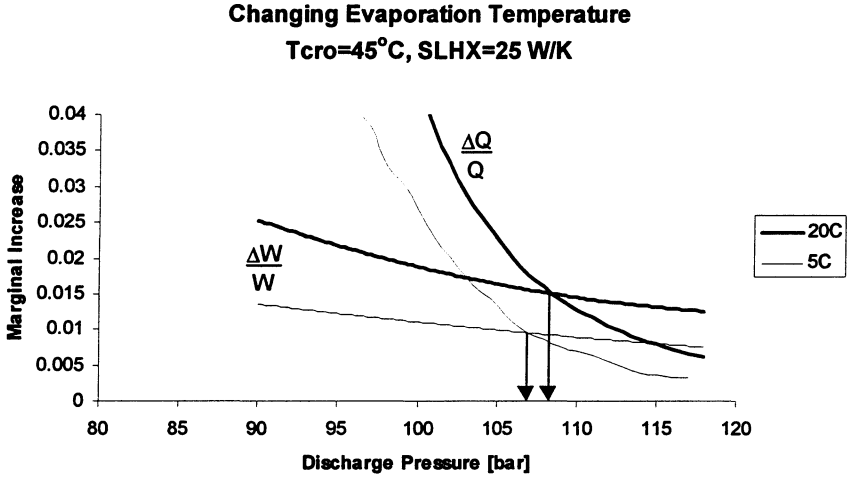

Figure 6.10. Sensitivity Curves for a Change in Evaporation Temperature

6.4 Effect of Compressor Efficiency

The next effect studied was that of compressor efficiency. This parameter is related to different compressor designs as well as different compressor speeds. For this set of model runs, two different compressor efficiency curves were used. These curves come from the experimental data presented in (11). Recalling that the maximum COP occurs when ($\Delta Q / Q = \Delta W / W$), changing the compressor efficiency should change the ($\Delta W / W$) term, thus causing a different pressure for the maximum COP.

From trigonometry it can be found that as the line for the compressor work slopes away from vertical (decreasing compressor efficiency), the term ($\Delta W / W$) increases. Therefore, the

(ΔQ / Q) term also needs to increase. From the discussion presented in the SLHX section, this would occur at lower high side pressures. The opposite would be true for increasing compressor efficiency. However, the magnitudes of these changes are of importance.

The model results for changing the compressor efficiency are shown in Figure 6.11. There are actually two sets of curves for each term, but neither the (ΔW / W) nor the (ΔQ / Q) terms change enough to make a difference in the location of the intersection.

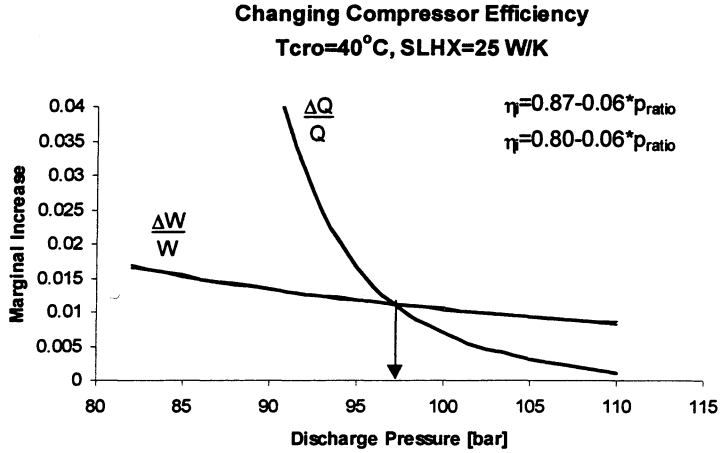

Figure 6.11. Sensitivity Curves for a Change in Compressor Efficiency

6.5 Summary of Steady Refrigerant Flow Operation

Several parameters have been studied for their influence on the value of the COP maximizing high side pressure. Figure 6.12 shows the model prediction for the baseline case, along with actual system data taken over a wide range of conditions. It is seen that this model works quite well in predicting the location for maximum COP pressure for steady refrigerant flow conditions.

6.6 Operation Near Critical Point

Since the critical temperature of CO_2 is near 32°C, it stands to reason that for some operating conditions, the system can be run in either transcritical or subcritical mode. In subcritical mode, the gas cooler would function as a condenser. Tests were performed at conditions that allowed for either subcritical or transcritical operation to see if one mode was superior to the other.

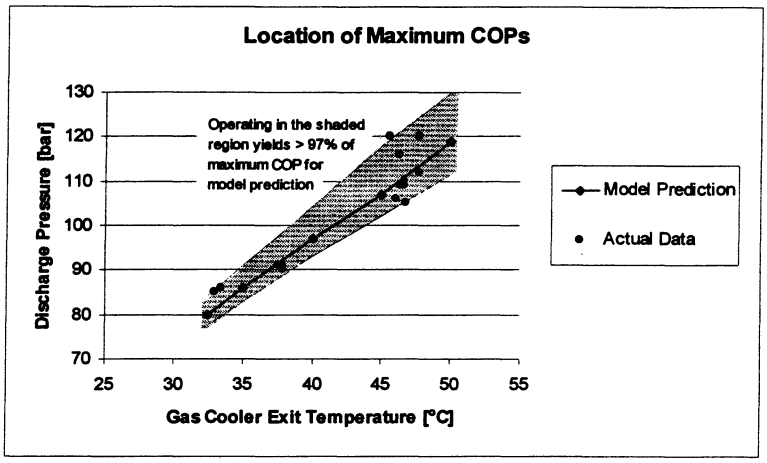

Figure 6.12. Model Predictions and Actual Data

Test data for the two conditions is shown in Figure 6.13. In both cases, it is seen that there is a sharp decrease in both COP and capacity once operation is taken from transcritical to subcritical. This seems to suggest that for this system, transcritical operation is the preferred mode, even when conditions permit subcritical operation.

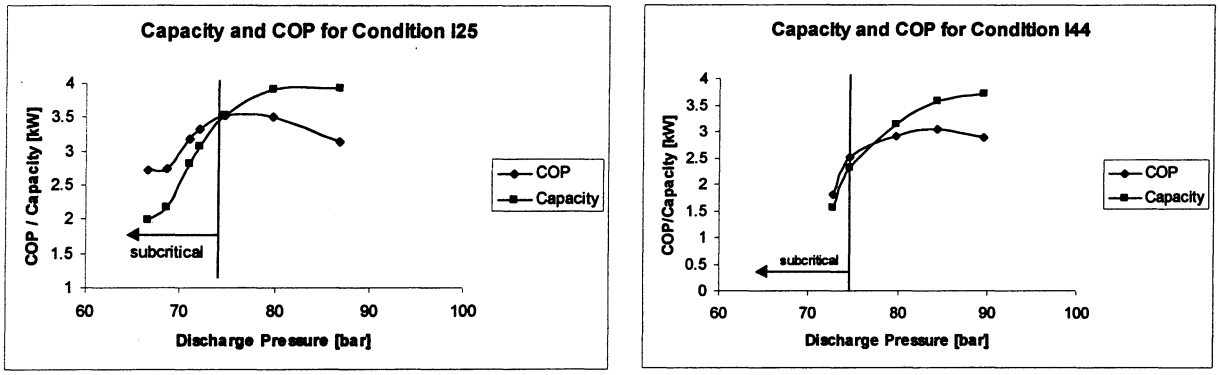

Figure 6.13. Transition from Transcritical to Subcritical High Side Pressure Operation

7 Cycling Operation of Transcritical R744 and Subcritical R134a Systems

There is an ongoing debate about methods used to control compressor capacity. There are three candidates: speed reduction, variable displacement compressors and clutch cycling. Speed control could be realized either by some mechanical speed reducer, or by use of an electrical motor. An electrical motor would be an excellent option from a control standpoint, but would require major changes in the vehicle's electrical generation and supply system. This idea would be feasible if the proposed switch to a 42V electrical system would be accepted.
In the mind of many experts that are currently creating R744 systems, using a variable displacement compressor is the dominant option. The reasons are numerous, but among the most important is the concern about the impact of clutch cycling on smooth driveability of cars with small engines.

The dominant control strategy in subcritical R134a systems is clutch cycling, not because of its technical advantages, but predominantly for economic reasons.

In this chapter, the results of the test runs using clutch cycling for a prototype transcritical R744 system with a fixed displacement compressor and a R134a system that uses clutch cycling with a fixed area expansion device will be presented. Both systems were operated over a wide range of conditions. The complete test matrix, as well as tables of results can be found in Appendix A.

7.1 System Operation

As stated in chapter 4, the sensor that caused the R134a system to cycle was a pressure switch placed on the suction accumulator. During the first experiments with R744, a similar, pressure-activated cycling control was tried, but did not work well. The decision was then made to cycle the R744 system based on the air temperature exiting the evaporator. This allowed the behavior of the R744 system to mimic the R134a system. Figure 7.1 is a graph that is representative for all conditions. It shows the air temperatures at the inlet and exit of the evaporator. It is seen that the inlet air temperature is well controlled to be constant. The outlet air temperature for the R744 system was then set at each condition a comparison wanted to be made to mimic the R134a system. As shown in Figure 7.1, using the air temperature as the control input allowed that to be done.

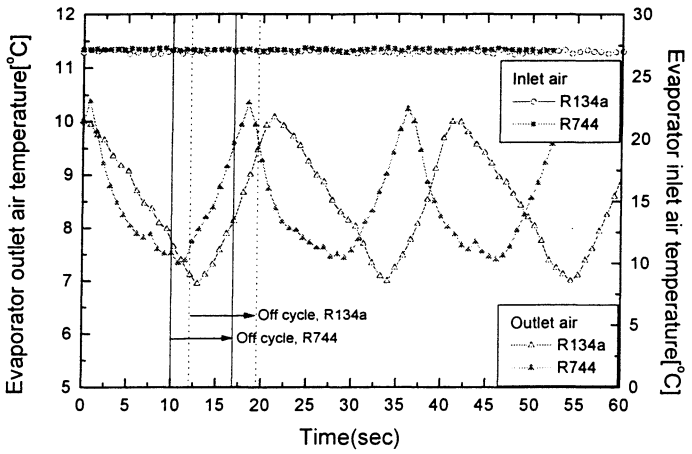

Figure 7.1. Indicators of the Similarity of Operation of the Two Systems (R744 and R134a)

7.2 Torque Behavior

This section will explore the behavior of the torque curves for cycling for all three setups (R744-manual valve, R744-needle valve, R134a). Figure 7.2 shows torque curves for the three setups for the same operating condition. It is important to note that the compressor speed is the same for all three curves shown here. If it were not the same, it would be the compressor power (torque and speed) that would be the important parameter to look at. One minor difference between the curves is that the data for both R744 curves was sampled at a faster rate (as can be seen by the small 'wiggles' in the data) than the R134a data (each dot is a data point). This explains why the torque curve at the end of the second on period for the R134a curve looks a bit different than the rest.

It is seen that the three different setups have quite different torque characteristics. For the R134a system, it is seen that the torque rises to its maximum value near the beginning of the cycle, then decreases to a steady value. For the R744 system with the backpressure valve, the curve is relatively smooth and holds steady throughout the on period. The torque for the R744 system with the needle valve rises throughout the on period of the cycle. Finally, in Table 7.3 it can be seen that these three distinct torque shapes produce nearly the same capacity and compressor power consumption.

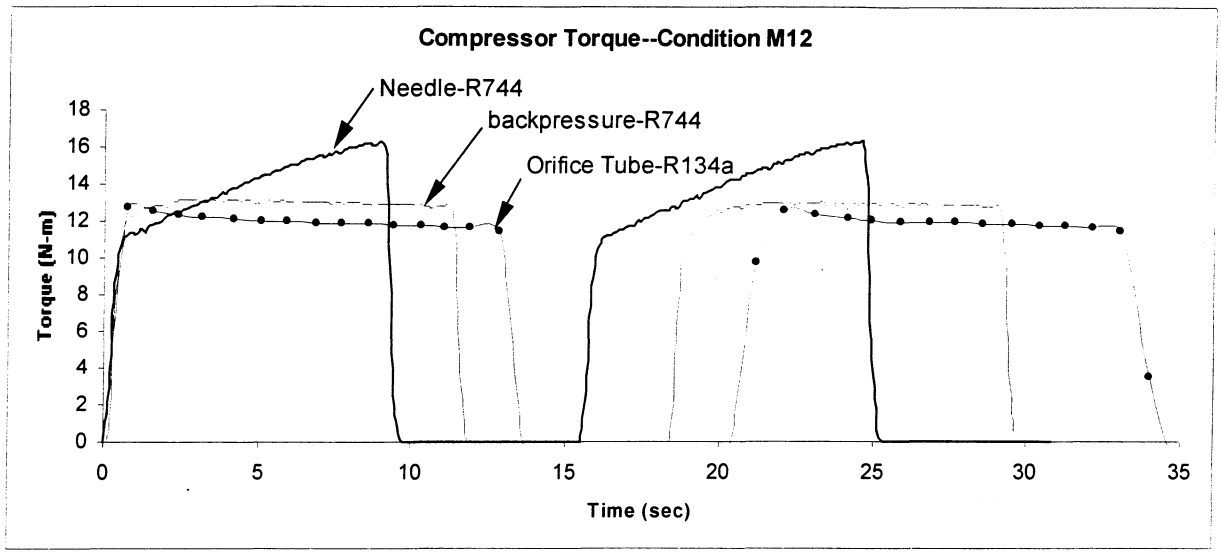

Figure 7.2. Torque on the Compressor Shaft for the Three Different Configurations

Table 7.3. Data for Condition M12

Test Condition	Average Power [kW]	Average Capacity [kW]	On Time [sec]	Off Time [sec]	COP
R744 Backpressure	1.45	2.62	11.6	5.2	1.80
R744 Needle	1.48	2.63	9.9	4.8	1.78
R134a	1.40	2.55	13.8	6.8	1.82

7.3 Refrigerant Flow Rate

Another system parameter that is significantly different among the three setups is the behavior of the refrigerant flow rate. Graphs are presented for each of the three setups showing refrigerant mass flow (mr), refrigerant pressures at the exit of the condenser (gas cooler) and evaporator, and the torques, each for the same condition as before, M12. The torques are provided to show whether the clutch is engaged or disengaged. Figure 7.4 shows the parameters for the R744 system with the backpressure valve. It can be seen that the mass flow does not exactly follow the torque curve. That is, there is a time delay between when the compressor engages and the mass flow rate comes up, as well as a delay between when the clutch disengages and the mass flow goes to zero (valve closed). It appears that the startup delay is longer than the shutoff delay. The startup delay is due to the time it takes for the compressor to build up the

pressure in the high side, as well as the valve design. The values of these delays are a function of the specific valve design used for this system.

Figure 7.5 shows the same parameters for the R744 system with a needle valve (fixed area). The mass flow behavior is quite different than the backpressure valve because the needle valve is always open, even during the off period. It is seen that the mass flow rate ranges from about 15 to 25 g/s for this valve while for the backpressure valve it ranges from 0 to 40 g/s. The flow rate for the needle valve is a function only of p_{cro} (for choked conditions) or p_{cro} and p_{ero} (for non-choked conditions).

The parameters for the R134a system are shown in Figure 7.6, however the mass flow rate is not shown. This is because the flow at the sensor was two phase and did not accurately display the average trends.

The system pressures also exhibit different behaviors for each setup. For the backpressure valve, it is seen that p_{cro} maintains a somewhat constant value over the on period, and bleeds off a little pressure during the off period. The majority of the bleeding that occurs during the off period would be through the compressor since the valve should be completely closed. However, for the R744 system with the needle valve, p_{cro} rises throughout the on period, and there is significant bleeding of pressure during the off period. In this case, most of the bleeding is through the open valve. The R134a system pressures exhibit different behavior than the other two. This is due to the differences in behavior of the flow through the expansion device, and the fact that the high side of the system contains liquid. Note that for the R744 setups, the torque and pressure shapes follow each other during the on period, while for the R134a system, they do not.

For the R744 systems, the high side pressure behavior is very important. It has been shown that there is a single value of high side pressure that gives the maximum COP for a given set of operating conditions during non-cycling operation. However, it will be shown later in this text that this result also holds for cycling mode. That means that for the system with the backpressure valve that operates mainly at one pressure, this pressure could be set to correspond to whatever pressure gives the maximum COP. However, for the needle valve, since the high side pressure varies over a wide range, the system will spend most of its time operating at a pressure which does not give the maximum COP.

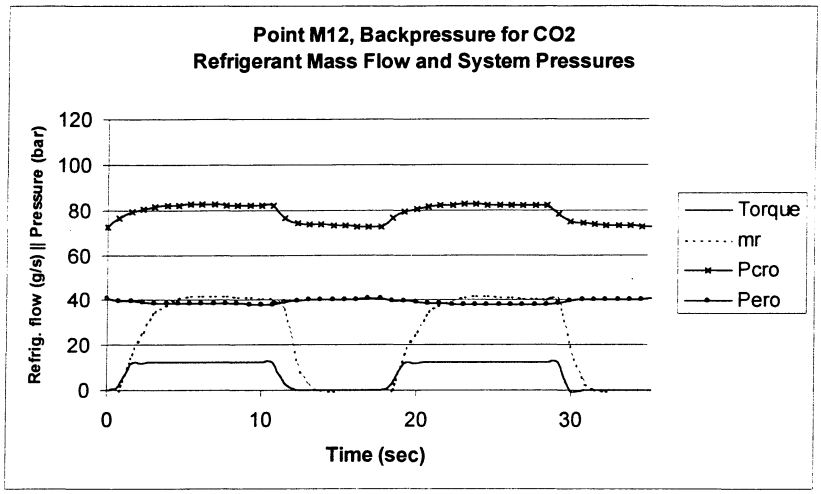

Figure 7.4. R744 System with Backpressure Valve

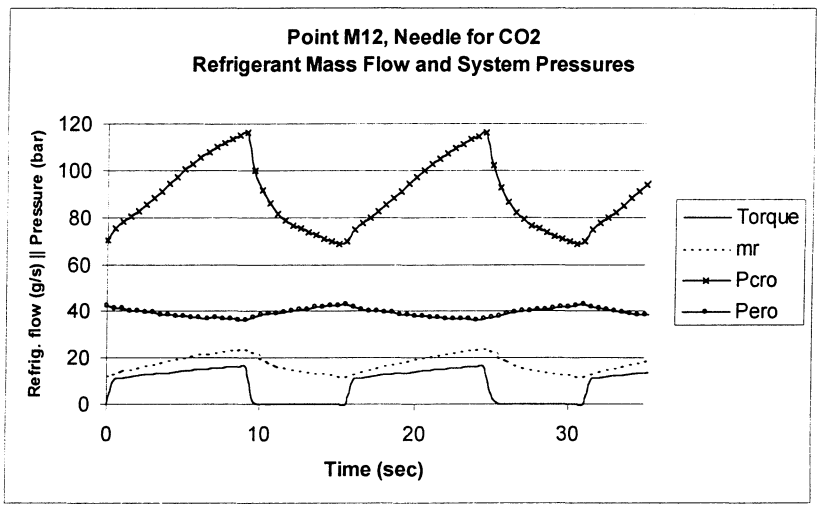

Figure 7.5. R744 System with Manual Needle Valve

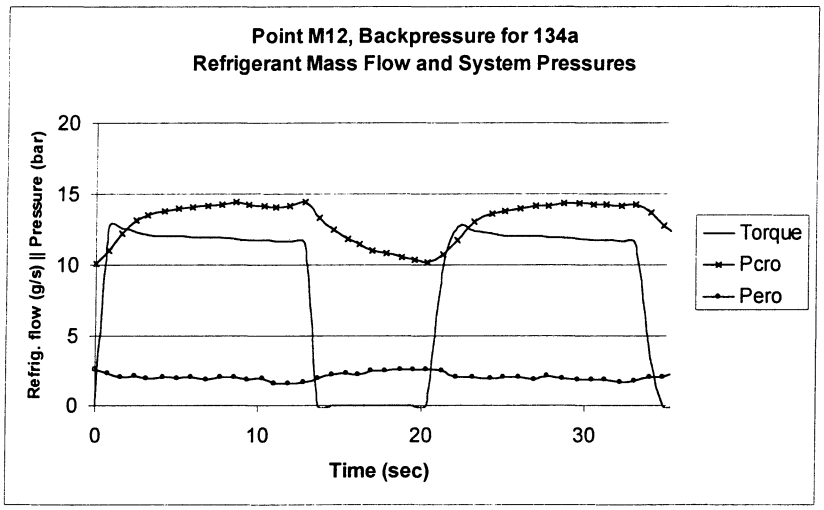

Figure 7.6. R134a System with Fixed Area Expansion Device

7.4 Evaporator Performance

This section will explore the differences in evaporator behavior for the three setups. This will be done by looking at the refrigerant temperatures entering and exiting the evaporator. The torque signal is shown in order to know if the compressor is engaged or not. Actually, the mass flow descriptions from the previous section have a great impact on what is happening to the evaporators. In the system with the backpressure valve, it is seen in Figure 7.7 that there is a large amount of superheat at the beginning of the on period, then two phase from the middle of the on period until the compressor is disengaged. This is due to the way the backpressure valve behaves, as described in the previous section. The valve remains somewhat closed until the high pressure side comes up to the setpoint value, then the valve is open as far as it is going to go. This has the effect of starving the evaporator during the first few moments of on-time operation.

Since the needle valve is open during the off period, the behavior shown in Figure 7.8 can be explained. There is sufficient refrigerant in the evaporator at the beginning of the on period to give two-phase operation. However, as the on time progresses, it is seen that there is not a good balance between what the evaporator requires and what it is being fed, and the outlet begins to superheat, and the amount of superheat grows as the on period continues.

The R134a behavior in Figure 7.9 shows the most balanced of the three. During the off period, it should behave somewhat like the needle valve in that the fixed area expansion device remains open, allowing refrigerant to flow from the high side to the low side. Also, during on time operation, it appears that the area of the expansion device is sufficient to provide enough refrigerant for the evaporator to operate at very low (or no) superheat during the entire on period.

These results might show that there is room for improvement in the way the refrigerant flow is controlled in the R744 system. That is, perhaps there is a better way to provide the proper amount of refrigerant to the evaporator. One option for doing this is to use an intermediate pressure receiver, rather than a low pressure receiver that was used for these two R744 setups.

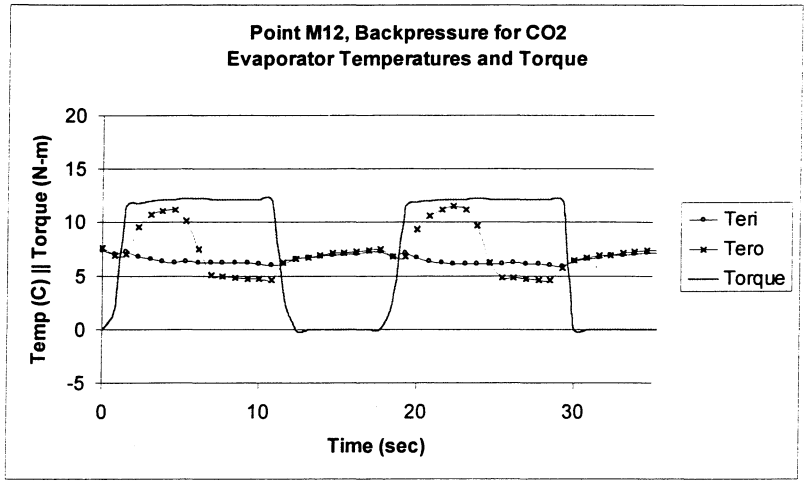

Figure 7.7. R744 System with Backpressure Valve - Indicators of the Evaporator Performance

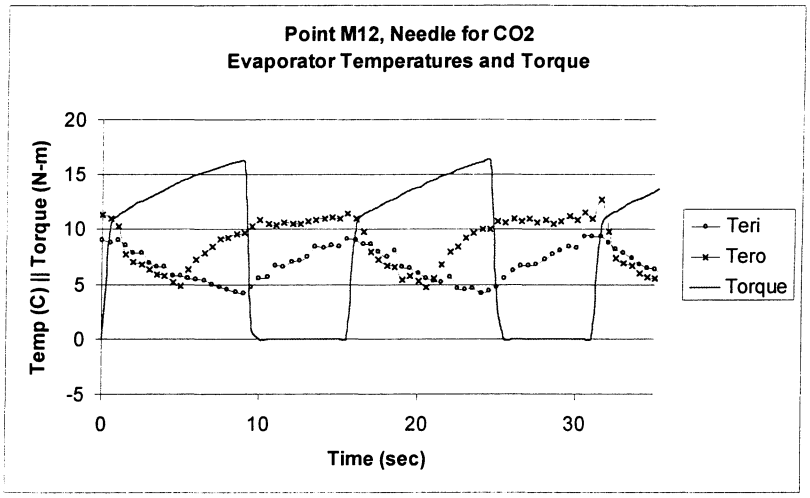

Figure 7.8. R744 System with Manual Needle Valve - Indicators of the Evaporator Performance

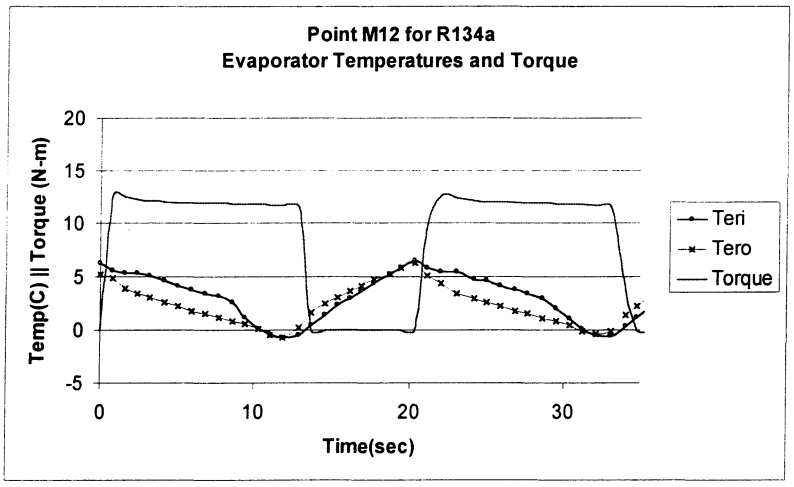

Figure 7.9. R134a System - Indicators of the Evaporator Performance

7.5 Influence of High Side Pressure on Cycling

The question of whether or not a maximum COP exists in transcritical cycling must be addressed. It must first be noted that the evaporator air outlet temperature was the variable used to decide whether or not the clutch was engaged. Thus, the cycling event was entirely evaporator driven. This means that if the lower temperature limit was held constant, along with air flow rate, the clutch will disengage when the evaporator surface reaches a certain low temperature. Likewise, if the upper temperature limit as to when the clutch is engaged is also kept constant, along with air flow rate, then the clutch will engage when the evaporator surface reaches a certain high temperature. Also keep in mind that the evaporator blower was running at all times whether or not the clutch was engaged, and the evaporator air inlet temperature was also constant. Therefore, for the evaporator to go from the low temperature to high temperature, it must absorb a certain fixed amount of energy. This energy is a function of the temperature differential and heat exchanger design, (Energy = m_{evap}* cp_{evap}* ΔT). The rate at which the evaporator warms up is a function of the thermal mass of the material, as well as the interactions with the refrigerant inside. If the interaction with the refrigerant is the same, and the assumptions above of what is constant are true, then one would expect that the rate at which the evaporator warms up should be constant. Since adjusting the high side pressure does not change any of these items that were assumed to be constant, the evaporator should warm up at the same rate with the same total energy exchange for a pressure setpoint change. Thus, the off cycle should be nearly identical for a range of high side pressure setpoints.

However, when the pressure setpoint is changed, the on cycle will change. Increasing the pressure setpoint will both increase refrigerating capacity (were the compressor not cycled off) and increase compressor power. This will have the effect of decreasing the on cycle time, due to the increase in refrigerating capacity, thus increasing the rate at which energy is removed from the evaporator. Again, to reach the low temperature, a certain fixed amount of energy must be removed from the evaporator. So, the compressor now will consume more power, but the on cycle will be shorter. Thus, this may increase or decrease the total energy consumption per cycle. All the while, the delivered cooling capacity should remain nearly constant. This suggests that maximum COP in cycling should be the point at which maximum COP occurs during the on cycle portion. We already know that for any set of conditions there is a pressure which gives the maximum COP, but as conditions change, so does the pressure to give maximum

COP. Therefore, it is necessary to examine the range of fluctuation of the parameters during cycling. Figures 7.10 and 7.11 show T_{cro}, as well as compressor torque and refrigerant mass flow rates as a function of time for two different high side pressures. The higher value of the pressure (in the on period) represents the setting of the back pressure valve. The lower value (in the off period) is a function of the valve design. The time for the pressure change indicates the leakage rate through the valve and the compressor.

The shape of the torque graph during the engagement period is almost identical. The major difference is the length of the on period. The shorter on periods at higher pressures indicate higher capacities during the on period. The off periods are almost unchanged – the heating of the system is independent of the cooling rate. Please note that the total, average capacity is almost identical.

It can also be seen that T_{cro} varies in approximately a 1°C band during the on time, with an average on time value of approximately 45.2-45.5°C for both tests. From the model prediction, this would correspond to an optimum high side pressure of approximately 107 bar. Table 7.12 shows the results for tests at this condition with varying high side pressure setpoints. It is seen that the highest COP occurs somewhere around 105-110 bars, in good agreement with the non-cycling model (Figure 6.12). Also note that the table shows that the off time of the cycle remains approximately constant, as described above.

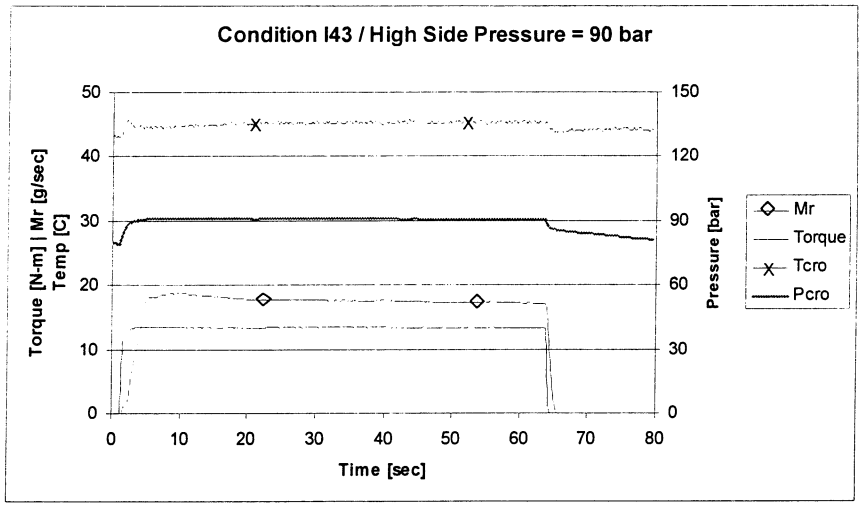

Figure 7.10. R744 System Performance at I43 at 90 bar

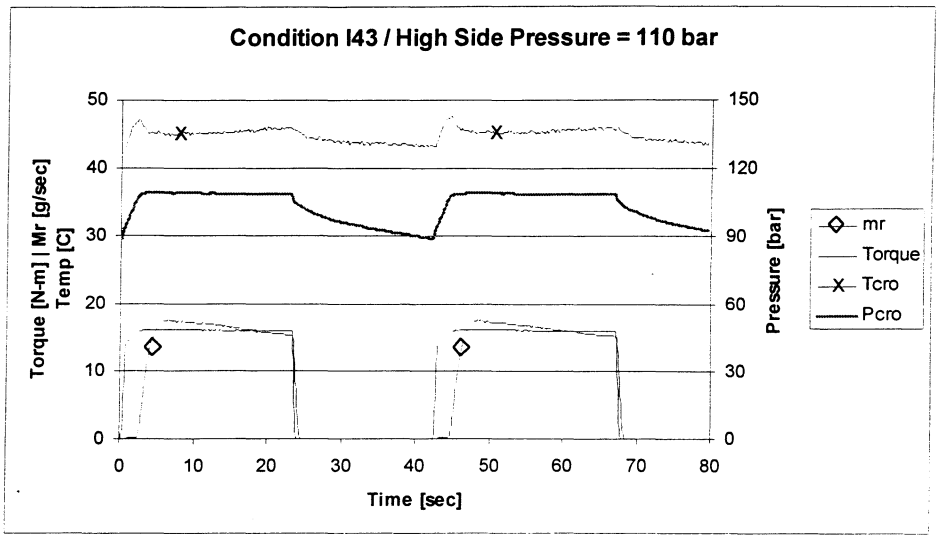

Figure 7.11. R744 System Performance at I43 at 110 bar.

Table 7.12. Results for Cycling Operation with Varying High Side Pressure Setpoints

Test Condition I43 with Air Temperature Limits at [4,7]°C					
Discharge Pressure [bar]	Cycle Time [sec]	On Time [sec]	Off Time [sec]	Capacity [kW]	COP
90	68.3	49.4	18.9	1.15	1.22
95	63.3	44.2	19.1	1.16	1.25
100	47.8	28.9	18.9	1.13	1.33
105	44.0	25.5	18.5	1.15	1.37
110	42.9	24.2	18.7	1.16	1.37

7.6 Compressor Speed-R744

Next, the influence of compressor speed on system behavior during cycling will be investigated. The two conditions selected were M23, shown in Figure 7.13, and I28, shown in Figure 7.14. The table showing the performance data for these two conditions is in Table 7.15. Note that both conditions are operated with the backpressure valve, and both conditions use approximately the same setting of this valve. From the table it is seen that the capacities are approximately equal, while the values of compressor power, and hence COP, are not. The on time for condition M23 is shorter, indicating higher on time capacity, however the off times for both are the same. This is due to the reasoning discussed earlier in this chapter. In both of these conditions, there is more bleeding of the high pressure during the off period than was seen earlier in condition M12. Within these two conditions, it seems that the valve opens faster for condition

M23 than for I28. This is perhaps due to slightly faster buildup of high side pressure, or higher mass flow rate for condition M23. Finally, it is seen that the fluctuations in the refrigerant temperature leaving the evaporator are similar.

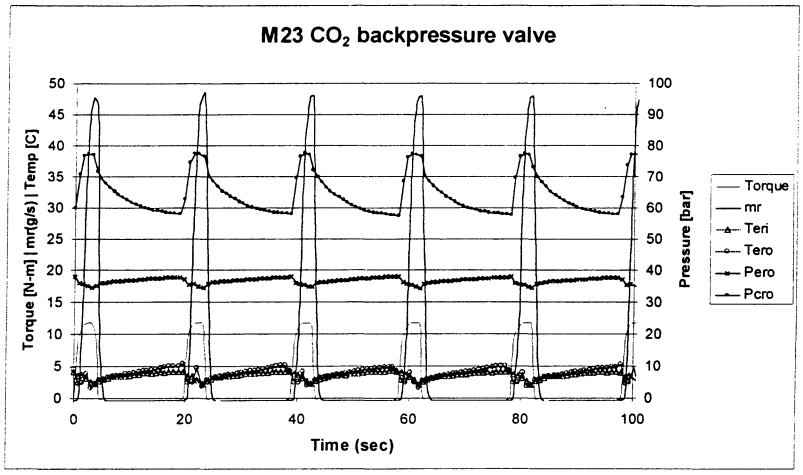

Figure 7.13. R744 System Behavior for Condition M23

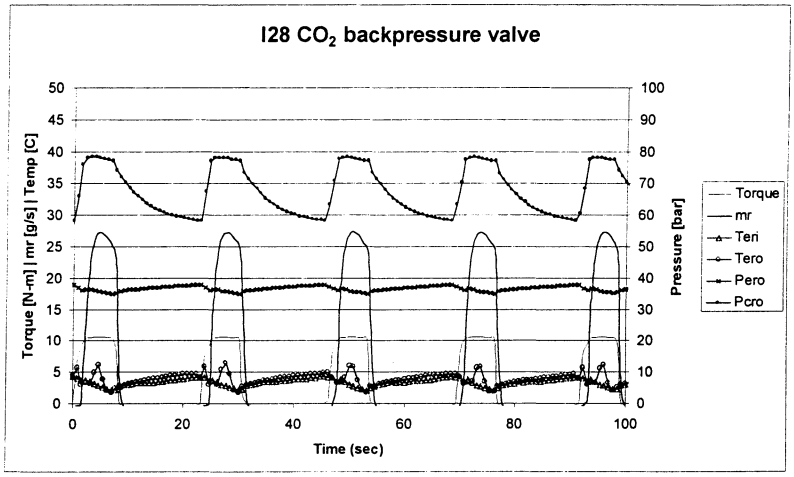

Figure 7.14. R744 System Behavior for Condition I28

Table 7.15. R744 System Performance Data for Selected Conditions

Test Condition	Average Power [kW]	Average Capacity [kW]	On Time [sec]	Off Time [sec]	COP
M23	0.38	1.15	4.6	14.8	3.06
I28	0.31	1.18	8.5	14.2	3.83
I23	0.51	1.23	12.3	12.8	2.39

7.7 Ambient Temperature-R744

The final parameter that will be studied is the difference that ambient temperature has on the system behavior. This is shown by comparing conditions I28 (as shown earlier), and I23, shown in Figure 7.16. The first item to note is that the torque is higher for condition I23. This is due to the setting of the backpressure valve being at a higher value. The valve is set at a higher value because it has been shown that in order to get maximum COP, the relationship says that as T_{cro} is increased, the high side pressure must be increased. Since T_{cro} is a strong function of the ambient temperature (which is higher for I23), it stands to reason that the pressure to achieve maximum COP should be higher.

However, even though the pressure setting is higher in I28, it is seen that the on time is longer. This is contrary to the understanding that as pressure is increased, the on time capacity should go up, and the on time will be shorter. In this case, however, the ambient temperature has also changed, thus actually giving a lower on time capacity, therefore the on time becomes longer. Again, both conditions exhibit more high pressure bleeding than presented earlier for condition M12. Also, the behaviors of the evaporator refrigerant temperatures are similar for these two conditions.

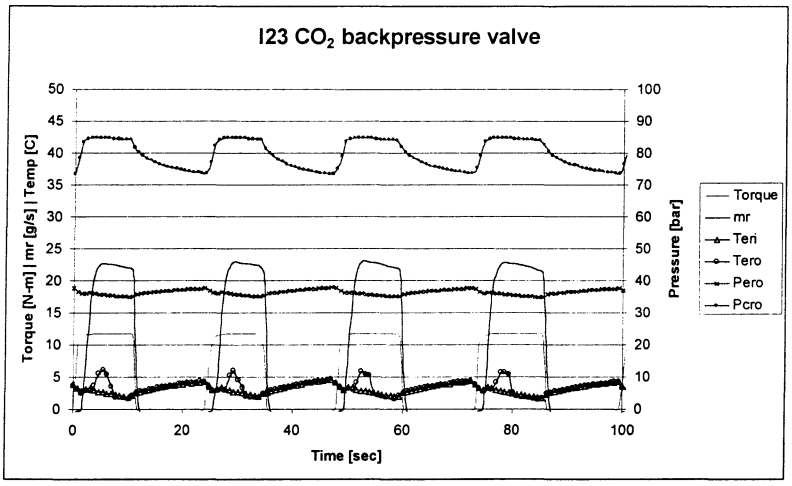

Figure 7.16. R744 System Behavior for Condition I23

8 Control Strategy Development

The fundamental control problem for an automotive A/C system is that of controlling the capacity. In general, the design condition of an automotive A/C system is the most extreme condition expected. Therefore, if a system can provide the required cooling capacity at that condition, it will be able to provide more than enough at more moderate conditions. Ideally, the capacity delivered should exactly match the capacity desired, and all of this should occur with the maximum performance possible for the system, without adding any extra cost or package volume. Of course, this is an impossible scenario, so it is up to the designer to specify the proper blending of the criteria to deliver a system matched to the customers' needs. Since this study is more focused on capacity and performance of the system, items such as cost and packaging will not be considered, but it is important to be aware of them.

In considering capacity and performance, there are two extremes. One extreme would be to design a control system that matched the desired capacity without regard to the COP. At the other extreme, the A/C system would be operated at maximum COP for the operating conditions, not worrying about whether not enough or too much cooling capacity was being delivered. However, as with most engineering problems, the solution desired is neither of the extremes, but a blend of the two.

Although some airside variables can be changed to help control capacity, such as evaporator airflow rate, usually some form of compressor modulation is also necessary. There are three methods of compressor modulation that are discussed, and two were tested. The three are clutch cycling, variable speed, and variable displacement. The two that were tested are clutch cycling and variable speed. However, there is great similarity in system behavior between variable speed and variable displacement operation. Basically, the only difference between the two is the compressor efficiency.

As of now, the most popular method for preventing evaporator freezing is to use a magnetic clutch attached to the compressor. This sensor also has the added benefits of providing capacity control and protection against low charge operation. This clutch is disengaged when the evaporating temperature drops too low and is engaged when the temperature comes back up to a specified level. This clutching of the compressor can lead to a decrease in driveability because of the sudden increase and decrease of the compressor power requirement, especially in small cars.

Several authors have presented papers developing control strategies for automotive air conditioning systems. The approach used in each paper is quite different, from straightforward linear theory (16) to fuzzy logic controllers (17). This is best explained by comments in (18) about this control problem. The difficulty in designing these control systems arises in the fact that this control problem does not fall into any category of traditional control theory for several reasons. First, the mechanical and electrical systems that comprise a vehicle control system are inherently nonlinear and cover a wide range of operating conditions. Other items that cause this problem to stray even further from a conventional control problem are that the goals of the system, especially occupant comfort, are not easily defined by precise mathematical formulas, much less linear formulas. Finally, it might be possible that the mechanical system cannot even provide enough heating or cooling to achieve the desired effect. All of these observations lead to the suggestion that a better way to design automotive climate control systems is to have a controller that can allow and correct for imprecision.

Most of the controller development presented here is somewhat general in nature and can be applied to any type of working fluid. However, there is one item that makes this controller development specifically tailored toward an R744 system, that being the requirement of some type of high side pressure control. In the transcritical R744 system, changing the high side pressure changes both system capacity and COP, the high side pressure which gives a maximum value for either of these parameters varies with operating conditions, and the maxima for the two parameters usually do not occur at the same high side pressure. Thus, it may be possible to trade COP for capacity and vice-versa by adjusting the high side pressure. (1)

In this paper, control strategies for transcritical R744 systems using a variable speed compressor, variable displacement compressor and clutch-cycled compressor will be developed. Although the variable speed compressor is not in use today, it could be in use when the internal combustion engine is no longer used to propel the automobile. Or, it could be put into use if a change in automobile voltage would allow for an electrically driven compressor. Also, variable speed operation gives good insight into variable displacement operation, with the main difference between the two being compressor efficiency. These systems are shown in the schematics in Figure 8.1. Note that all three systems use a low pressure receiver.

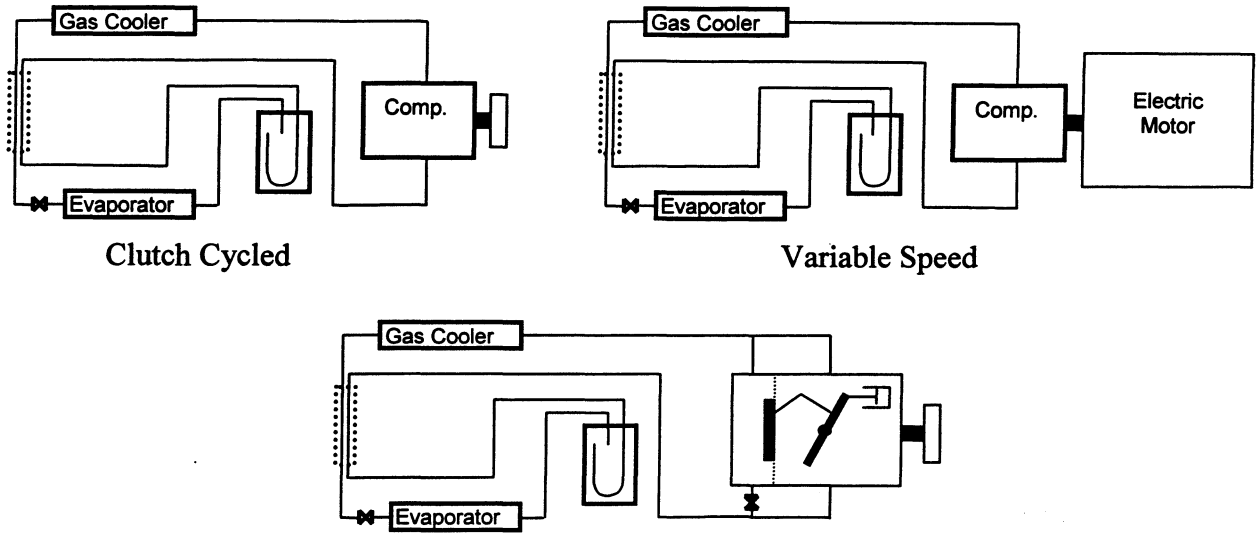

Figure 8.1. System Schematics

8.1 Controller Overview

The advanced controller developed here will concentrate on two regions of operation. The first is a pulldown situation, or when the cabin temperature is too high and needs to be reduced to a more comfortable level. This means that the system capacity must be higher than the load coming into the cabin, and the relative mismatch, along with the specific vehicle design, will determine the rate at which the temperature is pulled down. Generally, in this mode of operation the passengers are uncomfortable, and are not concerned with system efficiency. They want the temperature to be pulled down to a more comfortable level as quickly as possible. The logic for that situation would also apply to a situation where there is not sufficient capacity to bring the temperature down to the desired level. In either case, it is maximum capacity that is the focus.

After the pulldown situation has occurred for some time, the temperature will get to a level where the passengers are no longer uncomfortable. At that time, the second major type of system operation is under way. This is when the temperature in the cabin is relatively close to what the passengers desire. Thus, one would want the system capacity to be approximately equal to the load that is coming in. Also, since the passengers are more comfortable, the focus of operation should not only consider capacity, but efficiency as well.

These systems are also subject to safety constraints which the controller must be aware of. In the case of the R744 system, the safety aspects are maximum compressor discharge pressure and maximum compressor discharge temperature. These limits are functions of the heat exchanger, piping, and compressor design. The discharge temperature becomes an issue when the suction line heat exchanger is added to the system. If any control law runs up against one of these constraints, it must stop there and go no further. Generally, as discharge pressure is increased, so is discharge temperature, therefore, by decreasing high side pressure, the system can be brought back into a safe operating region. Another problem the controller must prevent is evaporator freezing.

8.2 Controller Development

The development of control strategies will begin by looking at a simple controller based on a fixed displacement, clutch-cycled system. After that, a more sophisticated control strategy will be discussed. The portion of the advanced control related to the pulldown region will be discussed, then the development will move to the strategy for the comfort region. After the advanced strategy has been developed, specific applications for clutch cycling, variable speed, and variable displacement compressors will be discussed.

8.2.1 Clutch Cycling Simple Control

For the simple control, the one parameter that is of interest is the high side pressure. The goal of this controller will be to operate the R744 system somewhat efficiently over the wide range of operating conditions. As shown in chapter 7, experimentation was done over a wide range of conditions for the clutch-cycled system. A model was presented earlier in the text for predicting the optimum high side pressures as a function of gas cooler refrigerant exit temperature. This curve is shown in Figure 8.2. Note that operating at any combination of temperature and pressure in the shaded region guarantees at least 97% of the maximum COP. Also note that the relationship is somewhat linear, then saturates at temperatures below 30°C. This is a consequence of data taken when operating the system at subcritical pressures, also shown earlier in the text. It was found that for this particular system, the efficiency and capacity dropped rapidly once the pressure was taken below critical (73.8 bar). Figure 8.2 also shows

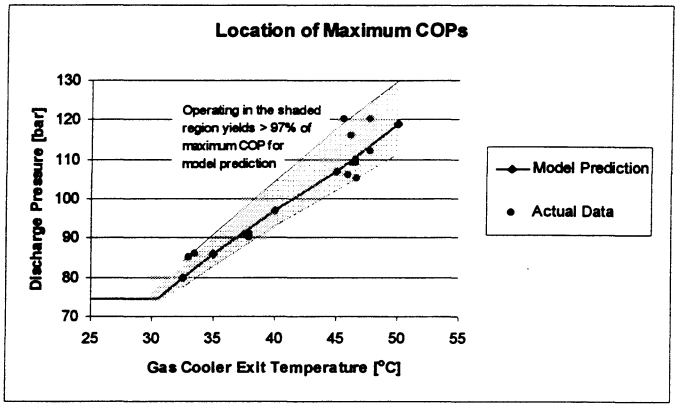

Figure 8.2. Maximum COP as a Function of T_{cro}

that running at a higher pressure than is specified is better than running at a lower pressure, especially in the region of lower gas cooler exit temperatures.

One way to control the high side pressure is by utilizing the expansion device. One such device that is not used presently is a variation of a backpressure regulating valve. This valve would use a temperature signal to change the setpoint of the valve, similar to a TXV (thermal expansion valve). However, this valve would be balanced when the backpressure achieves a specified value. This design could accomplish the task with no electronic feedback. That is, the pressure setpoint relationship could be designed into the device mechanically. It would also be an easy matter to design in the constraint that the high side pressure cannot exceed a specified limit. One possible valve design is discussed in (19). This valve does not need to be a high-precision device, and can be designed knowing the small range of flow rates it is likely to encounter in this application.

To prevent the evaporator from freezing, a temperature or pressure switch that disengages the clutch when the evaporating temperature (pressure) drops too low could be used.

The relationship between T_{cro} and high side pressure shown in Figure 8.2 was developed for non-cycling conditions. However, as shown earlier in this text, the same type of analysis can be extended to cycling conditions if an averaged T_{cro} is used. The thermal mass of the bulb could act as an averager and achieve this goal.

8.2.2 Advanced Control-Pulldown Region

This region will be defined as any time when the cabin temperature is at a level over 5°C above the user setpoint. The goal in this region is to get the cabin temperature reduced quickly. Thus, the compressor should be functioning at its maximum, or at a level that produces an evaporator surface temperature that is just above freezing, whichever occurs first. If the compressor capacity is not enough to bring the evaporation temperature that low, the next item to adjust would be the high side pressure. The remainder of this section will discuss the strategy related to adjusting the high side pressure. Since capacity will increase (in general) as high side pressure is increased, this would seem to suggest that the controller should just increase the high side pressure until one of the safety constraints is violated. Unfortunately, as the high side pressure is increased, the incremental gain in capacity is less than the incremental increase in compressor power, hence the falling COP, as seen earlier in the text. Therefore, some criteria must be established which limits the upper setting of the high side pressure. This limit will be a parameter specified by the designer who must decide what price in compressor power should be paid for increasing the capacity.

Rather than develop a system map for all sets of operating conditions to know what this pressure limit is, this controller will attempt to find the limit during operation. This requires that the controller select a starting point to begin observing the system. As a first step in selecting the pressure, the high side pressure is set to correspond to the pressure at which the model predicts 97% of maximum COP can be achieved with higher capacity than at maximum COP. This starting point was selected somewhat arbitrarily based on observation of system behavior. Another logical starting point which will not be explored here would be the pressure at which the model predicts maximum capacity, since maximum capacity (without too much compressor power penalty) is the goal in this region. However, it has been observed during system operation that usually a large price is paid in compressor power to get small gains in capacity near the maximum capacity, as seen in Figure 8.3. That is, the capacity versus high side pressure curve is rather flat at that region while the compressor power curve is increasing linearly. By starting at the 97% of maximum COP pressure, there is usually some slope in the capacity curve, giving a more favorable trade off of increasing capacity versus increasing compressor power. To select this pressure, a lookup table based on the T_{cro}-high side pressure relationship presented earlier in the text in Figure 8.2 is consulted. Next, the controller begins observing parameters in the

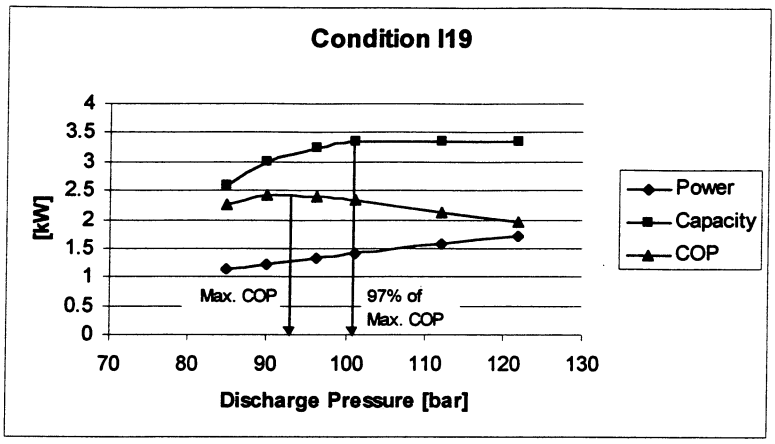

Figure 8.3. System Behavior for Different High Side Pressures

system. During this observation phase, if either of the safety constraints are violated, the high side pressure is reduced. Also, if the cabin temperature reaches the upper comfort limit, this control strategy is abandoned and the control is transferred to the design for the comfort region. After observation, the average air temperature difference across the evaporator is calculated. The observation time can be selected somewhat arbitrarily based on observed system response times in the lab. Then, the high side pressure is increased another 5 bar and the data is observed again.

The controller then decides whether or not increasing the pressure 5 bars was a wise decision. The way in which it does this is to compare the temperature difference across the evaporator with the previous value. This should give a rough idea of how much the capacity was increased after the pressure was increased. This is because the air flow rates should be roughly equivalent (the controller will fix the blower speed at maximum in this region), and the value of the flow rate can be measured during system development. It is also assumed that the ratio of latent to sensible capacity is unchanged. Looking at actual tests performed in this range of temperatures, and 40 to 50% relative humidity in the indoor chamber, it appears that an increase in ΔT of 1.0°C corresponds to approximately 350W of total cooling capacity. A sample of data showing this is given in Figure 8.4.

Also during actual system testing, it should be possible to get an idea of how much the compressor power increases when capacity is increased. In the case for this system at idle, the

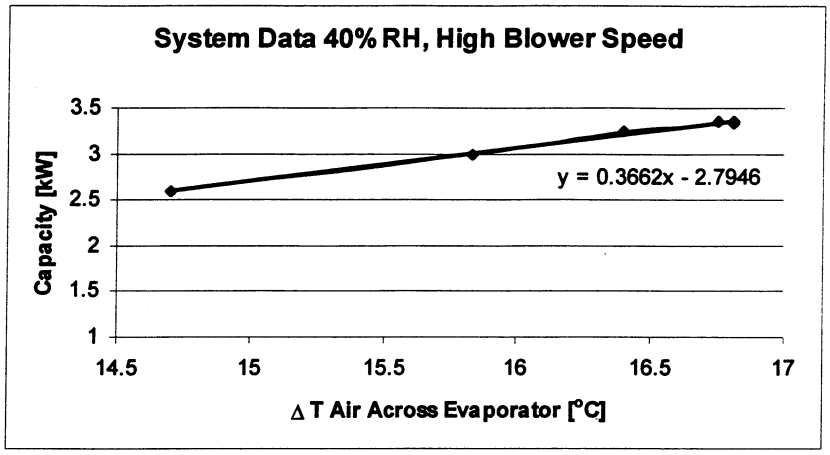

Figure 8.4. Capacity Versus ΔT Across Evaporator

increase was approximately 17.5 W/bar, as shown in Figure 8.5. There are 6 different conditions, each run at a variety of high side pressures, shown in Figure 8.5 which had different evaporator airflow rates, humidities, inlet temperatures, as well as different outdoor temperatures and airflow rates, all at idle conditions. It is important to note here that when the system was tested with a suction line heat exchanger at down-the-road conditions, it was found that the maximum COP and maximum capacity both occurred when the limit of compressor discharge temperature was met. Therefore, in that mode of operation, there will be no need to decide whether or not the pressure should be increased, it will already be on the verge of violating a safety constraint. That is why numbers for the idling mode of operation are used in this development. If it were found that the pressures used during down-the-road operation could

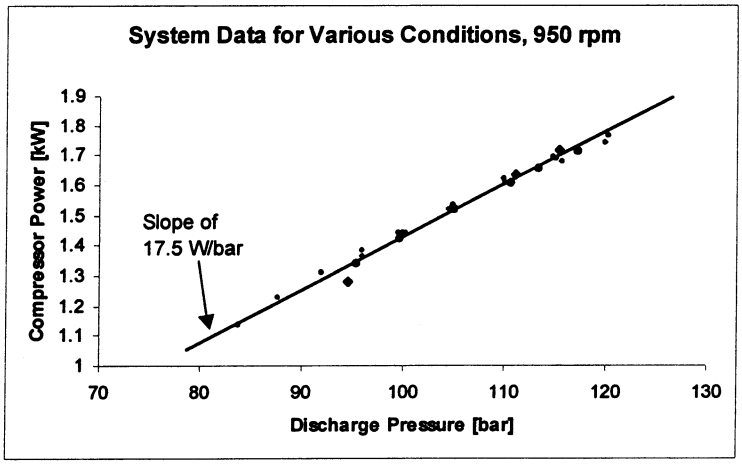

Figure 8.5. Data Showing Compressor Power Slope

provide peak COP, then those numbers would have to be considered in this portion of the control development. Moving back to the description of this particular controller, the designer must specify the tradeoff between increasing capacity and increasing compressor power. In this case, a pressure change will be acceptable if it can increase ΔT by 0.25°C, which means that, we will get at least the additional compressor work back in cooling power.

If the pressure change was worthwhile, then the pressure is increased again. If not, then the pressure level is returned to where it was. After holding for one minute, the pressure will be increased again to be sure that still no gain can be had by performing this action. This is necessary because the system will be operating in a transient nature and it is possible that with changing conditions, increasing the pressure could have a beneficial effect. The flowchart illustrating the control logic for this region is shown in Figure 8.6.

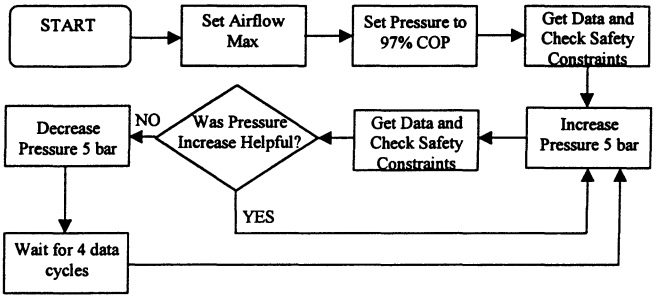

Figure 8.6. Flowchart for Pulldown Region

8.2.3 Advanced Control-Comfort Region

The next region that will be investigated is when the cabin temperature is somewhat comfortable. The most common way to control capacity now is to cool the air down more than necessary, then use waste heat from the engine to reheat the air to give the proper capacity. In general, the compressor will not need to operate at its maximum in this region. That is, if the compressor were operated at its maximum, it would either cause the evaporator to freeze, or it would provide more cooling capacity than is required.

There are other concerns besides capacity and COP when the evaporation temperature is raised by modulating the compressor. The major concern is what happens to the latent capacity. That is, when the evaporation temperature is raised, thus raising the mean surface temperature of the evaporator, will this be able to provide enough dehumidification performance? The answer depends on the outdoor conditions, the amount of fresh air that is entering the vehicle, and the

desired humidity in the cabin. In fact, it may be beneficial to have a humidity sensor as part of the control system if there is any question as to the dehumidification performance. This sensor could override the energy saving benefits of raising the evaporating temperature to provide more dehumidification. Or, perhaps there could be a button for the user to depress for defogging that could perform this override.

The basic structure of this controller will be made of two parts. The job of one part of the controller will be to observe the system and decide if more or less cooling is required and how much more or less. The second part of the controller will decide which actuators to use to provide more or less cooling. The terms "quantifier" and "selector", used in (20), will be used here to describe the two parts. This structure gives flexibility and insight into the controller behavior, thus making it easier to design for specific systems.

The quantifier observes what is happening in the system, then compares this to what the designer thinks should be happening. Depending on the difference between the two, the controller decides how much more or less cooling power is needed. In this case, the quantifier does this by observing the trend in the cabin temperature and comparing it to the trend that it is supposed to follow.

The trend, or trajectory, that the controller should follow is completely up to the designer. For this case, it is assumed that we want a smooth exponential trajectory for the cabin temperature, shown in Figure 8.7. However, since it will be the derivative that is tracked by this controller, any function with a continuous first derivative that approaches zero as the error

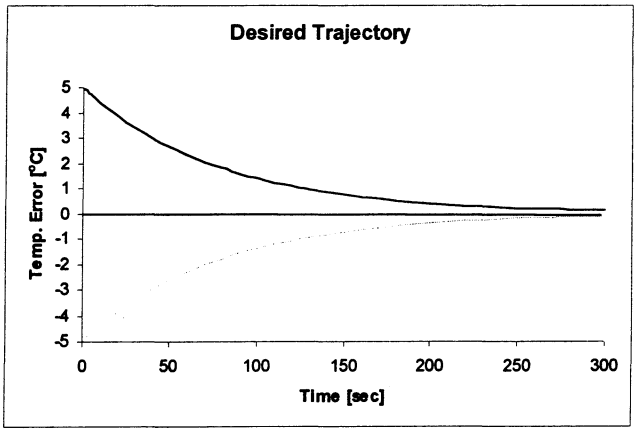

Figure 8.7. Trajectory Desired

approaches zero will work. For this design, we want the cabin temperature to go from T_{set}+5°C to within T_{set}+0.5°C of the setpoint in 180 seconds. The error in the cabin temperature, e, is defined by $e = T_{cabin}-T_{set}$. Or, $\dot{e} = \dot{T}_{cabin}$ if the setpoint does not change. Thus, this criterion means that we want e to go from 5 to 0.5 in 180 seconds. Mathematically, this means that we want the trajectory $e = 5 \cdot \exp(-k \cdot t)$. Therefore, since we want an exponential trajectory to approach T_{set}, this means that $e = 5 \cdot \exp(-k \cdot t)$, or $\dot{T}_{cabin} = k \cdot e$, where in this case, k is 1/78.2. This also means that when e is negative, we get the mirror image of what we described, shown in Figure 8.7 as a dotted line. From the physical system, we know that $m \cdot c_p \cdot \dot{T}_{cabin} = Q_{in} - Q_{out}$. Where mc_p and Q_{in} are functions of the vehicle and operating conditions, and Q_{out} is what the controller has to work with. Therefore, by increasing and decreasing Q_{out}, the quantity Q_{in}-Q_{out} will only change by the amount of change of Q_{out}, assuming Q_{in} is roughly constant. Thus, $\dot{T}_{cabin}$ will change. Since $\dot{T}_{cabin}$ is specified in this case to be k*e, the desired value of $\dot{T}_{cabin}$ is known. So, the quantifier then must decide how much more or less Q_{out} is required to bring $\dot{T}_{cabin}$ closer to the required value. Specifying the amount of change of Q_{out} is another decision left up to the designer. Chances are that this portion of the controller would have to be tuned for the specific vehicle that it is installed in due to different thermal masses, thus giving different sensitivities of $\dot{T}_{cabin}$ to a change in Q_{out}.

This change in the quantity Q_{in}-Q_{out} will be termed ΔQ. Therefore, for more cooling effect, ΔQ will be negative and for more 'heating' effect, ΔQ will be positive. For this development, ΔQ will be a linear function of the difference between $\dot{T}_{cabin}$ measured and $\dot{T}_{cabin}$ specified.

After ΔQ is calculated, this information is fed to the other part of the controller, the "selector" which decides what actions will be taken to fulfill this request. There will be three strategies used here to give ΔQ: adjusting blower speed, modulating the compressor, and adjusting the amount of reheat. A relationship for ΔQ and each of the adjustments is specified by the designer. The order in which these three strategies are used depends on the sign of ΔQ. Note that if less cooling power is required, reheat is the last strategy to be used. This is because blower speed reduction and raising the evaporating temperature are much more efficient ways to get the desired effect. Reheating is only used as a "last resort" means to match the delivered capacity to the desired capacity, mostly for reasons of dehumidification. That is, there is an

upper limit for the evaporating temperature in order to get adequate dehumidification. If the evaporating temperature is already that high and still less capacity is needed, this would be when reheat is used. If any one of these strategies saturates, or cannot provide the requested amount of adjustment, the next strategy is tried. This entire process is shown in the flowchart presented in Figure 8.8.

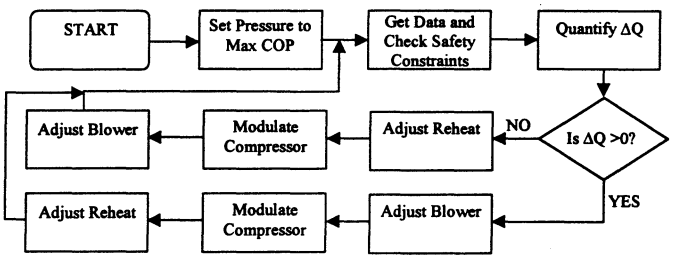

Figure 8.8. Flowchart for Comfortzone

Not only is the control idea necessary, but so are the numbers necessary to give the controller some idea of the sensitivity of the system to certain inputs. This allows the controller to choose reasonable values for the inputs and causes the system to have the desired reaction. The first relationship was to try to find out how fast the cabin air temperature changes based on the amount of mismatch between the energy coming in and the energy being pulled out. The basic equation describing this phenomenon is $m \cdot c_p \cdot \dot{T}_{cabin} = Q_{in} - Q_{out}$. So, we can calculate the sensitivity of $\dot{T}_{cabin}$ to the quantity Q_{in}-Q_{out} by assuming a volume of 5.66m^3 of air in the cabin. Then, the density and specific heat of air were considered for a wide range of relative humidities and temperatures. Namely, the four combinations that can be made from air temperatures of 21°C, 43°C, with relative humidities of 0% and 70%. After performing the calculations, it was found that this gave a thermal mass of the air to be between 6.30 kJ/K and 6.75 kJ/K. Therefore, a value of 6.5 kJ/K was selected and used to find that a 100W mismatch in the Q values corresponds to a temperature change of 0.23C° in 15 seconds.

The next relationship investigated was the sensitivity of sensible capacity to blower air flow rate. To discover the blower effect, actual system data corresponding to indoor conditions of between 21-26°C and 40-50% RH was used. From these data sets, it was determined that 100W of effect corresponded to changing the blower 1.1 units, where a blower setting of 1 corresponds to 0.057 kg/sec and a setting of 10 corresponds to 0.142 kg/sec. In a real controlled system, the parameter being controlled would be the blower voltage. Of course, there is an

additional relationship between voltage supplied, air temperature, duct and heat exchanger design, and flow rate. This relationship could be obtained by testing the real system, or as was done here, the system can be tested over a few conditions to get estimates of the values. In addition to just finding the numbers, some more insight was used to develop the actual blower relation. To prevent the passengers from thinking that something is wrong with the climate control system, the maximum change on the blower will be 3 steps, or 1/3 of the range. This prevents the blower from jumping from high to low speeds and back, which might be interpreted by the passengers as something wrong. As a final note, if the passenger uses the knob on the panel to select a fixed blower speed, the controller will not use the blower speed option to change the system capacity.

Finally, there is no data available to get a relationship for reheat, but this would be obtained in the same manner. A value is assumed in this study for illustrative purposes as 1 unit of reheat is equal to 100W, with limits at 0 units and 20 units.

These give the relationships shown in Figure 8.9. These are simple relationships based only on the value of ΔQ. However, if one wanted more refinement, these relationships could be made into surfaces or even hypersurfaces, functions not only of ΔQ, but also perhaps of actuator setting, operating conditions, etc.

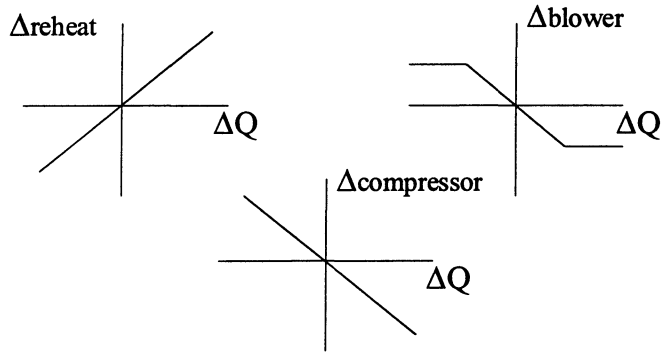

Figure 8.9. Actuator Relationships

8.3 Compressor Modulation

8.3.1 Clutch Cycling Control

Now that the strategies for the two regions of operation have been developed, the specifics of using clutch-cycling control will be discussed. For this type of control, the way in which the compressor is modulated is by engaging and disengaging the magnetic clutch. The

most common way to modulate the compressor now is to allow the evaporator temperature to go very near freezing. However, in a study by Håkansson (21), it was shown that this mode of operation is responsible for a large percentage of the energy consumption of the system. Also, this percentage increases as the climate becomes more moderate. In that study, the approach used was to increase the mean evaporation temperature by cycling the compressor at higher evaporation temperatures, which will be denoted as improved cycling.

Cycling and improved cycling were tested with the prototype R744 system. Table 8.11 shows the effects of using the improved cycling strategy for a selected operating condition. The sensor used to provide the limits was a thermocouple placed in the air stream exiting the evaporator. The only difference between the data points for each condition is the temperature cycling band. The effects of making the band wider and narrower (I45), along with changing the temperature band up and down (I48) are shown. It can be seen that when the band was made wider, the capacity increased and the COP decreased even though the operating conditions and arithmetic mean for the cycling limits did not. This is explained by the fact that the air exit temperature follows not a straight line path, but an exponential-type trajectory. This means that when the band is wider, the average air exit temperature over the cycle will be lower even though the limits are the same, as shown in Figure 8.10. Since the average exit air temperature is lower, it is expected that capacity should be higher and COP should be lower, which is what the data shows.

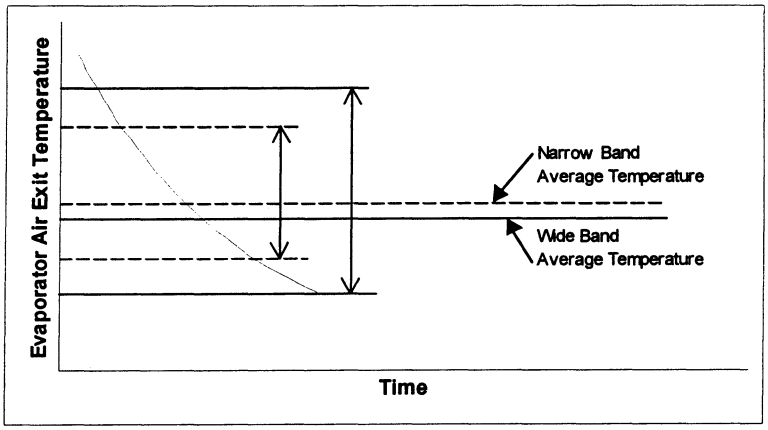

Figure 8.10. Effect of Temperature Band Width

In Table 8.11, it is seen that when the entire temperature band is shifted, a 50% reduction in capacity can be achieved at this condition with a 20% increase in COP. It appears

Table 8.11. Improved Cycling

Test Point	Temp. Limits [°C]	Cycle Time [sec]	On Time [sec]	Off Time [sec]	Capacity [kW]	COP
I45	[6,9]	42.2	24.3	17.9	1.11	1.35
	[5,10]	65.2	40.6	24.6	1.15	1.24
I48	[4,7]	32.1	14.1	18.0	1.33	2.49
	[6,9]	32.0	11.5	20.5	1.14	2.74
	[8,11]	33.8	9.6	24.2	0.92	2.87
	[10,13]	40.3	8.4	31.9	0.69	3.02

that improved cycling, that is, raising the cycling temperature limits, offers substantial benefits over traditional cycling when the system does not need to provide as much capacity.

No major changes need to be made to the pulldown region strategy described earlier to incorporate clutch-cycling control. The only thing needed is a sensor that gives some idea of the evaporator surface temperature, which in this case was a thermocouple in the evaporator exit air stream. For the pulldown region, the cycling limits will be set as low as possible to give maximum capacity while not freezing the evaporator.

The comfort region is somewhat more complicated, however. The method of modulating the compressor in this region will be by adjusting the mean value of the cycling limits. The effect of changing the cycling temperature can be approximated by $q_{change} = \dot{m}_{air} \cdot cp_{air} \cdot \Delta T$. Thus, at the low airflow rate, a change of 2°C in average cycling air temperature should approximately correspond to 100W. Since we do not want the evaporator to freeze, the lowest setting of the cycling band will be [4,7]°C. To prevent latent capacity from completely disappearing, the maximum limit of the cycling band should provide a surface temperature a few degrees below a comfortable dew point temperature. If one assumed a cabin of 21°C and 50% RH, this would correspond to a dew point of 10.2°C, thus giving cycling limits of [9,12]. If one wanted even more control over humidity, a humidity sensor could be installed in the cabin. This sensor would be used to override the action of raising the cycling band and would instead use reheat to properly match the capacity.

8.3.2 Variable Speed Control

Unlike clutch-cycling and variable displacement, in the pulldown region, the compressor capacity can be significantly increased by increasing the speed (to some limit), thus giving

another variable to adjust. Therefore, the effects of adjusting the speed to gain more capacity versus adjusting the high side pressure (as in the clutch cycled strategy), would need to be weighed. With adjustable speed, depending on design, it might be possible to bring the evaporation temperature very near freezing in this region for almost any condition, giving a very large cooling capacity and quick pulldown. Of course, this assumes that the other components (expansion device, heat exchangers) can 'keep up' with the increase in compressor capacity.

In the comfort region, the effects of reducing the compressor speed to give less capacity were investigated. Table 8.12 shows the effects of reduced compressor speed versus clutch cycling for two operating conditions. It is important to note that for the reduced speed data shown, the values represent the data at the maximum COP. Both the speed of the compressor and the high side pressure were varied to give the combination that provided the maximum COP for the same cooling capacity. It is seen that at a higher compressor speed (M28), there is a 20% increase in COP by reducing the speed to get less capacity. However, at a lower speed condition (I48), nothing is gained in the way of COP when the compressor speed is reduced. Therefore, the compressor consumes the same amount of power. This could simply be an effect of the design of the compressor, in that, the efficiency at low speeds drops way off, as shown in Figure 8.13. Since variable speed is allowed in this case, the designers could use a smaller displacement compressor that operated at higher speeds to overcome this problem. This type of design would still give the desired capacity at engine idle. In any case, for the control strategy, one would need the relationships between adjustment of speed and its effect on cooling capacity to be inserted into the controller for compressor modulation.

Table 8.12. Reduced Speed Data

Test Point	Cycling Limits [°C]	Compressor Speed [rpm]	Compressor ON%	Discharge Pressure [bar]	Capacity [kW]	COP
I48	[4,7]	950	40.9%	80.7	1.40	3.25
	N/A	375	100%	76.8	1.39	3.22
M28	[4,7]	1800	49.7%	100	2.39	1.94
	N/A	790	100%	86	2.39	2.33

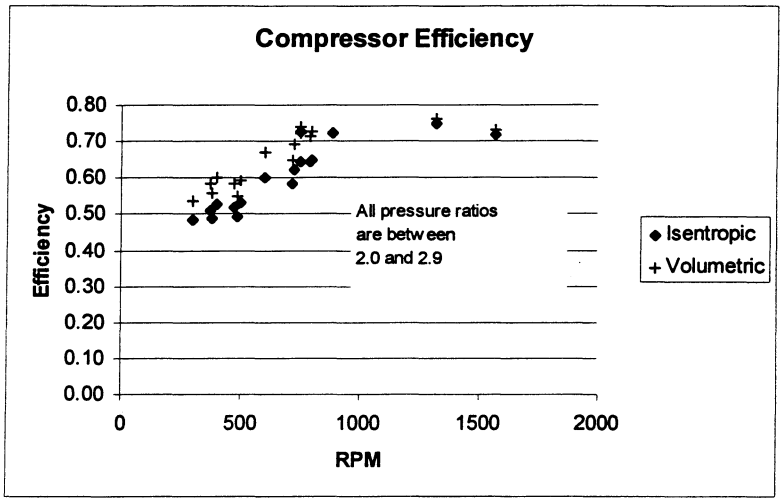

Figure 8.13. Compressor Efficiency as a Function of Speed

8.3.3 Variable Displacement Control

8.3.3.1 Internal Control

The internally controlled variable displacement compressor uses the compressor suction pressure as the input to adjust the displacement. Using this type of compressor would somewhat simplify the control strategy because the compressor modulation is handled by the compressor, not the controller. Only blower speed, high side pressure setpoint, and reheat value need adjustment. But, this method is not really comparable to the other two due to the lack of adjustability.

8.3.3.2 External Control

In the pulldown region, the strategy is similar to clutch-cycling because maximum displacement would be used, or displacement that caused the evaporation temperature to be just above freezing would be used.

Again, it is the comfort region that requires the most changes due to using this strategy. In general, the method of adjusting the compressor capacity is by providing a tap to the suction and discharge lines in the compressor crankcase. Then, some type of adjustable valve is used on one or both of these taps to set the crankcase pressure, thus adjusting the displacement. The lower the crankcase pressure, the smaller the compressor displacement. It is important to note

that by using this method, the low limit of the achievable crankcase pressure is equal to the suction pressure.

Instead of using the relationship between changing cycling limits and capacity, one would need to determine the relationship between adjustment of the displacement and capacity. Also necessary is the relationship between operating conditions, adjustment of the 'displacement' actuator, and compressor displacement. This relationship could be discovered through experimentation, or through modeling of the individual compressor and system. Either method would give the controller the necessary information so it could adjust the compressor displacement, based on the change in the amount of cooling power that is required.

8.4 Controller Summary

To summarize, control strategies were developed for the R744 system. Both a simple and advanced clutch cycling strategy were presented, along with the modifications necessary to introduce variable displacement and variable speed compressors. The advanced controller consisted of two main parts, one that handled the pulldown region and another that handled the comfort region. In the pulldown region, the main goal was fast temperature pulldown, but the tradeoff between extra capacity and lower COP was included in the goals. The controller uses closed-loop feedback in addition to a system map, developed by modeling, to determine what the high side pressure setting should be. In the comfort region, the main focus was efficiency. The controller uses a setting for high side pressure that corresponds to the maximum COP, as determined by the gas cooler exit temperature and the system map, developed by modeling. The controller decides how much more or less cooling power is needed to follow a design temperature trajectory. Then the controller decides how much to change each actuator (blower speed, compressor modulation, and reheat) based on how much more or less cooling power is needed.

8.5 Controller Simulation

Now that the controller has been completely specified from the conceptual stage all the way through making calculations for controller parameters it can be put into action by use of a simulation. This simulation uses the transient cabin model developed in Appendix B tied together with a simple model of the fixed displacement A/C system developed using actual test

data. The control code is also written in this simulation which will determine the operating parameters of the A/C system. The goal of the simulations is to show the fixed displacement advanced control in action and observe how some changes to the control logic and controller parameters will affect the outcome. The complete simulation development is in Appendix D, along with the controller pseudocode for the advanced controller. Only the highlights of the results will be featured here.

The first simulation is for a vehicle that has been thermally soaked at an outdoor temperature of 32°C, at idle conditions. The complete set of parameters for all of the simulation runs is shown in Table 8.14. The first set of results, Figure 8.15 shows the response for a controller with a control interval of 15 seconds. When this controller is switched from hightemp mode to comfortzone mode, it immediately calculates ΔQ and adjusts accordingly. It is seen that the controller functions well in the hightemp region, but has some problems when it switches modes. It overcorrects on the initial guess for how much the cooling power should change. This is because the controller in the comfortzone region does not have logic built in that anticipates the reduction in cooling power due to cabin temperature change and high side pressure change. To alleviate this problem, the control interval was changed to 10 seconds, with the thinking that the changing temperatures would not present as much of a problem over the smaller sampling interval. The controller performed much better, as seen in Figure 8.16, but there is still a large area where the cooling power is reduced too much when the controller changes modes.

Table 8.14. Simulation Conditions

Figure	Ambient Temperature [°C]	Initial Cabin Temperature [°C]	Setpoint [°C]	Control Interval [sec]
8.15	32	32	21	15
8.16	32	32	21	10
8.17	32	32	21	10
8.18	32	32	23	10
8.19	32	43	21	10
8.20	21	32	21	10

Finally, the controller was reprogrammed to only change the high side pressure during the first control action after the mode changed. The results of this change are shown in Figure 8.17. This change allowed the controller to not overcorrect as much, therefore this change

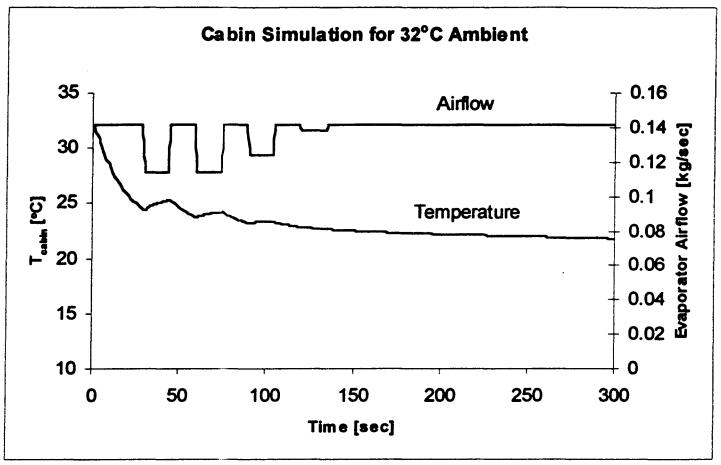

Figure 8.15. Cabin Simulation with 15 Second Control Interval

was kept in the control code. Note also that for this set of conditions, it takes the maximum blower speed to achieve the desired goal of setpoint temperature.

Figure 8.18 shows the results when the temperature setpoint is 23°C. Note that after some initial overcorrection, the controller smoothly adjusts the airflow until it finds the proper one. Figure 8.19 shows what would happen if the initial cabin temperature were 43°C. The behavior is quite similar to Figure 8.17, which has a 32°C initial cabin temperature.

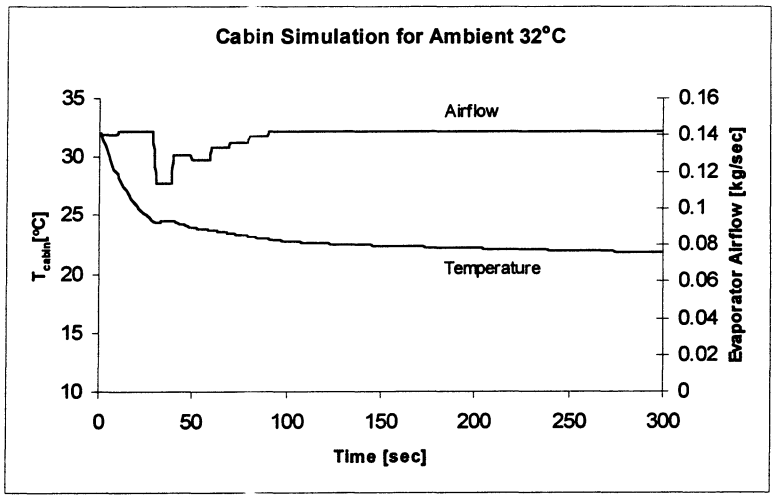

Figure 8.16. Cabin Simulation with 10 Second Control Interval

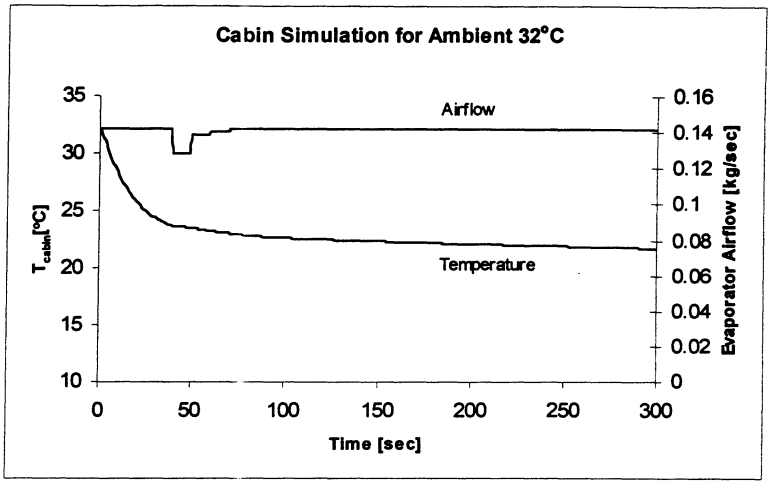

Figure 8.17. Cabin Simulation with Improved Comfortzone Control Logic

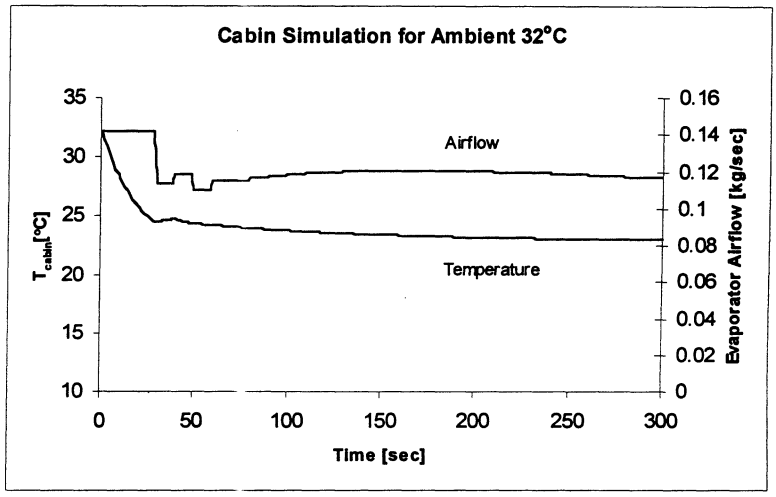

Figure 8.18. Cabin Simulation with 23°C Setpoint

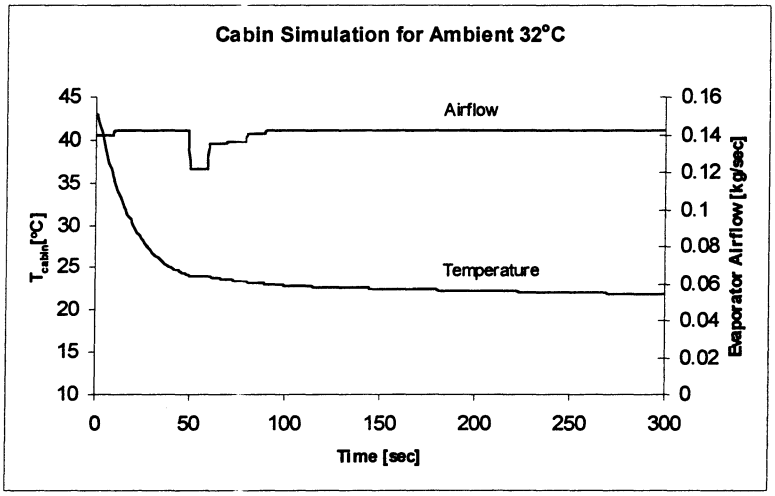

Figure 8.19. Cabin Simulation with 43°C Initial Cabin Temperature

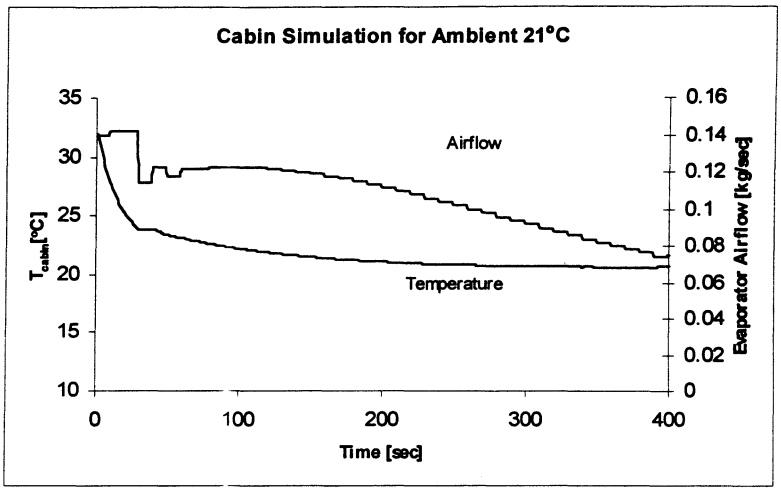

Figure 8.20. Cabin Simulation with 21°C Ambient

9 Conclusions

This work was concerned with control-related issues for transcritical R744 and subcritical R134a systems. The work began by giving background information on the systems that were studied in this work, as well as how the experimental methods used relate to actual operation of these systems. Next, the role of control systems as a part of air conditioning systems in general was discussed. The work then elaborated on several types of components that could be used as actuators in the system, including valve types and compressor types.

After the introductory material, the test facility and test procedures were elaborated upon. This section described such items as where to find the information on the environmental chambers and test equipment, as well as special considerations that were needed to operate these systems in cycling mode. Finally, the method of calculating some of the parameters that were special to the cycling case was discussed.

Focus then shifted to modeling the transcritical R744 system for steady, non-cycling conditions. The purpose of this model was to determine the sensitivity of the location of the COP maximizing high side pressure to several variables, such as SLHX UA values, evaporating temperature, and compressor efficiency. It was found that the most influential parameter was the temperature of the refrigerant exiting the gas cooler. The model predicted a somewhat linear relationship between the value of the COP maximizing high side pressure and the temperature of the refrigerant exiting the gas cooler. Some of the model conclusions were also verified with test data.

The next topic that was presented was an in-depth look into cycling operation of the R744 systems with backpressure regulator and needle valves, and the R134a system. It was found that the location of the COP maximizing high side pressure seems to follow the relationship for the non-cycling development because for this system, the temperature at the exit of the gas cooler did not fluctuate much. It also appears that there is room for improvement in the area of controlling the refrigerant flow during cycling for the R744 system. For both types of expansion devices, the evaporator showed signs of being starved, whereas the R134a system seemed to have enough refrigerant flowing into it.

Finally, two control strategies were developed that exploited the properties of the R744 system. The first strategy was a simple strategy that used the relationship from the model to design an expansion device that could operate the system near maximum COP for a wide range

of operating conditions. The second strategy that was developed was somewhat more complex in that it focused on two regions of operation. The main goal of this strategy was to provide maximum capacity in the regions where it was needed, then be able to provide maximum COP in the regions where that was appropriate. The controller would do this mainly by adjusting the evaporator air flow rate, as well as modulating the compressor, whether it be by cycling, variable speed, or variable displacement. The final adjustment the controller could use would be to adjust the reheat, but this is a last resort method, mainly in use for humidity control.

Acknowledgement

We acknowledge the contribution of Visiting Scholar Y. C. Park who has since returned to his position of Professor at Korea University, Seoul.

List of References

1. Boewe, D., Park, Y. C., Yin, J., Bullard, C. W., Hrnjak, P. S., 1999. The Role of a Suction Line Heat Exchanger in Transcritical R744 Mobile A/C Systems, SAE International Congress and Exposition, Paper 1999-01-0583.

2. Pettersen, J., Skaugen, G., 1994. Operation of Trans-critical CO_2 Vapor Compression Circuits in Vehicle Air Conditioning, Proceedings of the IIR Gustav Lorentzen conference - New Applications of Natural Working Fluids in Refrigeration and Air Conditioning, pp. 495-505.

3. Yin, J., Pettersen, J., McEnaney, R., Beaver, A., 1999. TEWI Comparison of R744 and R134a Systems for Mobile Air Conditioning, SAE International Congress and Exposition, Paper 1999-01-0582.

4. Alco Controls, Catalog

5. Eaton Corp, Anonymous, 1993. Thermostatic Valves for Automotive A/C Applications, University of Brighton Symposium.

6. Peterson, G., Kozinski, R., 1997. A Pressure Regulated, Flow Sensitive Variable Orifice Valve, SAE paper 971834

7. Laboe, K., Gondusky, J., Giasson, E., 1997. Variable Orifice Valve Development and A/C System Performance Testing, SAE paper 971824.

8. Heidorn, J.H., Refrigerating Apparatus with Compressor Modulating Means, U.S. Patent 3062020.

9. Taya, T., Kobayashi, H., Kawaguchi, M., Inagaki, M., 1992. 10PC20 Swash Plate Type Variable Displacement Compressor for Automotive Air Conditioners, SAE Paper 920260.

10. Park, Y. C., McEnaney, R., Boewe, D., Yin, J.M., Hrnjak, P.S., 1999. Steady State and Cycling Performance of a Typical R134a Mobile A/C System, SAE International Congress and Exposition, Paper 1999-01-1190.

11. Boewe, D., 1999. Comparative Experimental Study of Subcritical R134a and Transcritical R744 Refrigeration Systems for Mobile Applications, Thesis, University of Illinois at Urbana-Champaign.

12. McEnaney, R., Park, Y.C., Yin, J., Bullard, C.W., Hrnjak, P.S., 1999. Performance Of The Prototype Of A Transcritical R744 Mobile A/C System, SAE International Congress and Exposition, Paper 1999-01-0872.

13. Inokuty, H., 1928. Graphical Method of Finding Compression Pressure of CO_2 Refrigerating Machine for Maximum Coefficient of Performance, Proc. 5th Int. Congress of Refrigeration, Rome, pp. 185-192.

14. Boewe, D., Bullard, C., Yin, J., Hrnjak, P., 1999. Contribution of Internal Heat Exchanger to Transcritical R744 Cycle Performance,

15. Park, Y.C., Yin, J.M., Bullard, C.W., Hrnjak, P.S., 1999. Experimental and model analysis of control and operating parameters of transcritical CO2 mobile A/C system, Proceedings of Vehicle Thermal Management Systems 4 Conference.

16. Tabe, T., Matsui, K., Kakehi, T., Ohba, M. Automotive Climate Control, IEEE Control Systems Magazine, October 1986.

17. Gach, B., Lang, M., Riat, J., 1997. Fuzzy Controller for Thermal Comfort in a Car Cabin, SAE paper 970107.

18. Davis, L., Sieja, T., Matteson, G., Dage, G., Ames, R., 1994. Fuzzy Logic for Vehicle Climate Control, Proceedings of the Third IEEE Conference on Fuzzy Systems.

19. Denso Corporation, 1997. Pointing to the Future: Two Stage CO_2 Compression, IIR Conference-Heat Transfer Issues in Natural Refrigerants.

20. Mårdberg, B., 1997. An Algorithm for Automobile Climate Control, SAE paper 971790.

21. Håkansson, H., 1997. Development of an Energy Efficient Climate Controller, SAE paper 971789.

Appendix A Data for Cycling and Reduced Speed

Table A.1. Cycling Data for CO_2—Idle Speed

Test Point	T_{cai} [°C]	m_ca [kg/sec]	T_{eai} [°C]	RH	m_ea [kg/sec]	QE [kW]	Q_sens [kW]	Q_lat [kW]	Condensate [g/sec]	W_{comp} [kW]	COP	QC [kW]	Cycle Time [sec]	ON %	Dischg. Prs. [bar]	Temp. Limits [°C]
I22	32.3	0.454	21.0	0.50	0.057	1.34	0.83	0.51	0.19	0.65	2.08	1.85	36.9	0.57	85	[4,7]
I22	32.7	0.454	21.3	0.50	0.057	1.37	0.85	0.52	0.19	0.62	2.20	1.88	34.0	0.51	91	[4,7]
I22	32.6	0.454	21.2	0.50	0.057	1.39	0.84	0.55	0.20	0.65	2.14	1.92	34.2	0.51	95	[4,7]
I23	31.7	0.448	21.5	0.40	0.061	1.24	1.00	0.24	0.09	0.53	2.32	1.25	29.8	0.57	N/A	[4,7]
I28	21.1	0.452	21.5	0.40	0.061	1.18	0.96	0.22	0.08	0.31	3.83	1.33	22.7	0.37	81	[4.3,7]
I30	15.3	0.452	21.4	0.40	0.061	1.18	0.98	0.20	0.08	0.27	4.35	1.52	22.7	0.35	76	[4.2,6.8]
I43	43.9	0.456	21.1	0.40	0.057	1.23	0.93	0.30	0.12	1.03	1.20	1.79	86.2	0.79	90	[4,7]
I43	43.9	0.456	21.1	0.39	0.058	1.09	0.86	0.23	0.08	0.80	1.36	1.59	38.8	0.53	110	[4,7]
I43	43.7	0.449	21.0	0.40	0.057	1.15	0.92	0.22	0.09	0.94	1.22	1.67	68.3	0.72	90	[4,7]
I43	43.8	0.450	21.0	0.40	0.057	1.16	0.93	0.23	0.09	0.93	1.24	1.74	63.3	0.70	95	[4,7]
I43	43.6	0.450	21.0	0.40	0.057	1.13	0.92	0.21	0.09	0.85	1.33	1.65	47.8	0.60	100	[4,7]
I43	43.6	0.450	20.9	0.40	0.057	1.15	0.93	0.21	0.09	0.84	1.36	1.68	44.0	0.58	105	[4,7]
I43	43.6	0.451	21.0	0.40	0.057	1.16	0.90	0.26	0.10	0.85	1.37	1.70	42.9	0.56	110	[4,7]
I43	43.6	0.451	20.9	0.40	0.057	1.07	0.89	0.18	0.07	0.86	1.24	1.68	44.3	0.57	110	[4,7]
I45	43.6	0.455	21.0	0.50	0.057	1.35	0.88	0.46	0.17	1.13	1.19	2.11	84.4	0.81	95	[4,7]
I45	43.8	0.455	21.0	0.50	0.057	1.34	0.86	0.48	0.17	1.05	1.27	2.03	50.0	0.68	102	[4,7]
I45	43.6	0.454	21.0	0.50	0.057	1.30	0.86	0.44	0.16	1.07	1.22	2.02	45.3	0.64	108	[4,7]
I45	43.9	0.453	21.1	0.49	0.056	1.26	0.80	0.45	0.17	0.94	1.33	1.62	49.8	0.66	100	[5,8]
I45	43.9	0.453	21.0	0.50	0.057	1.11	0.74	0.36	0.13	0.82	1.35	1.47	42.3	0.58	100	[6,9]
I45	43.8	0.453	21.0	0.49	0.057	1.15	0.78	0.38	0.14	0.93	1.24	1.58	65.2	0.62	100	[5,10]
I45	43.8	0.453	21.0	0.49	0.057	1.21	0.81	0.40	0.15	0.92	1.32	1.66	93.9	0.64	100	[4,11]
I45	43.8	0.453	21.0	0.49	0.057	1.36	0.88	0.48	0.18	1.00	1.36	1.88	50.0	0.68	102	[4,7]
I48	21.6	0.450	21.3	0.49	0.057	1.33	0.85	0.48	0.18	0.53	2.49	2.13	32.1	0.44	92	[4,7]
I48	21.6	0.449	21.4	0.49	0.057	1.14	0.74	0.40	0.14	0.42	2.74	1.73	31.9	0.36	92	[6,9]
I48	21.2	0.449	21.0	0.51	0.057	0.92	0.66	0.26	0.10	0.32	2.86	1.42	33.8	0.28	92	[8,11]
I48	21.4	0.449	21.1	0.50	0.057	0.69	0.55	0.15	0.06	0.23	3.02	1.00	40.4	0.21	92	[10,13]

Table A.2. Cycling Data for CO_2—Medium Speed

Test Point	T_{cai} [°C]	m_ca [kg/sec]	T_{eai} [°C]	RH	m_ea [kg/sec]	QE [kW]	Q_sens [kW]	Q_lat [kW]	Condensate [g/sec]	W_{comp} [kW]	COP	QC [kW]	Cycle Time [sec]	ON %	Dischg. Prs. [bar]	Temp. Limits [°C]
M12	32.4	0.537	27.1	0.42	0.098	2.53	1.89	0.65	0.25	1.31	1.93	2.88	17.4	0.67	89	[7.5,10]
M23	21.4	0.526	21.5	0.40	0.061	1.15	0.97	0.18	0.07	0.38	3.06	1.32	19.4	0.24	82	[4.7,6.8]
M26	15.6	0.536	21.5	0.40	0.061	1.19	0.96	0.22	0.09	0.33	3.57	1.48	20.8	0.23	80	[4.6,6.9]
M28	32.2	0.538	21.1	0.50	0.099	2.33	1.50	0.83	0.31	1.32	1.77	3.56	21.0	0.57	90	[4,7]
M28	32.2	0.537	21.0	0.50	0.100	2.35	1.52	0.82	0.32	1.23	1.90	3.48	18.7	0.51	95	[4,7]
M28	32.5	0.537	21.5	0.49	0.100	2.39	1.51	0.88	0.31	1.23	1.94	3.53	18.3	0.50	100	[4,7]
M28	32.3	0.536	21.3	0.50	0.100	2.39	1.51	0.88	0.32	1.33	1.80	3.56	18.2	0.50	110	[4,7]

Table A.3. Reduced Speed Data for CO_2—System and Compressor

Test Point	W_{comp} [kW]	COP	Mr [g/sec]	Isentropic Efficiency	Volumetric Efficiency	P_{ratio}	P_{rcpi} [kPa]	P_{rcpo} [kPa]	T_{rcpi} [°C]	T_{rcpo} [°C]	Vc [RPM]
I13	1.31	1.89	19.2	0.72	0.72	2.65	3968	10710	32.5	111.2	883.5
I22	0.64	2.26	8.7	0.53	0.59	2.35	3564	8490	17.1	92.5	500
I22	0.61	2.21	8.3	0.52	0.58	2.31	3621	8477	16.7	90.8	475
I22	0.71	1.92	11.1	0.60	0.67	2.19	3585	7942	26.3	94.7	602.6
I22	0.67	2.12	8.1	0.49	0.55	2.47	3590	8956	14.5	95.6	490
I48	0.46	3.23	7.6	0.53	0.60	2.14	3558	7673	8.9	71.6	400
I48	0.43	3.22	7.1	0.51	0.58	2.11	3612	7676	8.4	70.6	375
I48	0.48	2.90	7.0	0.49	0.56	2.23	3614	8115	7.6	75.2	385
I48	0.34	3.37	5.8	0.48	0.54	2.03	3844	7859	8.5	67.8	305
M3	2.13	1.97	33.8	0.75	0.76	2.58	4372	11469	34.4	114.3	1320
M12	0.88	2.92	17.1	0.73	0.74	2.22	3847	8731	23.9	89.2	753
M28	1.12	2.26	15.6	0.65	0.73	2.54	3497	8997	25.3	99.4	801.8
M28	1.04	2.34	14.6	0.64	0.72	2.52	3538	9012	26.0	98.9	750.1
M28	1.00	2.37	14.1	0.62	0.69	2.48	3587	8998	23.4	98.3	724.9
M28	1.06	2.20	13.5	0.59	0.65	2.62	3597	9539	19.3	102.9	714.9
M28	1.03	2.33	15.5	0.64	0.71	2.38	3566	8616	24.7	98.1	789
H3	2.66	1.83	35.9	0.72	0.73	2.86	4093	11969	32.0	122.9	1571

Table A.4. CO_2 Reduced Speed Operation—Gas Cooler

Test Point	T_{cai} [°C]	T_{cao} [°C]	m_ca [kg/sec]	QC [kW]	P_{cri} [kPa]	P_{cro} [kPa]	Dpca [Pa]	T_{cri} [°C]	T_{cro} [°C]	T_{shi} [°C]	T_{sho} [°C]
I13	43.0	49.7	0.454	2.84	10508	10501	28.7	107.8	46.0	5.7	26.2
I22	32.2	34.9	0.454	2.06	8390	8449	31.0	86.8	33.1	2.8	15.6
I22	32.3	34.8	0.455	1.96	8380	8440	30.8	85.5	33.2	3.3	15.5
I22	32.3	34.2	0.455	2.01	7833	7883	30.8	89.7	34.2	2.6	25.2
I22	32.1	34.3	0.455	2.01	8860	8918	30.9	90.1	32.9	3.0	12.7
I48	21.2	22.8	0.449	2.27	7602	7665	25.4	68.0	21.6	2.9	5.0
I48	21.2	22.6	0.453	2.14	7607	7671	25.2	67.0	21.6	3.7	5.4
I48	21.2	22.1	0.454	2.17	8044	8112	25.3	71.1	21.5	4.2	5.5
I48	21.1	21.8	0.454	1.73	7794	7855	25.8	64.0	21.4	8.7	7.6
M3	42.9	51.4	0.541	5.02	11260	11125	43.1	111.3	48.2	10.1	29.9
M12	32.5	37.8	0.535	2.81	8535	8552	35.2	86.1	35.6	4.8	20.1
M28	32.3	36.6	0.535	3.55	8897	8912	38.4	95.5	34.7	1.1	17.5
M28	32.3	36.3	0.535	3.40	8903	8934	38.4	94.9	34.2	2.2	17.7
M28	32.3	36.1	0.535	3.35	8886	8921	38.4	94.2	34.0	2.6	17.4
M28	32.3	35.7	0.535	3.41	9432	9464	38.4	98.5	33.3	2.8	15.2
M28	32.2	36.1	0.535	3.42	8500	8521	38.5	94.1	35.2	2.5	21.0
H3	42.8	50.4	0.701	5.92	11704	11589	60.7	119.2	46.9	7.7	26.0

Table A.5. CO_2 Reduced Speed Operation—Evaporator

Test Point	T_{eai} [°C]	T_{eao} [°C]	m_ea [kg/sec]	RH	QE [kW]	Q_lat [kW]	Q_sens [kW]	Condensate [g/sec]	P_{eri} [kPa]	P_{ero} [kPa]	T_{ori} [°C]	T_{eri} [°C]	T_{ero} [°C]	DPea [Pa]
I13	27.2	8.9	0.100	0.39	2.47	0.69	1.78	0.258	4047	4013	36.9	7.1	6.9	104.8
I22	20.9	4.8	0.057	0.51	1.46	0.55	0.90	0.212	3593	3575	26.6	2.3	2.2	47.3
I22	21.0	5.3	0.057	0.51	1.35	0.47	0.89	0.180	3648	3630	26.5	3.1	3.0	46.9
I22	21.0	5.2	0.057	0.50	1.36	0.48	0.88	0.181	3625	3602	32.9	3.0	2.8	47.0
I22	21.0	5.1	0.057	0.51	1.43	0.55	0.87	0.209	3616	3599	25.2	3.0	2.9	47.4
I48	21.0	5.1	0.060	0.50	1.49	0.54	0.94	0.209	3583	3566	16.4	2.7	2.6	50.4
I48	20.9	5.5	0.058	0.50	1.39	0.51	0.88	0.196	3635	3618	16.6	3.3	3.2	47.9
I48	20.9	5.5	0.058	0.50	1.38	0.51	0.87	0.195	3637	3620	16.7	3.3	3.2	47.9
I48	20.9	7.4	0.058	0.50	1.16	0.39	0.77	0.149	3863	3847	18.1	5.5	5.6	47.4
M3	32.6	13.8	0.145	0.45	4.19	1.40	2.79	0.549	4566	4480	38.7	12.1	11.4	223.7
M12	26.6	8.7	0.100	0.39	2.57	0.76	1.81	0.278	3909	3879	29.8	5.6	5.4	105.6
M28	21.1	4.7	0.099	0.50	2.53	0.95	1.58	0.358	3570	3537	26.4	2.3	2.1	106.0
M28	21.1	5.1	0.099	0.50	2.44	0.88	1.56	0.337	3600	3571	26.7	2.6	2.4	103.7
M28	21.1	5.5	0.099	0.50	2.37	0.85	1.52	0.323	3645	3617	26.5	3.1	2.9	102.5
M28	21.1	5.6	0.099	0.50	2.32	0.85	1.47	0.315	3650	3623	25.1	3.2	3.0	101.7
M28	21.1	5.3	0.099	0.50	2.39	0.86	1.53	0.325	3634	3602	29.1	3.0	2.8	102.1
H3	32.5	12.6	0.145	0.40	4.86	1.89	2.97	0.710	4330	4238	35.5	9.7	8.9	198.1

Table A.6. R134a System During Cycling Operation—Idle and Medium Speed

Test Point	T_{cai} [°C]	m_ca [kg/sec]	Teai [°C]	RH	m_ea [kg/sec]	QE [kW]	Q_sens [kW]	Q_lat [kW]	Condensate [g/sec]	W_{comp} [kW]	COP	QC [kW]	Cycle Time [sec]	ON %
i21	32.2	0.453	20.9	0.68	0.058	1.68	0.78	0.90	0.33	0.60	2.78	2.39	41.9	0.61
i22	31.9	0.453	20.9	0.49	0.059	1.43	0.92	0.51	0.19	0.71	2.01	2.20	34.8	0.72
i23	32.4	0.453	21.3	0.39	0.060	1.22	0.94	0.27	0.11	0.64	1.90	1.98	27.6	0.65
i24	32.6	0.452	21.5	0.25	0.060	0.97	0.97	0.00	0.00	0.54	1.80	1.58	24.8	0.57
i26	21.8	0.451	27.1	0.40	0.058	1.78	1.18	0.60	0.23	0.59	3.00	2.13	29.9	0.63
i27	21.2	0.451	20.9	0.69	0.061	1.13	0.55	0.58	0.20	0.46	2.44	1.44	36.4	0.52
i28	21.3	0.452	21.3	0.39	0.059	1.14	0.93	0.21	0.09	0.43	2.67	1.70	27.7	0.48
i29	16.2	0.459	27.1	0.39	0.058	1.70	1.18	0.52	0.21	0.48	3.52	2.14	27.6	0.55
i30	15.7	0.451	21.3	0.40	0.059	1.13	0.95	0.19	0.08	0.36	3.11	1.77	30.5	0.43
i31	32.3	0.454	26.9	0.40	0.060	1.29	0.93	0.36	0.14	0.68	1.91	2.19	55.7	0.43
i32	26.8	0.452	26.9	0.40	0.059	1.26	0.93	0.33	0.14	0.56	2.26	1.96	46.2	0.67
i33	26.9	0.453	20.8	0.41	0.059	0.81	0.67	0.15	0.05	0.43	1.88	1.34	35.5	0.58
m9	43.9	0.539	21.3	0.29	0.143	2.05	2.05	0.00	0.00	1.53	1.34	3.71	18.8	0.76
m11	32.5	0.531	26.9	0.48	0.099	3.44	1.90	1.54	0.57	1.94	1.78	5.66	62.7	0.92
m12	32.5	0.537	26.9	0.40	0.099	2.55	1.71	0.83	0.32	1.40	1.82	4.18	20.7	0.67
m13	32.5	0.532	26.9	0.25	0.100	2.21	2.01	0.20	0.08	1.23	1.80	3.62	19.7	0.64
m14	32.3	0.537	21.1	0.39	0.101	1.52	1.50	0.03	0.00	1.09	1.39	3.19	14.3	0.56
m15	26.7	0.537	26.8	0.39	0.101	2.78	1.89	0.89	0.34	1.29	2.15	4.33	20.9	0.63
m16	26.8	0.539	21.2	0.39	0.102	1.87	1.48	0.39	0.14	0.91	2.05	2.94	14.6	0.49
m18	21.1	0.533	32.1	0.40	0.099	3.76	2.18	1.58	0.58	1.54	2.44	5.54	24.9	0.78
m19	20.9	0.534	32.0	0.25	0.100	3.00	2.44	0.55	0.22	1.26	2.39	4.42	18.7	0.61
m20	21.7	0.534	27.2	0.40	0.058	1.70	1.12	0.58	0.22	0.76	2.22	2.21	14.8	0.44
m21	21.2	0.538	21.1	0.68	0.060	1.74	0.74	0.99	0.35	0.75	2.31	1.85	14.8	0.46
m22	21.2	0.534	21.5	0.48	0.061	1.34	0.87	0.47	0.17	0.63	2.13	2.04	14.3	0.41
m23	21.4	0.536	21.4	0.39	0.059	1.11	0.94	0.17	0.08	0.54	2.03	1.66	14.0	0.33
m24	21.0	0.536	21.4	0.27	0.060	0.94	0.94	0.00	0.00	0.50	1.90	1.50	13.0	0.33
m25	16.1	0.537	27.1	0.39	0.058	1.66	1.14	0.52	0.21	0.65	2.56	2.30	15.1	0.39
m26	16.2	0.537	21.6	0.38	0.059	1.05	0.84	0.21	0.08	0.44	2.37	1.47	14.1	0.29
m27	26.4	0.538	21.5	0.39	0.060	1.13	1.12	0.01	0.10	0.60	1.87	1.62	13.5	0.35

Table A.7. R134a System During Cycling Operation—High Speed

Test Point	T_{cai} [°C]	m_ca [kg/sec]	Teai [°C]	RH	m_ea [kg/sec]	QE [kW]	Q_sens [kW]	Q_lat [kW]	Condensate [g/sec]	W_{comp} [kW]	COP	QC [kW]	Cycle Time [sec]	ON %
h5	42.5	0.709	21.4	0.67	0.141	3.64	1.75	1.89	0.69	3.15	1.15	6.92	52.1	0.94
h6	42.5	0.710	21.4	0.48	0.142	2.94	1.85	1.09	0.40	2.37	1.24	5.12	14.4	0.73
h7	43.2	0.711	21.4	0.39	0.144	2.35	1.96	0.39	0.15	2.09	1.12	4.40	12.7	0.65
h8	43.5	0.693	21.4	0.30	0.144	2.07	2.07	0.00	0.00	1.86	1.11	3.66	11.3	0.58
h9	32.3	0.695	26.9	0.65	0.098	3.75	1.60	2.15	0.78	2.57	1.46	6.72	19.0	0.79
h10	32.5	0.695	26.9	0.48	0.098	3.02	1.71	1.31	0.49	2.05	1.47	5.14	14.0	0.64
h11	33.0	0.688	27.0	0.39	0.099	1.69	1.69	0.00	0.00	1.77	0.95	4.36	13.1	0.57
h12	32.6	0.700	26.9	0.22	0.100	1.93	1.93	0.00	0.00	1.35	1.43	3.20	11.6	0.44
h13	20.6	0.706	21.5	0.69	0.060	2.16	1.46	0.70	0.27	0.92	2.34	2.52	11.9	0.35
h14	21.7	0.695	21.4	0.49	0.057	1.28	0.78	0.49	0.19	0.79	1.61	3.51	12.0	0.29
h15	21.7	0.696	21.4	0.39	0.057	1.09	0.82	0.26	0.11	0.71	1.52	3.25	11.4	0.27
h16	22.1	0.696	21.5	0.28	0.057	0.88	0.88	0.00	0.00	0.65	1.35	2.65	11.2	0.25

Table A.8. R134a System During Reduced Speed Operation—Evaporator

Test Point	T_{eai} [°C]	T_{eao} [°C]	m_ea [kg/sec]	RH	QE [kW]	Q_sens [kW]	Q_lat [kW]	Condensate [g/sec]	P_{eri} [kPa]	P_{ero} [kPa]	Dper [kPa]
i23r	20.9	10.9	0.056	0.41	0.60	0.56	0.04	0.01	272.5	263.9	8.6
i28r	20.9	10.2	0.058	0.41	0.65	0.60	0.05	0.01	270.5	262.9	7.5
i30r	20.9	10.4	0.058	0.41	0.64	0.62	0.02	0.01	281.8	274.8	7.1
m12r	26.9	11.6	0.099	0.41	1.90	1.55	0.35	0.14	289.0	270.0	19.0
m23r	20.7	11.0	0.057	0.41	0.61	0.56	0.05	0.02	263.9	256.6	7.3
m26r	20.7	10.3	0.057	0.41	0.68	0.62	0.06	0.03	272.0	264.9	7.1
h7r	21.4	5.6	0.144	0.40	2.94	2.28	0.66	0.25	304.7	266.9	37.8
h15r	21.5	11.8	0.098	0.39	1.08	0.92	0.15	0.05	280.0	271.7	8.3

Table A.9. R134a System During Reduced Speed Operation—Condenser

Test Point	T_{cai} [°C]	T_{cao} [°C]	m_ca [kg/sec]	QC [kW]	P_{cri} [kPa]	P_{cro} [kPa]	DPcr [kPa]
i23r	32.2	34.5	0.454	0.75	1027.7	1010.0	17.7
i28r	20.8	23.2	0.452	1.06	770.0	755.5	14.5
i30r	15.9	17.9	0.451	0.99	662.3	650.1	12.2
m12r	32.2	39.2	0.538	3.58	1272.6	1235.0	37.6
m23r	20.7	23.3	0.537	1.19	764.8	751.7	13.1
m26r	14.9	17.2	0.536	1.21	653.5	640.8	12.7
h7r	42.6	49.8	0.712	5.08	1730.7	1676.0	54.7
h15r	21.0	22.6	0.702	3.58	783.5	767.3	16.2

Table A.10. R134a System During Reduced Speed Operation—System and Compressor

Test Point	W_{comp} [kW]	COP	P_{ratio}	P_{rcpi} [kPa]	Vc [RPM]
i23r	0.41	1.45	3.75	273.8	442.7
i28r	0.27	2.38	2.79	275.9	352.5
i30r	0.20	3.14	2.38	278.8	303.4
m12r	1.01	1.89	4.77	266.8	902.3
m23r	0.27	2.30	2.89	264.5	353
m26r	0.21	3.15	2.43	268.6	324
h7r	2.01	1.47	7.17	241.5	1670
h15r	0.95	1.13	2.86	274.2	1211

Table A.11. Test Matrix

Compressor Speed, RPM	Condenser	Evaporator		Relative Humidity, %			
	Inlet air temp.,°C	Flow rate, m^3/sec	Inlet air temp.,°C	70	50	40	25
3000	43.3	0.1180	43.3		H1		
		0.1180	32.2		H2	H3	H4
		0.1180	21.1	H5	H6	H7	H8
	32.2	0.0826	26.7	H9	H10	H11	H12
	21.1	0.0472	21.1	H13	H14	H15	H16
1800	43.3	0.1180	43.3		M1	M0	
			32.2		M2	M3	M4
			26.7			M5	
			21.1	M6	M7	M8	M9
	32.2	0.1180	26.7			M10	
		0.0826			M11	M12	M13
		0.0826	21.1		M28	M14	
	26.7	0.0826	26.7			M15	
			21.1			M16	
		0.0472	21.1			M27	
	21.1	0.0826	32.2		M17	M18	M19
		0.0472	26.7			M20	
		0.0472	21.1	M21	M22	M23	M24
	15.5	0.0472	26.7			M25	
		0.0472	21.1			M26	
950	60	0.1180	43.3		I1		I0
		0.1180	32.2		I2	I3	I4
	54.4	0.1180	32.2		I5	I6	I7
		0.1180	26.7			I38	
	43.3	0.1180	43.3			I39	
		0.1180	32.2		I8	I9	I10
		0.1180	26.7			I11	
		0.0826		I34	I12	I13	I14
		0.0472				I42	
		0.1180	21.1	I15	I16	I17	I18
		0.0472			I45	I43	
	32.2	0.1180	26.7			I19	
		0.0826				I20	
		0.0472				I31	
		0.0472	21.1	I21	I22	I23	I24
	26.7	0.1180	26.7			I44	
		0.0472				I32	
		0.0472	21.1		I46	I33	
	21.1	0.1180	26.7			I25	
		0.0472				I26	
		0.0472	21.1	I27	I48	I28	
	15.5	0.0472	26.7			I29	
		0.0472	21.1			I30	

Appendix B Load Model

A model was constructed to simulate the transient nature of an automotive cabin. The goal of this model was to provide an idea of what the steady state system load would be for varying conditions. The model was constructed semi-empirically using data from an actual wind tunnel test. EES software was used to solve the set of differential-algebraic equations.

B.1 Model Construction

The automotive cabin was modeled as two thermal masses. These thermal masses are the cabin air and the vehicle mass, as shown in Figure B.1. Also shown in the figure are the various energy exchanges which lead to changing temperatures of these masses.

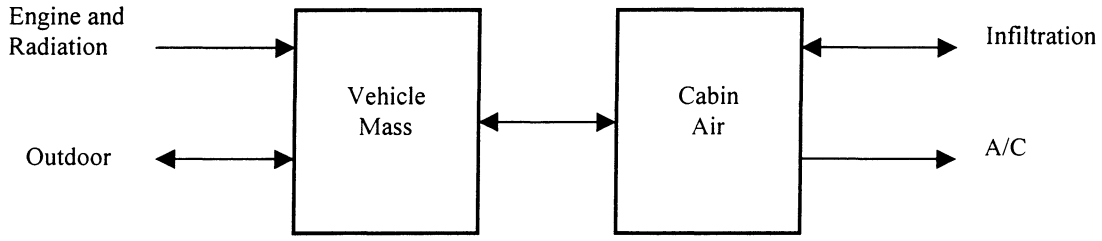

Figure B.1. Schematic of Transient Cabin Model

The energy exchanges associated with the vehicle mass are the engine and radiation loads, the energy exchanged with the outdoor environment, and the energy exchanged with the cabin air. The engine and radiation loads were assumed to be constant, and were combined into one parameter which was specified in the model. The energy exchanged with the outdoor environment was governed by a $UA\Delta T$ equation, as was the energy exchanged with the cabin air. All of the UA heat transfer coefficients were specified in the model, and the ΔT portions of the equations were calculated in the transient model.

The cabin air itself was modeled as exchanging energy with the vehicle mass, the infiltration air from outside, and the A/C system. The energy exchange with the vehicle mass was described above. The infiltration air was modeled as displacing the equivalent mass of air in the cabin. Finally, the energy exchange with the A/C system was modeled by fitting the data taken during the transient wind tunnel testing. Of course, these energy exchanges only kept track of sensible loads. The mass of water vapor present in the cabin was tracked separately. The source and sink for water vapor were the infiltration air and the A/C system, respectively. The

mass of water vapor and mass of air in the cabin were then used to calculate dew points and relative humidity. The summary of modeling can be seen in Table B.2.

Table B.2. Summary of Transient Cabin Model

Energy Exchange		Modeling Method
Vehicle Mass	Engine and Radiation	Assumed to be constant loads, combined into one parameter
	Outdoor	UAΔT
	Cabin Air	UAΔT
Cabin Air	Infiltration	Infiltration air displaced equivalent mass of cabin air
	A/C System	Curve fit actual data taken during transient wind tunnel test
Water Vapor Modeling		
Infiltration Air		Infiltration rate and outdoor relative humidity gave vapor rate
A/C System		Curve fit actual data taken during transient wind tunnel test

There were several inputs to the model which took into account various operating conditions. These were the outdoor ambient conditions, initial indoor conditions, and load provided by the engine and solar load. There were also inputs which modeled the vehicle itself. These included size of the cabin, thermal mass of the cabin, heat transfer coefficients between cabin surfaces and cabin air, heat transfer coefficient between the car and the ambient, and flow rate of infiltration air.

The A/C system itself was modeled using data from the actual transient wind tunnel test. The test performed was a thermal soak of the vehicle up to an initial cabin temperature of 60°C for ambient conditions of 43.3°C. When the vehicle cabin reached this temperature, the vehicle was started and began driving at 48.3 km/h with the A/C system engaged at a specified evaporator air flow rate. This condition was continued for 30 minutes. The data consisted of snapshots at certain periods of time during the test. The values provided were elapsed time, cabin temperature, cabin relative humidity, and evaporator air exit temperature and humidity. The data was then curvefit to produce relationships that could be used in the model. The data and curvefits are shown in Figure B.3. The total capacity and latent capacity (condensate removal rate) were curvefit, then the sensible capacity was found to be the difference between the two.

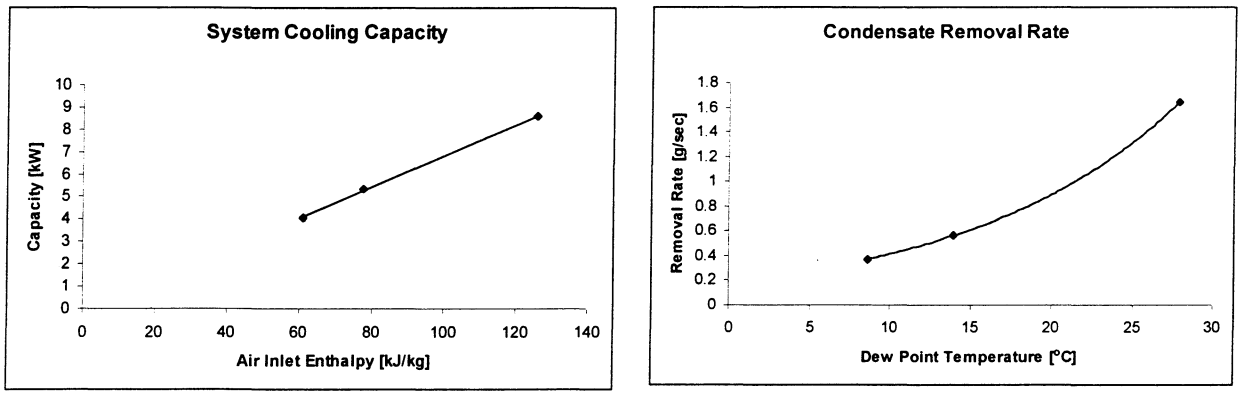

Figure B.3. Data from Actual Transient Wind Tunnel Testing

B.2 Model Results

The goal of this model was to get the model output to match the data taken during the wind tunnel testing. To do this, the input parameters were changed until the model output resembled the data. The final transient response is shown in Figure B.4. Once this occurred, it was assumed that the input parameters characterizing the automotive cabin were close approximations of the actual numbers. From these numbers, the steady state loads on the cabin could be determined. The final parameters are shown in Table B.5.

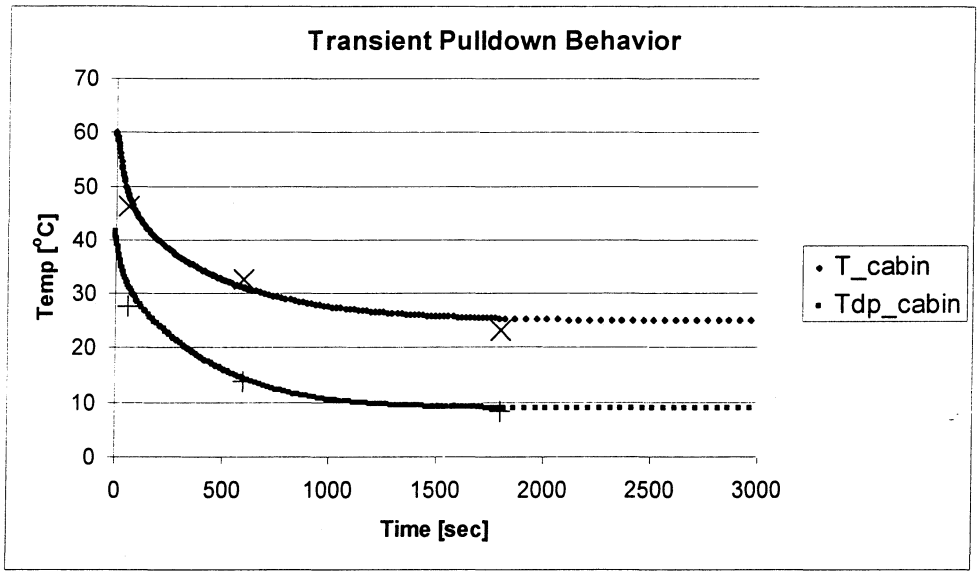

Figure B.4. Response of Transient Model and Actual Data Points

Table B.5. Final Values of Model Parameters

Symbol	Value	Description
V_cabin	5.66 m^3	Volume of cabin air
UA	265.9 W/K	Heat transfer coefficient from vehicle interior to cabin air
UA_vm	341.8 W/K	Heat transfer coefficient from vehicle interior to outdoor
Mcp_vm	189.9 kJ/K	Thermal mass of vehicle interior
k	633 W	Engine + radiation load

B.3 Determining Steady State Loads

Once the model results showed that the parameter values were appropriate, the transient portions of the model equations were set to zero. This allowed calculation of steady state load based on indoor and outdoor conditions. Therefore, load curves, shown in Figure B.6, could be developed and used in the study of the automotive A/C system.

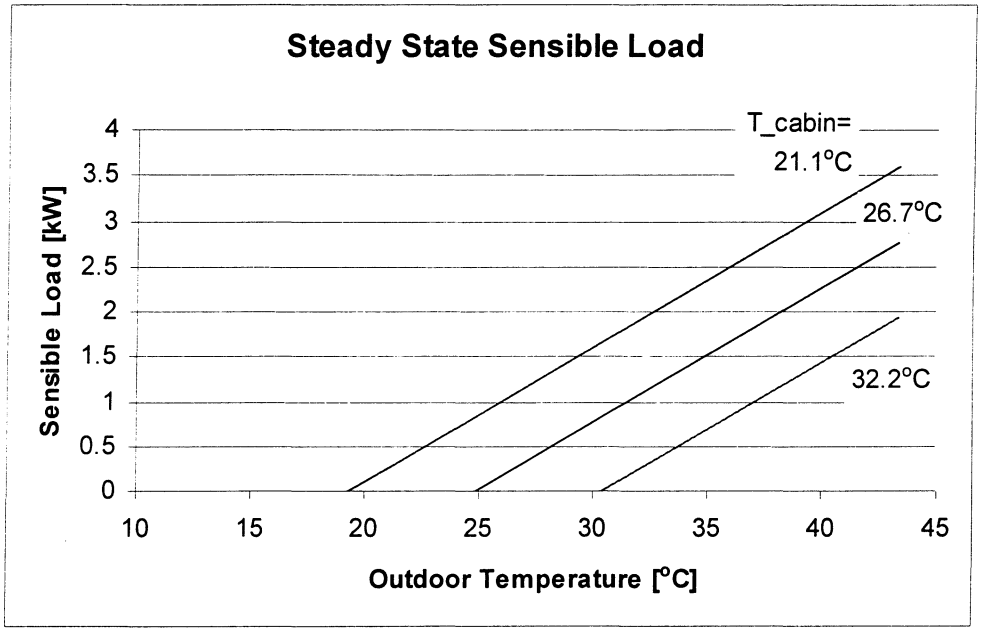

Figure B.6. Load Curves for Various Cabin Temperatures

B.4 Model Code

{Air Property Calculations}

p_atm=14.696
t_outdr=110
r_outdr=.40

```
t_init=140
t_vm_init=140
r_init=.4
den_init=density(airh2o,t=t_init,r=r_init,p=p_atm)
omega_init=humrat(airh2o,t=t_init,r=r_init,p=p_atm)
air_init=200*den_init-water_init
(1+omega_init)*air_init=200*den_init
den_cabin=density(airh2o,t=t_cabin,w=omega_cabin,p=p_atm)
mcp_cabin=200*den_cabin*specheat(airh2o,t=t_cabin,p=p_atm,w=omega_cabin)
omega_outdr=humrat(airh2o,r=r_outdr,t=t_outdr,p=p_atm)
den_outdr=density(airh2o,r=r_outdr,t=t_outdr,p=p_atm)
mdot_inf=10*den_outdr/60
mdot_inf_air=mdot_inf/(1+omega_outdr)
mdot_inf_wat=mdot_inf-mdot_inf_air
mdot_inf_airout=mdot_inf/(1+omega_cabin)
mdot_water_out=mdot_inf-mdot_inf_airout
H_outdr_air=enthalpy(air,t=t_outdr)
H_cabin_air=enthalpy(air,t=t_cabin)
H_cabin=enthalpy(airh2o,t=t_cabin,w=omega_cabin,p=p_atm)
Tdp_cabin=dewpoint(airh2o,t=t_cabin,w=omega_cabin,p=p_atm)
omega_cabin=water_cabin/air_cabin
air_cabin=air_init-(water_cabin-water_init)

{Equations Describing A/C System}

AC=(541.689*H_cabin-30.576)/3600
AC_lat=(432.366*exp(.04415*Tdp_cabin))/3600
AC_sens=AC-AC_lat
mdot_AC_remove=if(Tdp_cabin,47,0.00333*(Tdp_cabin-
32)/60,0.05/60,0.0253*exp(0.04291*(Tdp_cabin-32))/60)*(.2+.8*exp(-.028*time))

{Heat Transfer Coefficients and Load Constant}

hA=.14
mcp_vm=100
k=.6
hA_vm=.18


{Transient Portion of Model}

T_cabin=T_init+INTEGRAL((1/mcp_cabin)*((mdot_inf_air*H_outdr_air-
mdot_inf_airout*H_cabin_air)+hA*(T_vm-T_cabin)-AC_sens),time)
T_vm=T_vm_init+INTEGRAL((1/mcp_vm)*(k-hA*(T_vm-T_cabin)-hA_vm*(T_vm-
T_outdr)),time)
water_cabin=water_init+INTEGRAL((mdot_inf_wat-mdot_water_out-mdot_AC_remove),time)
```

Appendix C Sensitivity Model Code

```
{Thermodynamic R744 Procedures}

procedure TP(TC, P : Vkg,Hkg,Skg)
      R744=35;
        TK=TC+273.15
        CALL REFPROP(1, R744,1, TK, P : TK', P, V, H, S, Q)
       MW=44.01;   Vkg=V/MW;        Hkg=H/MW;        Skg=S/MW
end
procedure TQ(TC, Q : P, Vkg, Hkg, Skg)
      R744=35;
        TK=TC+273.15
        CALL REFPROP(1, R744 ,5, TK, Q : TK', P, V, H, S, Q)
       MW=44.01;  Vkg=V/MW;  Hkg=H/MW;   Skg=S/MW
end
procedure PQ(P, Q : TC, Vkg, Hkg, Skg)
      R744=35;
        CALL REFPROP(1, R744 ,6, P, Q : TK, P', V, H, S, Q)
       TC=TK-273.15
       MW=44.01; Vkg=V/MW;  Hkg=H/MW;  Skg=S/MW
end
procedure PS(P, Skg : TC, Vkg, Hkg)
        R744=35;   MW=44.01
      S=Skg*MW
        CALL REFPROP(1 ,R744 ,4 , P, S : TK, P, V, H, S, Q)
        TC=TK-273.15
      Vkg=V/MW;  Hkg=H/MW
end

{Set Conditions}

t_evap=9
p_high=11800
t_cro=35

{Compressor}

eta_isen=.01*(92.6-7.9*p_ratio)    "950 rpm"
eta_vol=.01*(105-11.43*p_ratio)
p_ratio=p_high/p_low
p_1=p_low
p_2=p_high
(h_2-h_1)*(eta_isen/.85)=(h_2s-h_1)
call tp(t_1,p_1 : v_1,h_1,s_1)
call ps(p_2,s_1 : t_2,v_2,h_2s)
m_dot=eta_vol*348.33*density(carbondioxide,t=t_1,p=p_1)/1000000
```

```
{Gas Cooler}

p_3=p_high
t_3=t_cro
call tp(t_3,p_3 : v_3,h_3,s_3)

{SLHX parallel}

length=1.0
segment=length/5
UA=.024  "kW/K/m"
UA_seg=UA*segment
T_33a=(T_3+T_3a)/2
T_3a3b=(T_3a+T_3b)/2
T_3b3c=(T_3b+T_3c)/2
T_3c3d=(T_3c+T_3d)/2
T_3d4=(T_3d+T_4)/2
m_dot*(H_3-H_3a)=UA_seg*(T_33a-T_66a)
m_dot*(H_3a-H_3b)=UA_seg*(T_3a3b-T_6a6b)
m_dot*(H_3b-H_3c)=UA_seg*(T_3b3c-T_6b6c)
m_dot*(H_3c-H_3d)=UA_seg*(T_3c3d-T_6c6d)
m_dot*(H_3d-H_4)=UA_seg*(T_3d4-T_6d1)
call tp(t_3a,p_high:v_3a,h_3a,s_3a)
call tp(t_3b,p_high:v_3b,h_3b,s_3b)
call tp(t_3c,p_high:v_3c,h_3c,s_3c)
call tp(t_3d,p_high:v_3d,h_3d,s_3d)
call tp(t_4,p_high:v_4,h_4,s_4)
call tp(t_6a,p_low:v_6a,h_6a,s_6a)
call tp(t_6b,p_low:v_6b,h_6b,s_6b)
call tp(t_6c,p_low:v_6c,h_6c,s_6c)
call tp(t_6d,p_low:v_6d,h_6d,s_6d)
T_66a=(T_6+T_6a)/2
T_6a6b=(T_6a+T_6b)/2
T_6b6c=(T_6b+T_6c)/2
T_6c6d=(T_6c+T_6d)/2
T_6d1=(T_6d+T_1)/2
H_6a-H_6=H_3-H_3a
H_6b-H_6a=H_3a-H_3b
H_6c-H_6b=H_3b-H_3c
H_6d-H_6c=H_3c-H_3d
H_1-H_6d=H_3d-H_4

{Expansion}
H_5=H_4
```

```
{Evaporator}
p_low=pressure(carbondioxide,t=t_evap,x=.5)
call pq(p_low,1:t_6,v_6,h_6,s_6)

{System Parameters}
Q=m_dot*(h_6-h_5)
P=m_dot*(h_2s-h_1)/eta_isen
COP=Q/P
```

Appendix D Controller Pseudocode and Simulation Development

D.1 Fixed Displacement Advanced Control Code

```
    initialize controller
    set cyclelimits=[4,7]
    is cabin temperature within setpoint + 5°C?
        if yes, goto comfortzone
        if no, goto hightemp
hightemp:
    set airflow rate = 10
    set pressurelookup to 97% COP at high capacity, based on lookup table
    set cabin_lolimit to (setpoint + 5°C , goto comfortzone)
    set cabin_hilmit to none
    call logdata
    increase morepressure to 5 bar
    call logdata
    if the pressure was changed, did ΔT across evaporator increase by more than 0.25°C?
        if yes, increase morepressure by 5 bar
        if no, decrease morepressure by 5 bar
    have 4 datalogging cycles passed without pressure change?
        if yes, increase morepressure by 5 bar
    repeat

comfortzone:
    set morepressure = 0
    set cabin_lolimit to none
    set cabin_hilimit to (setpoint + 7°C, goto hitemp)
    call logdata
    call quantify
    call select
    repeat
logdata
```

```
    set timer for 15 sec
        gather parameters
        is cabin_lolimit violated?
            if yes, take cabin_lolimit action
        is cabin_hilimit violated?
            if yes, take cabin_hilimit action
        is air temperature after the evaporator below lo_cycle_limit?
            if yes, then disengage clutch
        is air temperature after the evaporator above hi_cycle limit?
            if yes, then engage clutch
        are any safety limits violated?
            if yes, then increase safety by 1 bar
        is pressure@pressurelookup+morepressure > 150?
            if yes, then set pressure to 150-safety
            if no, then set pressure to (pressure@pressurelookup + morepressure - safety)
        add parameters to running totals
        repeat until timer expires
    calculate average values
    calculate start and end values

quantify
    ΔQ=[(ΔT_cabin_trajectory@average T_cabin)-(T_cabin_end-T_cabin_start)]*(100/0.23)

select
    Q_remaining=ΔQ
    if ΔQ < 0 (require more cooling)
        is reheat at minimum?
            if yes, skip to cycle limits
            if no, then
                use relationship to determine reheat adjustment for Q_remaining
            {if no, then}
```

```
            subtract amount adjusted from Q_remaining
        are cycle limits at minimum?
            if yes, skip to blower
            if no, then
                use relationship to determine cycle limit adjustment for Q_remaining
                subtract amount adjusted from Q_remaining
        determine blower adjustment for Q_remaining
        make adjustments
    if ΔQ>0
        is blower limit at minimum?
            if yes, skip to cycle limits
            if no, then
                use relationship to determine blower adjustment for Q_remaining
                subtract amount adjusted from Q_remaining
        are cycle limits at maximum?
            if yes, skip to blower
            if no, then
                use relationship to determine cycle limit adjustment for Q_remaining
                subtract amount adjusted from Q_remaining
        determine reheat adjustment for Q_remaining
        make adjustments
{End Fixed Displacement Advanced Control}
```

D.2 Simulation Development

A simulation of an automotive cabin was developed using the transient model of the automotive cabin presented in Appendix B, the controller pseudocode presented above, and a model of an automotive A/C system. Visual Basic was used to code the controller and cabin model, and EES was used to model the automotive A/C system. Visual Basic was also used to coordinate all of the pieces. The structure of the program was that the controller would calculate the desired operating parameters via the control structure presented above, then VB would feed those parameters, along with the current information from the transient cabin model, into the A/C

model in EES. EES would then calculate the A/C system outputs based on the controller and cabin inputs and return these to the VB program. Finally, the VB program would update the cabin model and then again use the controller code to continue the process. This is shown graphically in Figure D.1.

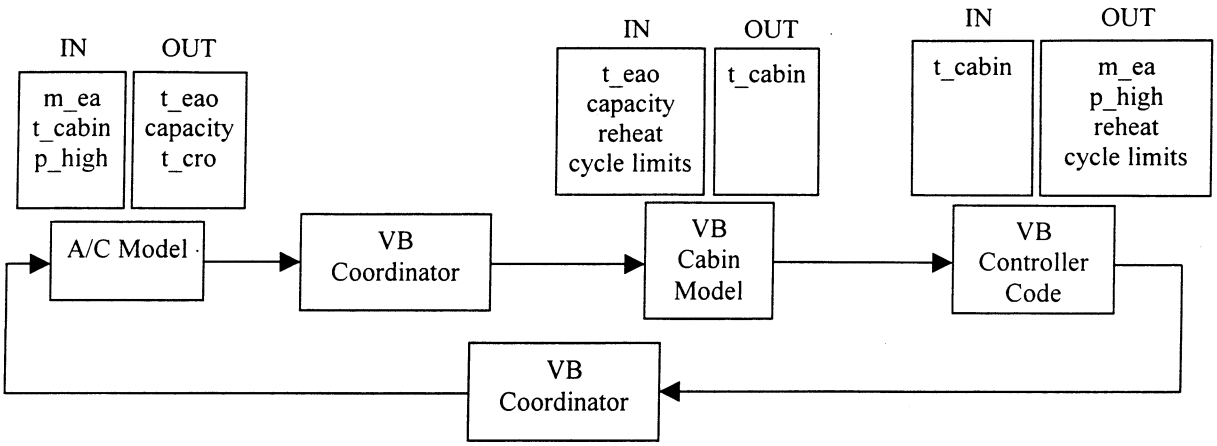

Figure D.1. Information Flow in the Controller Simulation

The cabin model is implemented in VB rather than in EES, as in Appendix B. This is because the model is relatively simple. Only a minor simplification is necessary to code it in VB, the properties of the air in the cabin needed to be simplified. Therefore, in this simulation, no humidity effects were used and the specific heat of the air was assumed to be constant over the range of temperatures encountered. Other than that, the model is exactly the same as in Appendix B.

The only new part of the simulation is the model of the A/C system. In the real system, the parameters that need to be specified are airflow rates and inlet temperatures to both heat exchangers, relative humidity at the evaporator air inlet, compressor speed, and high side pressure. Then, the model should be able to calculate all of the other operating parameters which in this case means the capacity, air exit temperature from the evaporator, and T_{cro}.

The time step used for this simulation was 1 second. Therefore, a main goal for developing the A/C system model was computational speed since this model had to be called hundreds of times during a simulation run. However, realistic reactions to the inputs were also desired. Some aspects of the actual system behavior and what conditions would be simulated were investigated to produce a model to meet both of the goals.

The equations for compressor efficiencies, both isentropic and volumetric, were determined from system data, as in Appendix C. The compressor speed was assumed to be a constant 950 rpm during the simulations. Also assumed to be constant were the airflow rate and air temperature entering the gas cooler. This allowed a simple relationship between refrigerant mass flow rate and T_{cro} to be developed for each set of gas cooler operating conditions. The refrigerant mass flow rate was found to be the most influential parameter in determining T_{cro}, based on examining system data for relevant operating conditions. The suction line heat exchanger was modeled exactly the same way as in Appendix C, however only 3 divisions were used instead of 5. Finally, the evaporator was modeled with the equation $Q=UA\Delta T$ where ΔT was the log-mean temperature difference and the UA value was determined from matching the Q value obtained in the model with actual system data.

There were other simplifications that were necessary for the model. Since there was no data to correlate the position of the reheat flap with the heat transfer associated with it, a value of 100W per 1 unit of flap opening was assumed. Also, since this model only calculated steady state parameters, some method of dealing with cycling was needed. For this simulation, the cooling power that was applied to the cabin air was equal to the cooling power supplied by the steady state A/C system, minus the reheat value, then the loss in capacity due to cycling operation was subtracted. The loss in capacity due to cycling was calculated by realizing the difference between the air exit temperature and the cycling limit air temperature. Then, the difference in heat transfer is roughly given by $q_{reduced}=m\_dot_{air}*cp_{air}*(T_{cyclim}-T_{eao})$. Of course, all of these simplifications make the model more unlike the real system, but the main purpose of this simulation is to test the controller, so the system just needs to behave in a somewhat realistic manner. The next step in approximating the system would call for models of the gas cooler and evaporator that calculated heat transfer coefficients, which would greatly increase the computation time of the model.